Republic of Iraq
Ministry of Higher Education and
Scientific Research
University of Babylon
College of Engineering
Dept . of Mech . Eng

Theoretical and Experimental Study of Heat Transfer and fluid Flow Through Pipe

A Thesis

Submitted to the College of Engineering

University of Babylon in Partial Fulfillment of the

Requirements for the award of degree of Master of Science in

Mechanical Engineering

(Power Mechanics)

By

Sawsan Abdul Settar Owadh

B. Sc ., (Mech.Eng.)

Supervised by

Dr.Adil Abbas Alwan Almoosawy

Asst. Prof.

2008 A.M **1429 A.H**

يَرْفَعِ اللَّهُ الَّذِينَ آمَنُوا مِنكُمْ وَالَّذِينَ أُوتُوا
الْعِلْمَ دَرَجَاتٍ وَاللَّهُ بِمَا تَعْمَلُونَ خَبِيرٌ

المجادلة (11)

صَدَقَ اللَّهُ العَظِيم

Dedication

To My Family

To My Mother And Father

To My Supervisor

With Respect

And Love

Certification

I certify that this thesis entitled "*Simulation of Heat transfer Mechanism of Fluid flow through pipe*" which was prepared by "*Sawsan Abdul Settar Owadh* " under my supervision at the University of Babylon / Department of Mechanical Engineering ,as a partial requirements for the award of the degree of Master of Science in Mechanical Engineering.

Signature:

Dr. Adil A. Al-Moosawy

Assistant professor.

/ / 2008

جمهورية العراق
وزارة التعليم العالي والبحث العلمي
جامعة بابل/ كلية الهندسة
قسم الهندسة الميكانيكية

دراسة نظرية وعملية
لانتقال الحرارة و جريان مائع خلال انبوب

رسالة
مقدمة إلى كلية الهندسة في جامعة بابل وهي جزء من متطلبات نيل درجة ماجستير علوم في الهندسة الميكانيكية (ميكانيك قدرة)

أعدت من قبل
سوسن عبد الستار عوض
بكالوريوس في الهندسة الميكانيكية

أشراف
د.عادل عباس علوان الموسوي
أستاذ مساعد

1429 هـ 2008 م

Dedication

To My Family

To My Mother And Father

To My Supervisor

With Respect

And Love

Abstract

The flow and heat transfer in a tube of circular cross section have for some time been extremely popular subjects for analysis due to the enormous number of practical applications of this geometry, such as heat exchangers, boilers, condensers , evaporators , and a host of other process equipments such as electrical resistance ,nuclear reactors and radiant systems.

This research includes two parts. The first part represents a theoretical study which deals with the developing steady, laminar, Newtonian and incompressible fluid flow and heat transfer through circular tube .The effects of heat conduction, body force, free convection, heat generation and viscous dissipation within the fluid are neglected.

A computer program was built by using Gaussian elimination method to perform the numerical solution for two case of heating ,constant wall temperature and constant wall heat flux boundary conditions. This approach provides a picture of the variation of the velocity and temperature profiles through the tube. The computational algorithm is able to calculate all the hydrodynamic properties such as velocities and pressure drop . Also it is able to predict all the thermal properties such as the temperature, bulk temperature, and local Nusselt number.

The velocity profile becomes fully developed at approximately $\frac{Le}{2a} = 0.05\,\mathrm{Re}$, and the temperature distribution becomes fully developed at approximately $\frac{Le_t}{2a} = 0.05\,\mathrm{Re}\,.\,\mathrm{Pr}$, as expected.

The second part presents an experimental work which has been done to measure the pressure drop at the entrance region of laminar water flow through circular tube of (L =6.35 m , d=3.125 cm) for different values of Reynolds number ,also the pressure drop at the fully developed region at a range of Reynolds numbers within laminar and turbulent flow. It has been shown that there is a good agreement between the theoretical and the experimental pressure drop.

الـخلاصة

الجريان وانتقال الحرارة خلال الأنابيب ذات المقاطع الدائرية دائما ما كان من المواضيع الشائعة للتحليل نضـرا للتطبيقـات العديـدة لهـذا الشـكل مثـل ,المبـادلات الحراريـة ,المسـخنات ,المكثفات,المبخرات,وجملـة مـن الأجهزة العملية مثل المقاومات الكهربائية ,المفاعلات النووية والأنظمة الإشعاعية .

يتضمن البحث الحالي جزأين.يمثل الجزء الأول دراسة نظرية للجريان الطبائقي غير تام التطوّر لمائع غير قابل للانضغاط,(يخضع لقوانين نيوتن) وانتقال الحرارة لمنطقة النمو خلال مجرى دائري. تم إهمال تأثير كل من انتقال الحرارة بالتوصيل , قوة الجسم (body force) , انتقال الحرارة بالحمل الحر , الحرارة المتولدة و تشتت اللزوجة للمائع.

تم بناء برنامج لإنجاز الحل العددي لحالتين من الشروط الحدودية الحرارية: حالة بثبوت درجة حرارة الجدار و الأخرى بثبوت الفيض الحراري للجدار باستعمال طريقة (Gaussian elimination) . هذا الأسلوب يعطينا صورة لاختلاف السرع و درجات الحرارة ضمن كامل الأنبوب.الخوارزمية الحسابية قادرة على حساب الخواص الهايدروديناميكية مثل توزيع السرعة وفرق الضغط ,كذلك له إمكانية توقع الخواص الحرارية مثل توزيع درجات الحرارة و متوسط درجة الحرارة ورقم نسلت الموضعي.

شكل توزيع السرع يصبح كامل النمو عند حوالي ($\frac{Le}{2a} = 0.05\,\mathrm{Re}$) وشكل توزيع درجات الحرارة يصبح كامل النمو عند حوالي ($\frac{Le_t}{2a} = 0.05\,\mathrm{Re}.\mathrm{Pr}$), كما متوقع .

الجزء الثاني يمثل دراسة عملية لقياس فرق الضغط خلال منطقة الدخول لجريان الماء الطباقي خلال انبوب دائري (L=6.35 m , d=3.125 cm) لقيم مختلفة من أرقام رينولدز,كذلك حساب فرق الضغط خلال منطقة التشكيل التام ضمن مدى لأرقام رينولدز يتضمن كل من الجريان الطباقي والمضطرب. لقد تبين ان هنالك توافق جيد بين النتائج النظرية والعملية لفرق الضغط .

Acknowledgment

First, thanks are due to the Almighty **ALLAH** for enabling me to achieve this work. I wish to express my deepest gratitude and sincere thanks to my supervisor, **Assistant Professor Dr. Adil A. Alwan Almoosawy** for his guidance, invaluable discussions and constructive comments, which greatly improved the structure and presentation of the thesis. His patience and encouragement in the preparation of the thesis and extra time given from a busy schedule is greatly appreciated .

Sincere thanks are also expressed to the staff of the mechanical engineering department at University of Babylon for the encouragement , cooperation and helping in many intangible ways during this work.

I record my sincere gratitude to my husband and family for their love, patience and support during the period of preparing this work.

Finally, I am grateful to all those who have helped me in carrying out this work.

Sawsan

2008

Examining Committees Certificate

We certify that we have read this thesis, entitled "***Theoretical and Experimental Study of Heat Transfer and fluid Flow Through Pipe",*** and as examining committee, examined the student ***"Sawsan Abdul Settar Owadh"*** in its contents and in what is connected with it, and that in our opinion it meets the standard of a thesis for the degree of Master of Science in Mechanical Engineering.

Signature:
Name: Asst. Prof.
Dr. **Adil A. Al- moosawy**
(Supervisor)
Date: / /2008

Signature:
Name: Asst. Prof.
Dr. **Alaa Abbas**
(Member)
Date: / /2008

Signature:
Name: Asst. Prof.
Dr. **Abdul Kareem .A. Wehab**
(Member)
Date: / /2008

Signature:
Name: Asst. Prof.
Dr. **Majid H. Majeed**
(Chairman)
Date: / /2008

Approval of the Mechanical Engineering Department.

Head of the Mechanical Engineering Department
Signature:
Name: Asst. Prof. Dr. **Adil A. Al- moosawy**
Date: / /2008

Approval of the Deanery of the College of Engineering.

Dean of the College of Engineering .
Signature:
Name: Asst. Prof. Dr. Salah Tawfeeq Al-Bezzaz
Date: / /2008

Introduction

1.1. General

Heating and cooling of fluids flowing inside conduits are among the most important heat transfer processes in engineering. The design and analysis of heat exchangers require a knowledge of heat transfer coefficient between the wall of the conduit and the fluid flowing inside it .The sizes of boilers, economizers ,superheaters ,and preheaters depend largely on the heat transfer coefficient between the inner surface of the tubes and the fluid . Also ,in the design of air-conditioning and refrigeration equipment , it is necessary to evaluate heat transfer coefficient for fluids flowing inside ducts.

In long ducts , where the entrance effects are not important , the flow is laminar when Reynolds number values approach 2300. In the rang of Reynolds numbers between 2300 and 10,000 ,a transition from laminar to turbulent flow takes place , the flow in this regime is called transitional .At a Reynolds number 10,000 ,the flow becomes fully turbulent . But when the conduit is short ,in addition to Reynolds number and Prandtl number , several other factors such as entrance effects can influence heat transfer by forced convection in a duct. Therefore, When dealing with internal flows in short ducts, it is important to be cognizant of the extent of " the entry region ", depending on whether the flow is laminar or turbulent. [1]

1.2. Hydrodynamic Boundary Layer

Any fluid flowing in a pipe had to enter the pipe at some location. The region of flow where the fluid enters the tube is termed the entrance region and illustrated in figure (1-1). The fluid typically enters the tube with a nearly uniform velocity profile at section (1). As the fluid moves through the tube, viscous effects cause it to stick to the tube wall (the no slip boundary condition).

This is true whether the fluid is relatively inviscid air or a very viscous oil. Thus, a boundary layer (in which viscous effects are important) is produced along the tube wall such that the initial velocity profile changes with distance along the tube, z, until the fluid reaches the end of the entrance length, section (2), beyond which the velocity profile does not vary with z.

If the turbulence in the entering fluid stream is high , the boundary layer will quickly become turbulent. Irrespective of whether the boundary layer will remains laminar or becomes turbulent , it will increase in thickness until it fills the entire duct . From this point on , the velocity profile across the duct remains essentially unchanged, the flow is then said to be fully developed, section (2). The distance from the entrance at which this condition achieved and termed the hydrodynamic entry length (L_e)as shown in figure (1-1).

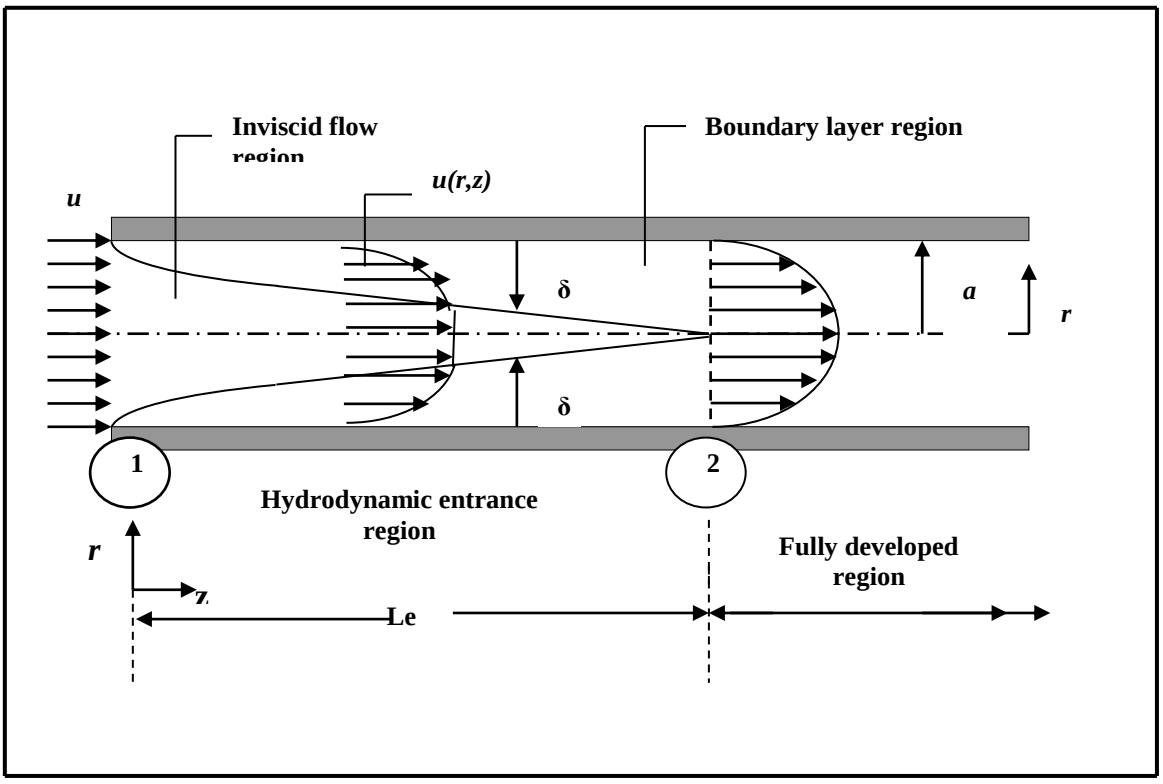

Figure (1-1) hydrodynamic boundary layer development in a heated circular tube as depicted in Ref. [2].

The fully developed velocity profile is parabolic for laminar flow in a circular tube. For turbulent flow, the profile is flatter due to turbulent mixing in the radial direction [2].

For laminar flow in a circular tube (Re ≤ 2300) the hydrodynamic entry length at which the velocity profile approaches its fully developed shape can be obtained from the relation [3] :

$$\frac{L_e}{d} = 0.05\,\mathrm{Re} \qquad \ldots.(1.1)$$

Lien [5] showed that the relationship for entrance length for turbulent flow is:

$$\frac{L_e}{d} \cong 4.4\,Re^{\frac{1}{6}} \qquad \ldots.(1.2)$$

Once the fluid reaches the end of the entrance region , section (2) of figure (1-1), the flow is simpler to describe because the velocity is a function of only the distance from the pipe centerline, r, and independent of z [2].

An important feature of hydrodynamic conditions in the fully developed region is that :

$$v = 0 \qquad \ldots.(1.3)$$

and

$$\frac{\partial u}{\partial z} = 0 \qquad \ldots.(1.4)$$

Hence, the axial velocity component depends only on r , $u(z,r) = u(r)$ [2].

1.3. Thermal Boundary Layer

If fluid enters the tube of figure (1-2) at a uniform temperature $T(r,0)$ that is less than the surface temperature, convection heat transfer occurs and a thermal boundary layer begins to develop. Moreover, if the tube surface condition is fixed by imposing either a uniform temperature (T is constant) or a uniform heat flux (q'' is constant), a thermal fully developed condition is eventually reached.

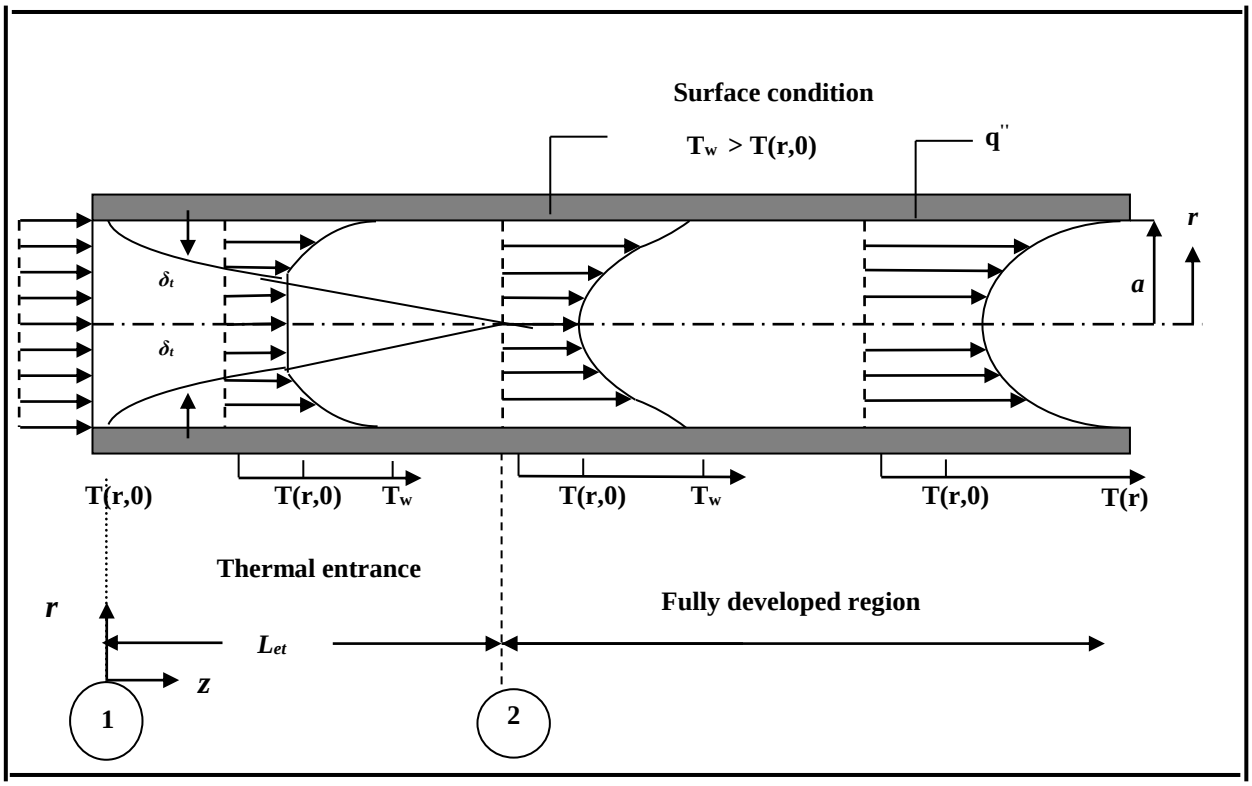

Figure (1-2) thermal boundary layer development in a heated circular tube as depicted in. Ref. [2].

The shape of the fully developed temperature profile $T(r,z)$ differs according to whether a uniform surface temperature or heat flux is maintained. For both surface conditions, however, the amount by which fluid temperatures exceed the entrance temperature increases with increasing z, Ref [2].

For laminar flow, reference [3] showed that the thermal entry length may be expressed as :

$$\frac{L_{et}}{d} = 0.05\,\mathrm{Re}\,.\,\mathrm{Pr} \qquad \text{....(1.5)}$$

Since the existence of convection heat transfer between the surface and the fluid dictates that the fluid temperature must continue to change with z, one might legitimately question whether fully developed thermal conditions can ever be reached. The situation is certainly different from the hydrodynamic case, for which $\left(\frac{\partial u}{\partial z} = 0\right)$ in the fully developed region. In contrast, if there is heat

transfer $\left(\frac{\partial T_b}{\partial z}\right)$, as well as $\left(\frac{\partial T}{\partial z}\right)$ at any radius r, is not zero. Accordingly, the temperature profile T(r) is continuously changing with z, and it would seem that a fully developed condition could never be reached. This apparent contradiction may be reconciled by working with a dimensionless form of the temperature [2].

Analyses have often been simplified by working with dimensionless temperature differences, as for transient conduction and the energy conservation equation. Introducing a dimensionless temperature difference of the form $(T_w - T)/(T_w - T_b)$, conditions for which this ratio becomes independent of z are known to exist. Although the temperature profile T(r) continues to change with z, the relative shape of the profile no longer changes and the flow is said to be thermally fully developed. The requirement for such a condition is formally stated as:

$$\frac{\partial}{\partial z}\left[\frac{T_w(z) - T(r,z)}{T_w(z) - T_b(z)}\right] = 0 \qquad \ldots.(1.6)$$

where T_w, is the tube wall temperature, T is the local fluid temperature, and T_b is the bulk (mean) temperature of the fluid over the cross section of the tube [1]. The Prandtl number is a nondimensional group of fluid transport properties :

$$\mathrm{Pr} = \frac{\mu . C_p}{K} \qquad \ldots.(1.7)$$

If the numerator and denominator are multiplied by density ,the Prandtl number can be written as :

$$\mathrm{Pr} = \frac{\nu}{\alpha} = \text{ kinematics viscosity / thermal diffusivity} \qquad \ldots.(1.8)$$

The kinematics viscosity is the diffusivity for momentum ,or for velocity ,in the same sense that the thermal diffusivity is the diffusivity for heat , or for temperature .(Diffusivity is defined as the rate at which a particular effects is diffused through the medium).

If the Prandtl number is 1,then heat and momentum are diffused through the fluid at the same rates ; if the velocity and temperature are both uniform at the entrance to a tube , the velocity and temperature profiles develop together .

If (Pr > 1), the hydrodynamic boundary layer develops more rapidly than the thermal boundary layer ($L_e < L_{et}$), while the inverse is true for (Pr < 1) ,that was shown in reference [1].

The Prandtl number for any particular fluid generally varies somewhat with temperature , but only over a limited range .due to the wide range of applications, fluid prandtl numbers usually vary between (0.01 < Pr < 1000) which covers a wide range of liquid metals , encompassing gases, water ,light organic liquids and highly viscous liquids such as automotive oils.

1.4. Objective of the Present Work

In the present work, developing steady laminar flow and heat transfer in the entrance region through circular tube will be studied within two parts: The first part represents a theoretical study which deals with the developing steady, laminar, Newtonian and incompressible fluid flow and heat transfer through circular tube .The effects of heat conduction, body force, free convection, heat generation and viscous dissipation within the fluid are neglected.

The second part presents an experimental work which has been done to measure the pressure drop by using U- tube Manometer at the entrance region of laminar water flow through circular tube of (L =6.35 m , d=3.125 cm) for different values of Reynolds number ,also the pressure drop at the fully developed region at a range of Reynolds numbers within laminar and turbulent flow.

Literature Review

Many fundamental studies of the flow in straight ducts can be found. The researchers in these studies emphasis on the velocity and temperature fields, hydraulic parameters such as Nusselt number and Reynolds number.

The analysis of hydrodymically developing laminar flows inside ducts of cylindrical geometry has been a subject of great interest as demonstrated by the currently literature , mainly to the interest in flows within circular ducts.

2.1. Theoretical Analysis

Moller [6] presented Nusselt number data in laminar flow for conditions of either uniform wall temperature or uniform heat flux in fully-developed flow. Flow that was thermally-developing (where the heated section was preceded by an isothermal length exceeding the hydrodynamic entry length), and flow that was developing simultaneously both thermally and hydrodynamically. The effect of variable fluid properties was considered and a correction for radial viscosity variation in liquids was recommended, but no correction was felt necessary for gases, following an assessment of the available data. For mixed convection conditions only a uniform wall temperature condition was considered. Nusselt number data were given for buoyancy-assisted flow in vertical tubes (heated up flow and cooled down flow) and for buoyancy-opposed flow. Data were also provided for flow in horizontal tubes. The ranges of conditions for which the recommended correlations have been tested were tabulated for the mixed convection conditions.

Schmidt and **Zeldin [7]** investigated numerically the case for the evaluation of the rate of heat transfer in the thermal entrance region of ducts with axial conduction. The velocity profile was fully developed and flow in a tube and between parallel plates was studied. Local and average Nusselt numbers and mixing temperatures were presented as a function of the peclet number. A criterion was also established which proves usefulness for predicting the conditions under which axial conduction may be ignored.

Coney and **El-shaarawi [8]** showed the laminar heat transfer in entrance region of concentric annuli with rotating inner walls. They obtained a numerical solution of the boundary-layer equations representing laminar flow with constant physical properties for that region .They showed the extent to which the rotation of the inner cylinder affects the entrance region laminar flow of heat transfer .The speeds of rotation of the inner cylinder are lower than the critical speed at which the Taylor voracities are generated. They concluded that the boundary layer near the wall is warmer than the wall itself owing to the heat generation that resulted from friction force, hence, relative velocities was very large.

Emery and **Gessner [9]** computed the velocity and temperature profiles for turbulent flow, both in the entrance region and the fully developed state in a duct with heated parallel plates. They started the calculations at the duct inlet and used a finite difference technique and a three- dimensional mixing length originally defined for corner flows. It was possible to predict axial flow behavior and the non-asymptotic approach to fully developed flow with and without associated heat transfer. The used boundary conditions were **(**$u(0,y)=u_{in}$**,** $u(x,0)=0$**,** $v(x,0)=0$ for $x \geq 0$).

Render [10] behavior of laminar, incompressible flow in the entrance region of a tube under the influence of sinusoidal velocity pulsations superposed on a mean through flow was studied. The resultant flow characteristics and wall heat transfer rates were studied for the range of conditions over which no flow reversal takes place. A numerical computation technique has been developed which solves the unsteady momentum an energy equations in an explicit fashion, eliminating iteration. The solution program permits a tube wall temperature which varies with axial distance and temperature-dependent fluid viscosity. Key elements in the solution technique are a coordinate transformation to a system involving the stream function as a radial dimension, integration of the governing differential equations over a control volume to yield difference equations. Assumptions concerning variation of unknowns to eliminate matrix inversion or iteration, and determination of the local, time-dependent longitudinal pressure gradient from local flow phenomena.

Kuehn and **Goldstein [11]** described the effect of the Prandtl number and the diameter ratio over the range needed for more applications on the heat transfer between annuli. A parametric study took into consideration the Prandtl number and diameter ratio are each varied over several orders of magnitudes ($0.001< Pr < 1000$, $1.0 < D_o/D_i < \infty$). They determined their influences on the natural convection flow and local/and mean heat transfer in horizontal annuli. From their study, they concluded that as the Prandtl number increase above 1.0, the dimensionless velocities become invariant.

Ching and **Jenq [12]** studied laminar and turbulent heat transfer in pipe flow for liquid metals. Three flow regions, namely fully-developed, developing thermal, and developing thermal and velocity regions were considered. The Van Driest mixing length hypothesis was adapted to model the turbulent shear stress.

The thermal damping constant was redetermined in the study for the fully-developed region as well as other developing regions. Correlation for heat transfer calculation was given for boundary conditions at Constant Heat Flux and Constant Wall Temperature. The effect of the variation of physical properties was also studied. Coefficient of heat transfer calculation when the property is variable was given in a simple form of a liquid sodium eutectic

Al-Ali [13], a new integral method of solution for the combined hydrodynamic and thermal-entrance-region problem for laminar flow through parallel-plate channels and circular tubes, was developed. The new analysis adapts the hydrodynamic inlet-filled region to the thermal entry length problem. A new thermal-transition region, called the thermally-filled region, was introduced between the thermal inlet boundary-layer region and the fully developed region. A thermal shape factor for the thermally-filled region was properly defined. This factor guaranteed smooth transition of all pertinent thermal quantities from the inlet boundary-layer region to the fully developed region. With the new model, the velocity and temperature profiles, the skin friction factors, and the local Nusselt numbers approached their corresponding fully developed conditions asymptotically. Solutions were obtained for the combined entry length problem for laminar flow through circular tubes and parallel-plate channels for the constant wall temperature and constant wall heat flux boundary conditions. Results for variation of the local Nusselt number with axial distance agreed well with numerical solutions.

Uysal and **Sozbir [14]** investigated numerically the transient laminar forced convection inlet with hydrodynamical developed and thermally developing air flow . A numerical study of unsteady laminar forced convection of the inlet temperature was presented .Numerical solution for the parabolic velocity profile

was obtained under the boundary condition of the fifth kind which is verified with a range of Reynolds number . A second order accurate explicit finite difference scheme , numerical results were obtained with the fully developed parabolic velocity profile under the boundary experiments .

Alan Brigg [15] studied the heat transfer behavior associated with a thermal transient in a forced convection. the effects of the duct wall heat capacity and convection from the ambient were considered, while axial conduction was neglected. The fluid inlet temperature was varied periodically with time. Incompressible, hydrodynamically developed laminar flow of non-Newtonian fluid flow was assumed. The transient conjugate heat transfer problem for fully-developed laminar flow of non-Newtonian fluids in circular duct was studied by numerical analysis. Control volume based finite difference method was adopted in the numerical procedure for the integration of the governing equations. For the non-Newtonian fluid part, power-law model was used. Heat generation from viscous dissipation was also taken into account and was represented by Brinkman number. The study investigated the effects of non-dimensional parameters on wall, fluid and bulk temperatures. In this dissertation, special focus was placed on the effects of the flow index, Brinkman, and Nusselt numbers.

Bigyani Das [16] showed the steady, laminar, isothermal entrance region flow of the Hershel–Bulkley fluid in a tube by using the momentum integral and the momentum energy integral techniques. The resulting nonlinear ordinary differential equations on the dimensionless boundary layer thickness were solved numerically by using the Runge–Kutta method. The results for the plug core velocity, boundary layer thickness, pressure drop, entrance length and loss coefficient were obtained for a wide range of yield numbers and the flow behavior index. Significant effect of viscous dissipation was observed on the velocity

distribution and boundary layer growth, whereas the effect of viscous dissipation on pressure drop was negligible. In both the methods, the values of entrance length and loss coefficient were found to be reduced with increasing values of Hershel–Bulkley number and flow behavior index. However, in the case of the momentum energy integral method the values of entrance length and loss coefficient were appreciably higher than those obtained by using the momentum integral method.

Zhao and **Cheng [17],** a numerical investigation **,** has been carried out for a laminar incompressible reciprocating flow in a circular pipe with a finite length . An examination of the governing equation and boundary conditions indicates that a sinusoidally reciprocating flow is governed by three similarity parameters: the kinetic Reynolds number Re_{ω} **,**the dimensionless oscillation amplitude A_o **,**and the length to diameter ratio L/D. The numerical solution for the velocity profiles of a developing reciprocating flow shows that at any instant of times , there exist three flow regimes in the pipe , namely , an entrance regime ,a fully–developed regime and an exit regime. The numerical results for the fully–developed region are shown to be in excellent agreement with the analytical solution .Based on the numerical results ,a correlation equation of the space-cycle averaged friction coefficient for a laminar developing reciprocating pipe flow has been obtained in terms of the three similarity parameters.

Cuccuruiio and **Beradi [18]** illustrated the simultaneously developing of velocity and temperature profiles in the entrance pipe flow. the flow was assumed to be steady state for a non- Newtonian fluid in incompressible laminar pipe flow ,the fluid behavior was assumed to follow the Ostwald- Dewaele power law model .The developing velocity and temperature profiles were solved by the integral method. Results were presented and discussed in terms of axial and radial

velocity profiles, Fanning friction factors and Nusselt numbers for different fluid properties and thermal boundary condition.

Benhamou and **Laneville [19]** modeled numerically the transient developing laminar flow of a Newtonian incompressible fluid in a straight horizontal pipe oscillating around the vertical diameter at its entrance. The impulsive start of the latter generates a transient pulsating flow, whose duration increases with the axial distance. In any cross-section, this flow consists of a pair of symmetrical counter-rotating vortices which are alternatively clockwise and anti-clockwise. The circumferentially averaged friction factor and the axial pressure gradient fluctuate with time and are always larger than the corresponding values for a stationary pipe. On the other hand, local axial velocities and local wall shear stress can be smaller than the corresponding stationary pipe values during some part of the pipe oscillation. The fluctuation amplitude of these local variables increases with the axial distance and can be as high as 50% of the corresponding stationary pipe value, even at short distances from the pipe entrance. Eventually, the flow field reaches a periodic regime that depends only on the axial position. The results show that the transient flow field depends on the pipe oscillation pattern (initial position and/or direction of initial movement).

Shariff and **Greywall [20]** studied a new algorithm to compute paralyzed axisymmetric flows with heat transfer. These computations require using χ, distance along the centerline of the duct, and ξ, the stream function, as the independent variables. The dependent variables used are $\mathbf{U(\chi,\xi)}$, the streamwise velocity, $\mathbf{T(\chi,\xi)}$, the temperature, and $\mathbf{R(\chi,\xi)}$, the cross-stream coordinate of the stream surface ξ. Sample computations were carried out for the flow of the standard air, through a pipe of constant diameter, with a hydrodynamically fully

developed flow condition at the entrance. Results of the computations are in a close agreement with the available analytical results.

Barber and Emerson [21] computed the effects of the Reynolds number on the hydrodynamic development lengths in circular and parallel plate ducts. The study was conducted using a two- dimensional finite-volume Navier-Stokes solver developed by the Computational Engineering Group at CLRC Daresbury Laboratory. The solver was specifically adapted for the simulation of non-continuum flows by the inclusion of appropriate tangential slip-velocity boundary conditions at the solid perimeter walls. However, in the case of the parallel plate geometry, entrance development lengths in the slip-flow regime are approximately 25% longer than the corresponding continuum solution.

Patnaik and **Gowda [22]** investigated enumerates finite-element based prediction of internal flow problems with heat transfer. The present numerical simulations employ a velocity correction algorithm, with a Galerkin weighted residual formulation. Two problems each in laminar and turbulent flow regimes were investigated, by solving full Navier-Stokes equations. Flow over a backward-facing step was studied with extensive validations. The effect of wall conductivity in turbulent heat transfer was also studied by performing a conjugate analysis. Temporal evolution of flow in a channel due to circular, square and elliptic obstructions was investigated to simulate the vortex dynamics. Flow past an in-line tube bank of a heat exchanger shell was numerically studied. Resulting heat and fluid flow patterns were analyzed. Important design parameters of interest such as the Nusselt number, skin friction coefficient, pressure drop etc. were obtained. It was successfully demonstrated that the velocity correction approach with a Galerkin weighted residual formulation was able to effectively simulate a wide range of fluid flow features.

Viana, Nascimento, Quaresma and **Macedo [23]**, related momentum and energy equations describing the heat and fluid flow of Herschel-Bulkley fluids within concentric annular ducts, were analytically solved using the classical integral transform technique. They permit accurate determination of parameters of practical interest in engineering such as friction factors and Nusselt numbers for the duct length. In analyzing the problem, thermally developing flow was assumed and the duct walls were subjected to boundary conditions of first kind. Results were computed for the velocity and temperature fields as well as for the parameters cited above with different power-law indices, yield numbers and aspect ratios.

Tien-Chien ,Sunil ,and Guang-Jyh [24], a numerical study was conducted on laminar flow of an incompressible viscous fluid through a triangular channel in the hydrodynamically fully developed flow region .The triangular channel was subjected to a span –wise rotation ,and secondary flow motions were introduced by the Coriolis forces. A pair of counter –rotating ,longitudinal vortices appears at low rotation speed (small $\mathrm{Re}\,\mathrm{Re}_{\Omega}$). For moderate to large rotation speed ,the vortices split into two pairs of counter –rotating vortices .In certain region ,the counter – rotating vortices become highly unstable ,oscillating between two solutions ,i.e., one pair vortices and two pair vortices. Isosceles triangular channels with three aspect ratios ($\gamma = 0.287, 0.5, 0.866$) had been studied . A large rang of ($\mathrm{Re}\,\mathrm{Re}_{\Omega}$) and R_o(Rossby) numbers was calculated. The critical Reynolds number with respect to Rossby number , where the flow instability occurs , was calculated and the dual solution region presented . The results obtained from the computations cover a broad range of parameters ,especially from low rotational speed to high rotational speed .The friction factor ,velocity profile ,and streamline patterns were

presented . A comparison of the numerical results with the available theoretical data was also presented.

Maia and **Gasparetto [25]** incompressible, isothermal, laminar and steady flow of a power-law fluid in a, concentric annulus, were solved by a finite difference implicit method. The Newtonian case was solved used for validation of the method and then compared to reported results. For the non-Newtonian case a pseudo plastic power-law model was assumed and the equations were transformed to obtain a pseudo-Newtonian system which enabled its solution using the same technique as that used for the Newtonian case.

Iyad Al-Zaharnah [26], heat transfer and entropy analysis for flow through a pipe system was considered. The Reynolds number and the pipe wall temperature effects on entropy distribution and total entropy generation in the pipe were investigated. Numerical scheme employing a control volume approach was introduced when solving the governing equations. Steel was selected as pipe material, while water was used as fluid. It was found that increasing pipe wall temperature and Reynolds number increases the entropy production rate, in which case, entropy generation due to heat transfer dominates over that corresponding to fluid friction.

Ercan and **Yalcin [27]** investigated the two dimensional numerical analysis of entropy generation during transient convective heat transfer for laminar flow between two parallel plate. The fluid was incompressible and Newtonian and the flow was the hydrodynamically and thermally developing. The plates were held at constant equal temperatures higher than that of the fluid. The bottom plate moves in either parallel or in inverse direction to the flow. The governing equations of the transient convective heat transfer were written in two-dimensional Cartesian coordinates and solved by the finite volume numbers of 102 and 103 and

Prandtl number equal to one. After the flow field and the temperature method with simple algorithm. The solutions were carried for Reynolds distributions were obtained, the entropy values and the sites initiating the entropy generation were investigated. The lowest average number of the entropy generation on the bottom plate was obtained in parallel motion. The corners of the channel plates at the entrance play the role of active sites where the generation of entropy was triggered.

Ahmet and **Rached [28]** computed the numerical solution to the entropy generation in a circular pipe. Radial and axial variations were considered. Navier-Stokes equations in cylindrical coordinates were used to solve the velocity and temperature fields. Uniform wall heat flux was considered as the thermal boundary condition. The distribution of the entropy generation rate was investigated throughout the volume of the fluid as it flows through the pipe. Engine oil was selected as the working fluid. In addition, water and Freon were used in a parametric study. The total entropy generation rate was calculated by integration over the various cross-sections as well as over the entire volume.

Mzychka and **Yovanovich [29]** developed a new model for predicting Nusselt numbers in the combined entrance region of non – circular ducts and channels .This model predicts both local and average Nusselt numbers and was valid for both isothermal and isoflux boundary conditions .The model was developed using the asymptotic results for convection from a flat plate, thermally developing flows in non- circular ducts , and fully developed flow in non – circular ducts .Through the use of a novel characteristic length scale ,the square root of cross- sectional area, the effect of duct shape on Nusselt number was minimized. Comparisons were made with several existing models for the circular tube and parallel plate channel and with numerical date for several non – circular ducts .

Oyumi, S.M. [30] studied The continuity equation and the simplified version of the time dependent boundary layer momentum and energy equations simultaneously for flow between two parallel plates, used an explicit numerical procedure. Solved the three equations simultaneously eliminates the need to assume the shape of the velocity and temperature profiles. Furthermore, this approach provides a picture of the variation of the velocity and temperature within the entire channel. The steady-state solution is obtained by letting time become very large. The shape of the velocity and temperature profiles seem to be consistent with theoretical expectations.

Ibrahim [31] investigated numerically the developing turbulent flow and heat transfer through rectangular and circular duct . The study includes the numerical solution of the continuity, momentum, and energy equations together with the two equations of the (k-ε) turbulence model. The clustering of the grid in the radial direction near walls for each duct was used in the numerical solution. The results showed that, thermal entry length lies between, x/D(1.4 to 1.6) for the two ducts which means that the development of thermal boundary layer was so fast because the very high heat transfer coefficients which were resulted from very high velocities near walls and very small selected dimensions of each duct. The very high velocities near walls may result from the use of the wall function with a very small size of spacing between the clustered nodal points especially near walls.

Shaker[32] developed laminar flow of a Newtonian incompressible fluid and heat transfer in the entrance region of a two parallel plate channel were investigated. The continuity, x-momentum, and energy equations were solved as a steady state in two dimension equations. The dimensionless technique was used. These equations have been represented by finite difference technique. The study

was made for two case of heating : constant wall temperature and constant heat flux respectively**.**

Shirely and **Joao [33],** the generalized integral transform technique (GITT) was applied to the solution of the momentum equation in a hydrodynamically developing laminar flow of a non-Newtonian power-law fluid inside a circular ducts. A primitive variables formulation was adopted in order to avoid the singularity of the auxiliary eigen value problem in term of Bessel functions at the centerline of the duct when the GITT approach was applied. Results for the velocity field and friction factor ,Reynolds number product were computed for different power –law indices. They were tabulated and graphically presented as functions of the dimensionless coordinates.

2.2. Experimental Work

Babus'haq [34] studied the local heat transfer characteristics for air flowing turbulently inside a smooth heat transfer pipe of 29.1mm inside diameter and length equal to 179.1cm . (x/D=61.5) have been determined experimentally over a range of Reynolds numbers from 12000 to 56000. A wall boundary heating condition of uniform heat flux was imposed. The entrance configurations investigated was included a long calming section (x/D=69) and four short calming sections (x/D=50, 30 and 15) for which previous data are limited.

Goswami [35] analyzed velocity profiles for flow through circular tubes in laminar, turbulent, and transition region flows and how they affect measurement by flow meters. Experimental measurements of velocity profiles across the cross-section of straight circular tubes were made using laser Doppler velocimetry. In addition, flow visualization was done using the hydrogen bubble technique. Velocity profiles in the laminar and the turbulent flow were quite predictable

which allow the determination of meter factors for accurate flow measurement. However, the profiles can not be predicted at all in the transition region. Therefore, for the accuracy of the flow meter, it must be ensured that the flow was completely in the laminar regime or completely in the turbulent regime. In the laminar flow a bend, even at a large distance, affects the meter factor.

Nikuardse [36] conducted experiments with water in circular pipes to study the laminar and turbulent regions , covering Reynolds number from 600 to 1000,000 .The inner diameter of the pipes were (25 , 50 and 100 mm) .The pressure drop was measured at several intermediate location using pressure probes of 2mm outside diameter that extended to the center of the pipe. The laminar region of the experiments conducted was toward the lower Reynolds range of this experiment. The flow measurement does not seem to be influenced by this measurement techniques. It is estimated that the uncertainty to the flow measurement is quite low. The turbulent transition also investigated through direct flow visualization .

Fall [37] conducted experiments with the use of the (TQ H16) system "Losses in Piping Systems" apparatus. It requires a controlled water flow rate, which will be provided by the weight tank apparatus (TQ H1). By running water through the piping system on the apparatus at a known flow rate. The pressure losses for flow through the 15.7 mm and 32.4 mm diameter straight sections of pipe were measured using U–tube manometer for a large enough range of the Reynolds number to cover laminar, transitional, and turbulent regimes. The suggested upper limit of the Reynolds number was 15000**.**

2.3. Summary

It has been shown from the previous researches reported here, that mainly study concentrate on laminar or turbulent fluids flow and heat transfer through different geometrical shape such as rectangular duct ,triangular ,two parallel plat channel , concentric annulus and circular pipe by using different method like similarity, two dimensional finite volume Navier –Stokes equations, integral transform technique (GITT) and others. These studied covered either entrance region or fully developed region or both.

More progress is needed in new technique which presented in the present work ,where in its theoretical part the hydrodynamic and thermal boundary layer are considered to develop simultaneously, where this consideration is achieved by assuming uniform velocity and temperature profile at entrance of circular tube. Also an experimental work has been done to measure the pressure drop at the entrance region of laminar water flow through circular tube for different values of Reynolds number .Also the pressure drop at the fully developed region for a range of Reynolds number within both laminar and turbulent flow.

Mathematical Model and Numerical Solution

3.1. Introduction

Theoretical analysis was presented for the partial differential equations which described the developing laminar fluid flow and heat transfer through circular tube, assuming incompressible and constant property flow for developing velocity and temperature profile through the circular tube.

The model usually assumed for the entrance flow in a circular tube was the boundary layer model near the tube walls with a potential core toward the center of the tube which accelerates as the boundary layer grows. This model does an adequate job in most respects, it is questionable only near the tube inlet where transverse momentum effects are important and hence the boundary layer model breaks down. In the core region viscous effects may actually be present. One other aspect of this type of model is that the velocity distribution at the inlet of the tube is assumed to be uniform.

3.2. Mathematical Analysis

3.2.1. Assumptions and Governing Equations

The following study deals with developing laminar fluid flow and heat transfer through a circular tube. This study will be achieved for two cases, constant wall temperature and constant heat flux respectively. Figure (3-1) represents the laminar flow mechanism through pipe, and the coordinate system for the flow.

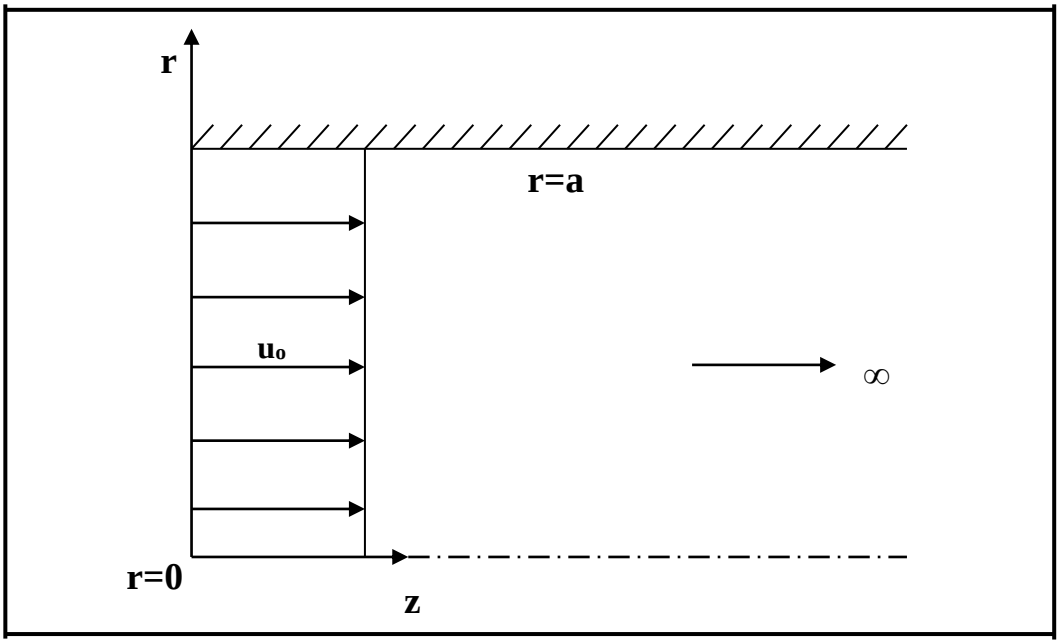

Figure (3-1) Schematic diagram of the problem, Ref.[38].

For two dimensional developing, steady state, incompressible laminar flow in a circular tube the effects of heat conduction, body force, free convection, heat generation and viscous dissipation within the fluid were neglected.

The equations of motion (mentioned by Hornbeck [38] and Adems [39]) were assumed to be :

Continuity equation

$$r\frac{\partial(\rho.u)}{\partial z}+\frac{\partial(\rho\cdot v\cdot r)}{\partial r}=0 \qquad \ldots.(3.1)$$

For incompressible flow , $\rho = constant$,and the continuity equation reduces

$$r\frac{\partial u}{\partial z}+\frac{\partial(v.r)}{\partial r}=0 \qquad \ldots.(3.2)$$

z-Momentum equation

$$\rho.u\frac{\partial u}{\partial z}+\rho.v\frac{\partial u}{\partial r}=-\frac{dp}{dz}+\mu.\left(\frac{\partial^2 u}{\partial r^2}+\frac{1}{r}\frac{\partial u}{\partial r}\right) \qquad \ldots(3.3)$$

For constant dynamic viscosity ,equation (3.3) becomes :

$$u\frac{\partial u}{\partial z}+v\frac{\partial u}{\partial r}=-\frac{1}{\rho}\frac{dp}{dz}+\nu\left(\frac{\partial^2 u}{\partial r^2}+\frac{1}{r}\frac{\partial u}{\partial r}\right) \quad \ldots.(3.4)$$

The term $\left(\frac{1}{r^2}\frac{\partial^2 u}{\partial \theta^2}\right)=0$ due to symmetry.

Equation (3.4) is the z-component of momentum equation for a steady, two dimensional, laminar, constant-property boundary-layer flow of a Newtonian fluid in forced convection. The two terms on the left hand side are the nonlinear convection terms. The two terms on the right hand side arise from inertial forces and viscous shearing forces, respectively.

Adems and Rogers [39] Assumed that $\partial v/\partial z << \partial u/\partial z$ and $\partial v/\partial r << \partial u/\partial r$, then the r –component of the momentum equation reduces as :

$$\frac{dp}{dr}=0 \quad \ldots.(3.5)$$

The energy equation for incompressible, constant property flow was uncoupled from the momentum equation once the velocity distribution was known. When viscous dissipation is neglected, the energy equation may be written as:

Energy equation

$$u\frac{\partial T}{\partial z}+v\frac{\partial T}{\partial r}=\alpha\left(\frac{\partial^2 T}{\partial r^2}+\frac{1}{r}\frac{\partial T}{\partial r}\right) \quad \ldots.(3.6)$$

The two most commonly considered thermal boundary conditions for confined flows were constant wall temperature and constant wall heat flux per unit length in the flow direction. Both of these conditions were considered in this formulation.

The solution to the energy equation, for the entry region was more difficult to obtain, since velocity and temperature now depend on (z) as well as (r). The simplest solution for the thermal entry length problem was based on assuming that thermal conditions were developed in the presence of a fully developed velocity profile .

3.2.2. Boundary Conditions

The requirement that the dependent variable or its derivative must be satisfied on the boundary of the partial differential equation was called the boundary condition. The boundary conditions represented the statements of physical facts at specified values of the independent variable. Any fluid moves over a surface whose temperature differs from it, will lead to transfer of heat by convection. Hence, the thermal and hydrodynamic boundary layer considerations will be encountered. These considerations should be precisely treated especially when laminar boundary layer was faced. In order to achieve this purpose, suitable boundary conditions should be applied on the selected problem. Therefore, reference [38] showed that the boundary conditions according to the geometry will be written as follows:

3.2.2.1. Entrance Region Boundary Conditions

Uniform temperature and velocity profile at the entrance region of circular tube was assumed. All entrance boundary conditions can be written as follows:

$$\left.\begin{aligned} u(r,0) &= u_o \\ p(0) &= p_o \\ T(r,0) &= T_o \end{aligned}\right\} \quad \ldots.(3.7)$$

Note: $u(r,0) = u_0$(Assumed constant here, although a function of (r) was also permissible).

3.2.2.2. Wall Boundary Conditions

All velocity components are zero at the walls, hence:-

$$\left.\begin{aligned} u(a,z) &= 0 \\ v(a,z) &= 0 \end{aligned}\right\} \quad \ldots.(3.8)$$

A number of temperature boundary conditions at the wall are possible. Two commonly employed conditions will be considered here constant wall

temperature or constant wall heat flux. The complete boundary conditions for the problem are :-

$$T(a,z) = T_w \quad (\textit{constant wall temperature}) \qquad \ldots.(3.9)$$

$$-k\frac{\partial T}{\partial r}(a,z) = q'' \quad (\textit{constant wall heat flux}) \qquad \ldots.(3.10)$$

Where

$$q'' = \frac{q}{A}$$

3.2.2.3. Centerline of Tube Boundary Conditions

At centerline of tube the boundary conditions are:

$$\left.\begin{aligned} &\frac{\partial u}{\partial r}(0,z) = 0 \\ &v(0,z) = 0 \\ &\frac{\partial T}{\partial r}(0,z) = 0 \end{aligned}\right\} \qquad \ldots.(3.11)$$

3.2.3. Dimensionless Variables

Before undertaking a numerical solution, the first step should invariably place the equations to be solved in a dimensionless form having as few parameters as possible. This may be accomplished for equations (3.2), (3.4) and (3.6) by employing the following dimensionless variables :

$$\left.\begin{aligned} U &= \frac{u}{u_o} \\ V &= \frac{v}{u_o} \\ R &= \frac{r}{a} \\ Z &= \frac{z}{a} \\ P &= \frac{p_o - p}{\rho . u_0^2} \end{aligned}\right\} \qquad \ldots.(3.12)$$

where the characteristic velocity (u_o) will usually be chosen as the upstream velocity from the body, and a typical length (a) is the radius of the circular tube .

The choice of the dimensionless temperature variable was dependent on the thermal boundary condition which was to be considered. The remaining dimensionless variables were the same for both boundary conditions. The dimensionless variables chosen were :

For the constant wall temperature, the thermal boundary condition will be:

$$\theta = \frac{T - T_w}{T_o - T_w} \qquad \text{….(3.13)}$$

For the constant wall heat flux, the thermal boundary condition will be:

$$\theta = \frac{k}{q'' a}\left(T - T_o\right) \qquad \text{….(3.14)}$$

The following dimensionless quantities will be used in the present work:

Reynolds number :

$$\mathrm{Re} = \frac{\rho . u_o . d}{\mu} \qquad \text{….(3.15)}$$

Prandtl number:

$$\mathrm{Pr} = \frac{c_p \mu}{k} = \frac{\nu}{\alpha} \qquad \text{….(3.16)}$$

Nusselt number:

$$Nu = \frac{h.d}{k} \qquad \text{….(3.17)}$$

Where d is the diameter of the tube.

3.2.4. Dimensionless Boundary Conditions

The boundary conditions may be put in dimensionless form by the choice of the dimensionless variables (3.12), (3.13) and (3.14):

3.2.4.1. Entrance Region Dimensionless Boundary Conditions

Uniform temperature and velocity profile at the entrance region of the circular tube is assumed. All entrance boundary conditions was shown by Ref . [38] and can be written as:

$$\left.\begin{aligned} U(R,0)&=1\\ P(0)&=0 \end{aligned}\right\} \quad \text{….(3.18)}$$

For the constant wall temperature, the thermal boundary condition will be:

$$\theta(R,0)=1 \quad \text{….(3.19)}$$

For the constant wall heat flux, the thermal boundary condition will be:

$$\theta(R,0)=0 \quad \text{….(3.20)}$$

3.2.4.2. Wall Dimensionless Boundary Conditions

All dimensionless velocity components are zero at walls, hence:

$$\left.\begin{aligned} U(1,Z)&=0\\ V(1,Z)&=0 \end{aligned}\right\} \quad \text{….(3.21)}$$

A number of dimensionless temperature boundary conditions at the wall are possible:

For the constant wall temperature, the thermal boundary condition will be:

$$\theta(1,Z)=0 \quad \text{….(3.22)}$$

For the constant wall heat flux, the thermal boundary condition will be:

$$\frac{\partial\theta}{\partial R}(1,Z)=1 \quad \text{….(3.23)}$$

3.2.4.3. Centerline of Tube Dimensionless Boundary Conditions

At centerline of the tube, the dimensionless boundary conditions are:

$$\left.\begin{aligned} \frac{\partial U}{\partial R}(0,Z)&=0\\ V(0,Z)&=0\\ \frac{\partial\theta}{\partial R}(0,Z)&=0 \end{aligned}\right\} \quad \text{….(3.24)}$$

3.2.5. Dimensionless Governing Equations

The dimensionless form is often more convenient to express the equations where each term is dimensionless. It is developed to simplify the solution of many engineering problems and to avoid large quantities in calculation.

The continuity equation may be put in dimensionless form by substituting the dimensionless variables as shown in (3.12)in equation (3.2) as:

$$R.a\frac{\partial(U u_0)}{\partial(Z.a)}+\frac{\partial(V u_0.R.a)}{\partial(R.a)}=0 \qquad \ldots.(3.25)$$

where (u_o) and (a) are constant:

$$\left(\frac{u_0.a}{a}\right)R\frac{\partial U}{\partial Z}+\left(\frac{u_0.a}{a}\right)\frac{\partial(V.R)}{\partial R}=0 \qquad \ldots.(3.26)$$

Now divide equation (3.26) by u_0:

Continuity equation

$$R\frac{\partial U}{\partial Z}+\frac{\partial(V.R)}{\partial R}=0 \qquad \ldots.(3.27)$$

The z-momentum equation may be put in dimensionless form by substituting the dimensionless variables in (3.12) and (3.15) in equation (3.4):

$$Uu_0\frac{\partial(U.u_0)}{\partial(Z.a)}+Vu_0\frac{\partial(U.u_0)}{\partial(R..a)}=-\frac{1}{\rho}\frac{\partial(P\rho.u_0^2)}{\partial(Z.a)}+\frac{\mu}{\rho}\frac{\partial^2(U.u_0)}{(\partial(R.a))^2}+\frac{1}{R.a}\frac{\partial(U.u_0)}{\partial(R.a)} \qquad \ldots.(3.28)$$

where (u_o),(a) and (ρ) are constant:

$$U\frac{\partial U}{\partial Z}\left[\frac{u_0^2}{a}\right]+V\frac{\partial U}{\partial R}\left[\frac{u_0^2}{a}\right]=-\frac{\partial P}{\partial Z}\left[\frac{\rho.u_0^2}{\rho.a}\right]+\nu\left[\left(\left(\frac{u_0}{a^2}\right).\frac{\partial^2 U}{\partial R^2}+\left(\frac{u_0}{a^2}\right).\frac{1}{R}\frac{\partial U}{\partial R}\right)\right] \qquad \ldots.(3.29)$$

Now divide equation (3.29) by $\frac{u_0^{\,2}}{a}$:

$$U\frac{\partial U}{\partial Z}+V\frac{\partial U}{\partial R}=-\frac{\partial P}{\partial Z}+\left[\frac{\partial^2 U}{\partial R^2}+\frac{1}{R}\frac{\partial U}{\partial R}\right].\left[\frac{\nu}{a.u_0}\right] \qquad \ldots.(3.30)$$

z-momentum equation

$$U\frac{\partial U}{\partial Z}+V\frac{\partial U}{\partial R}=-\frac{\partial P}{\partial Z}+\frac{1}{\mathrm{Re}}\left[\frac{\partial^2 U}{\partial R^2}+\frac{1}{R}\frac{\partial U}{\partial R}\right] \qquad \ldots.(3.31)$$

The energy equation for constant wall temperature may be put in dimensionless by substituting the dimensionless variables shown in equations (3.12), (3.13), (3.15) and (3.16) in equation (3.6):

$$Uu_0\frac{\partial\left(\theta\left(T_0-T_w\right)+T_w\right)}{\partial\left(Za\right)}+Vu_0\frac{\partial\left(\theta\left(T_0-T_w\right)+T_w\right)}{\partial\left(R.a\right)}=$$
$$\frac{k}{\rho.c_p}\left[\frac{\partial^2\left(\theta\left(T_0-T_w\right)+T_w\right)}{\partial\left(R^2.a^2\right)}+\frac{1}{R.a}\frac{\partial\left(\theta\left(T_0-T_w\right)+T_w\right)}{\partial\left(R.a\right)}\right] \quad \ldots.(3.32)$$

where (T_o-T_w),(T_w) and (a) are constant:

$$U\frac{\partial\theta}{\partial Z}\left[\frac{u_0\left(\left(T_0-T_w\right)+T_w\right)}{a}\right]+V\frac{\partial\theta}{\partial R}\left[\frac{u_0\left(\left(T_0-T_w\right)+T_w\right)}{a}\right]=$$
$$\frac{k\left(\left(T_0-T_w\right)+T_w\right)}{\rho.c_p.a^2}\left[\frac{\partial^2\theta}{\partial R^2}+\frac{1}{R}\frac{\partial\theta}{\partial R}\right] \quad \ldots.(3.33)$$

Now multiply equation (3.33) by $\left(\frac{a}{u_o\left(\left(T_o-T_w\right)+T_w\right)}\right)$:

$$U\frac{\partial\theta}{\partial Z}+V\frac{\partial\theta}{\partial R}=\frac{k}{\rho.c_p.a.u_0}\left(\frac{\partial^2\theta}{\partial R^2}+\frac{1}{R}\frac{\partial\theta}{\partial R}\right) \quad \ldots.(3.34)$$

Now multiply equation (3.34) by $\left(\frac{\mu}{\mu}\right)$:

where $\Pr=\frac{c_p.\mu}{k}$, $\mathrm{Re}=\frac{\rho.u_0.d}{\mu}$

Energy equation for constant wall temperature

$$U\frac{\partial\theta}{\partial Z}+V\frac{\partial\theta}{\partial R}=\frac{1}{\Pr.\mathrm{Re}}\left[\frac{\partial^2\theta}{\partial R^2}+\frac{1}{R}\frac{\partial\theta}{\partial R}\right]$$

….(3.35)

In the same way, the energy equation for constant wall heat flux may be put in dimensionless form by substituting the dimensionless variables shown in equations (3.12), (3.14), (3.15) and (3.16) in equation (3.6):

$$Uu_0\frac{\partial\left(\frac{\theta.q''.a}{k}+T_0\right)}{\partial(Z.a)}+Vu_0\frac{\partial\left(\frac{\theta.q''.a}{k}+T_0\right)}{\partial(R.a)}=$$
$$\frac{k}{\rho.c_p}\left[\frac{\partial^2\left(\frac{\theta.q''.a}{k}+T_0\right)}{\partial R^2.a^2}+\frac{1}{R.a}.\frac{\partial\left(\frac{\theta.q''.a}{k}+T_0\right)}{\partial R.a}\right] \quad \ldots.(3.36)$$

where (q''),(a),(T_o) and (k) are constant:

$$U\frac{\partial\theta}{\partial Z}\left[\frac{u_0\left(\frac{q''.a}{k}+T_0\right)}{a}\right]+V\frac{\partial\theta}{\partial R}\left[\frac{u_0\left(\frac{q''.a}{k}+T_0\right)}{a}\right]=$$
$$\left(\frac{k}{\rho.c_p}\right)\left(\frac{\frac{q''.a}{k}+T_0}{a^2}\right)\left[\frac{\partial^2\theta}{\partial R^2}+\frac{1}{R}.\frac{\partial\theta}{\partial R}\right] \quad \ldots.(3.37)$$

Now multiply equation (3.37) by $\left(\frac{a}{u_o\left(\frac{q''.a}{k}+T_o\right)}\right)$:

$$U\frac{\partial\theta}{\partial Z}+V\frac{\partial\theta}{\partial R}=\frac{k}{\rho.c_p.a.u_0}\left[\frac{\partial^2\theta}{\partial R^2}+\frac{1}{R}\frac{\partial\theta}{\partial R}\right] \quad \ldots.(3.38)$$

Now multiply equation (3.38) by $\left(\frac{\mu}{\mu}\right)$:

where $\Pr=\frac{c_p.\mu}{k}$, $\mathrm{Re}=\frac{\rho.u_0.d}{\mu}$

Energy equation for constant wall heat flux

$$U\frac{\partial\theta}{\partial Z}+V\frac{\partial\theta}{\partial R}=\frac{1}{\Pr.\mathrm{Re}}\left[\frac{\partial^2\theta}{\partial R^2}+\frac{1}{R}\frac{\partial\theta}{\partial R}\right] \quad \ldots.(3.39)$$

3.2.6. Heat Transfer Solution

3.2.6.1. Bulk Temperature

In order to solve for the heat transfer in confined flow situation, it is first necessary to find the bulk (mixed-mean) temperature. Ref .[38] is defined for the circular tube as

$$T_b \equiv \frac{\int_0^a 2.\pi.r.u.T.dr}{\int_0^a 2.\pi.r.u.dr} \qquad \ldots.(3.40)$$

The bulk temperature for constant wall temperature boundary condition may be put in dimensionless form by substituting the dimensionless variables (3.12) and (3.13) in (3.40) as:

$$\theta_b \equiv \frac{\int_0^a 2.\pi.R.a.U.u_0.\theta\left(\left(T_0 - T_w\right) + T_w\right).dR}{\int_0^a 2.\pi.R.a.U.u_0.dR} \qquad \ldots.(3.41)$$

So ,The dimensionless bulk temperature for constant wall temperature boundary condition is:

$$\theta_b \equiv \frac{\int_0^1 2.\pi.U.R.\theta.dR}{\int_0^1 2.\pi.R.U.dR} \qquad \ldots.(3.42)$$

where :

$$\theta_b = \frac{T_b - T_w}{T_o - T_w}$$

In the same way, the bulk temperature for constant heat flux boundary condition may be put in dimensionless form by substituting the dimensionless variables (3.12) and (3.14) in (3.40) as:

$$\theta_b \equiv \frac{\int_0^a 2.\pi.R.a\left(\frac{\theta.q''.a}{k}+T_0\right)U.u_0.dR}{\int_0^a 2.\pi.R.a.U.u_0.dR} \qquad \ldots.(3.43)$$

So ,the dimensionless bulk temperature for constant wall heat flux boundary condition is:

$$\theta_b \equiv \frac{\int_0^1 2.\pi.U.R.\theta.dR}{\int_0^1 2.\pi.R.U.dR} \qquad \ldots.(3.44)$$

where

$$\theta_b = \frac{k}{q''.a}(T_b - T_o)$$

So ,dimensionless Bulk Temperature:

$$\theta_b = \frac{\int_0^1 2.\pi.R.U.\theta.dR}{\int_0^1 2.\pi.R.U.dR} = \int_0^1 2.\pi.R.U.\theta.dR \qquad \ldots.(3.45)$$

Where

$$\int_0^1 2.\pi.R.U.dR = 1$$

3.2.6.2 Local Nusselt number

The local Nusselt number is given by Ref .[38] as:

$$Nu_z = \frac{2ha}{k} \qquad \ldots.(3.46)$$

where

$$h(T_w - T_b) = k\left.\frac{\partial T}{\partial r}\right|_{r=a} \qquad \ldots.(3.47)$$

so

$$Nu_z = \frac{-\left.\frac{\partial T}{\partial r}\right|_{r=a}.(2a)}{T_b - T_w} \qquad \ldots.(3.48)$$

The local Nusselt number for constant wall temperature boundary condition can be put in dimensional form by substituting the dimensionless variables (3.12) and (3.14) in (3.48) as:

$$Nu_z = \frac{-2a\left.\frac{\partial(\theta(T_o - T_w) + T_w)}{\partial(R.a)}\right|_{r=a}}{T_b - T_w} \qquad \ldots.(3.49)$$

where (T_o-T_w), (T_w) and (a) are constant

$$Nu_z = \frac{-2(T_0 - T_w)\left.\frac{\partial\theta}{\partial R}\right|_{R=1}}{T_b - T_w} \qquad \ldots.(3.50)$$

where $\theta_b = \frac{T_b - T_w}{T_o - T_w}$ ….(3.51)

So, the dimensionless local Nusselt Number for constant wall temperature:

$$Nu_z = \frac{-2\left.\frac{\partial\theta}{\partial R}\right|_{R=1}}{\theta_b} \qquad \ldots.(3.52)$$

In the same way, the local Nusselt number for constant wall heat flux boundary condition may be put in dimensionless form by substituting the dimensionless variables (3.12) and (3.14) in (3.48) as:

$$Nu_z = \frac{-2a\left.\dfrac{\partial\left(\dfrac{\theta.q''.a}{k}+T_o\right)}{\partial(Ra)}\right|_{r=a}}{T_b - T_w} \quad \ldots.(3.53)$$

where $\left(\dfrac{q''.a}{k}\right)$, *($T_o$) and (a) are constant*

$$Nu_z = \frac{-2a\dfrac{\partial\theta}{\partial R}\left(\dfrac{q''.a}{k.a}\right)}{T_b - T_w} \quad \ldots.(3.54)$$

where $\left(\dfrac{\partial\theta}{\partial R}=1\right)$ *at wall for constant heat flux*

$$Nu_z = \frac{-2a\left(\dfrac{q''}{k}\right)}{T_b - T_w} \quad \ldots.(3.55)$$

Now adding and subtracting (T_o) from the denominator of equation (3.55):

$$Nu_z = \frac{-2}{\dfrac{k}{q''.a}(T_b - T_w + T_o - T_o)} \quad \ldots.(3.56)$$

$$Nu_z = \frac{-2}{\dfrac{k}{q''.a}(T_b - T_o) - \dfrac{k}{q''.a}(T_w - T_o)} \quad \ldots.(3.57)$$

$$\theta_b = \frac{k}{q''.a}(T_b - T_o) \quad \ldots.(3.58)$$

$$\theta_w = \frac{k}{q''.a}(T_w - T_o) \quad \ldots.(3.59)$$

So, the dimensionless local Nusselt Number for constant heat flux :

$$Nu_z = \frac{-2}{\theta_b - \theta_w} \quad \ldots.(3.60)$$

3.3. Numerical Techniques

The numerical analysis for the partial differential equations was achieved by using special Finite Difference Method (FDM) to transform these non-linear equations to an algebraic equations.

The calculation region for circular tube is shown in figure (3-2)which shows the mesh of the upper region of the tube only, due to symmetry (symmetric in boundary conditions and dimensions).

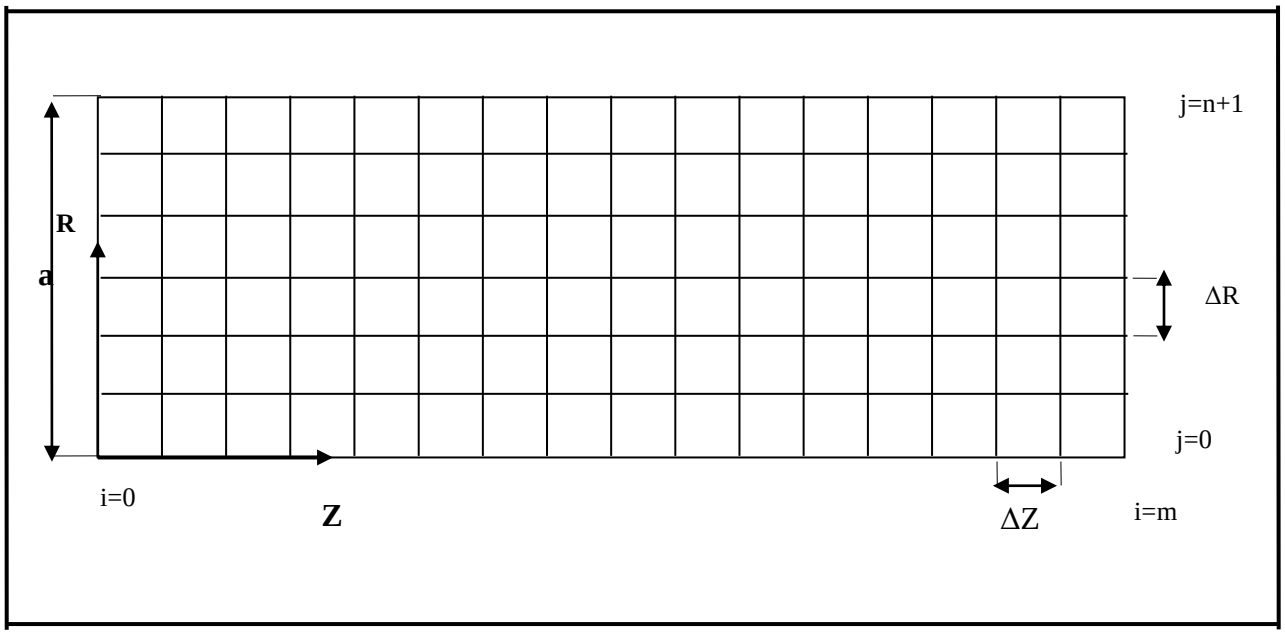

Figure (3-2)dimensionless nodal grid for circular tube .

The nodal points are specified by using the two indexes, (*i*) in the dimensionless axial direction (*Z*)which was divided into a number of (ΔZ) and (*j*) in the dimensionless vertical direction (*R*) which was divided into a number of (ΔR).

where

($i = 0, m$, $j = 0, n+1$).

And

(j=n+1) denote the wall of the tube.

A finite difference representation is chosen for continuity, momentum and energy equations . The finite difference grid is shown in figure (3-3). The difference form selected for equation (3.31) is as highly implicit since not only all R-derivatives evaluated at (*i+1*), the coefficients of the nonlinear convective terms are also evaluated at (*i+1*). The usual implicit scheme, does give correct results if the secondary velocity is of the order of the primary velocity or larger.

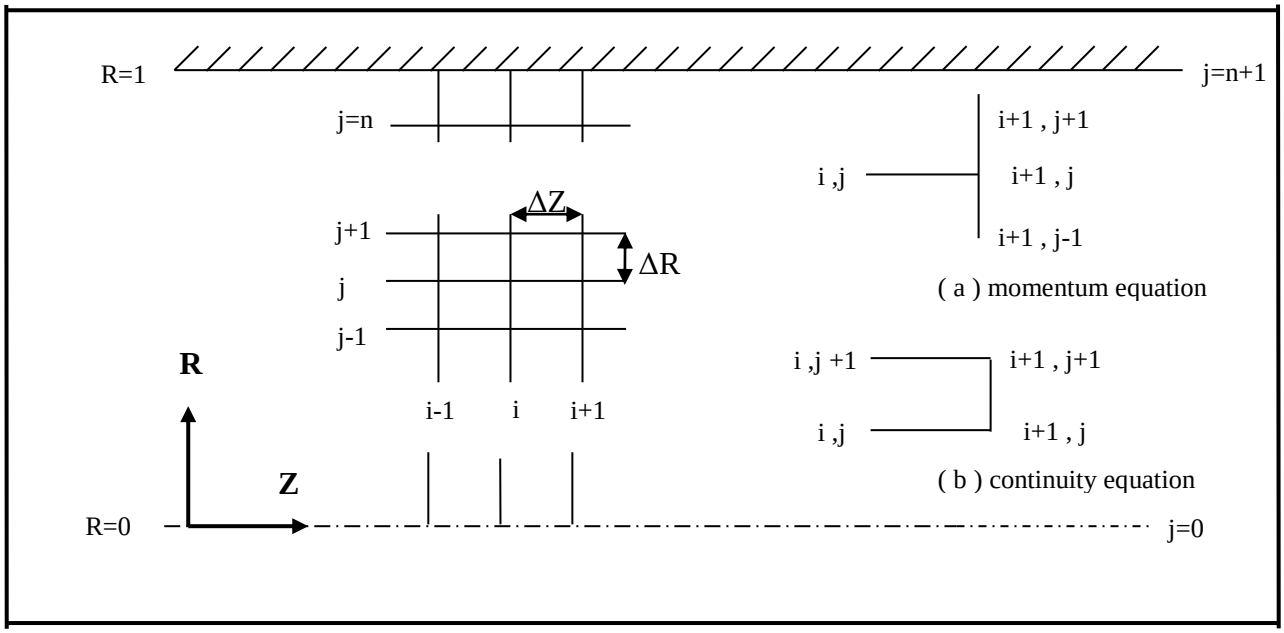

Figure (3-3) finite difference representation to be used with basic equations.

The continuity, momentum, and energy equations will be solved by using Gauss- Elimination method. A computer program which was built in the present work solving all the resulting algebraic form of all equations.

3.3.1. Finite Difference Representation for Dimensionless Momentum and Continuity Equations

The special Finite Difference Method (FDM) will be used to solve the momentum equation (3.31) for a steady, two-dimensional, laminar, constant-property boundary-layer flow of a Newtonian fluid in forced convection. The two

terms on the left side are the nonlinear convection terms. The two terms on the right side arise from inertial forces and viscous shearing forces, respectively.

Horenbec [38] showed that the numerical formulation for the dimensionless form of z-momentum equation with respect to figure (3-3 a) is :

$$U_{i,j}\frac{U_{i+1,j}-U_{i,j}}{\Delta Z}+V_{i,j}\frac{U_{i+1,j+1}-U_{i+1,j-1}}{2(\Delta R)}=$$

$$-\frac{P_{i+1}-P_i}{\Delta Z}+\frac{1}{\mathrm{Re}}\left[\frac{U_{i+1,j+1}-2U_{i+1,j}+U_{i+1,j-1}}{(\Delta R)^2}+\frac{1}{R_j}\frac{U_{i+1,j+1}-U_{i+1,j-1}}{2(\Delta R)}\right] \qquad \ldots.(3.61)$$

And Horenbec [38] showed that the numerical formulation of continuity equation (3.27) with respect to figure (3-3 b) is :

$$\left[\frac{R_j(U_{i+1,j}-U_{i,j})}{2(\Delta Z)}+\frac{R_{j+1}(U_{i+1,j+1}-U_{i,j+1})}{2(\Delta Z)}\right]+\frac{V_{i+1,j+1}R_{j+1}-V_{i+1,j}R_j}{\Delta R}=0 \qquad \ldots.(3.62)$$

In any application includes the solution of conservative equations in polar coordinates for duct laminar or turbulent flow, there is a problem will be faced in the center of this duct. This problem comes from getting the radius of the duct (r) the value zero at the center of the duct , which causes the division by zero or the " singularity " at any term in the governing equation contain (r) in the denominator. .

Adems and Rogers [39] showed that when the cylinder is solid rather than hollow ,special consideration must be given to the central node at r=0,the second term in equation (3.31), $\left(\frac{1}{R}\right)\left(\frac{\partial U}{\partial R}\right)$ is indeterminate. This may be accomplished by applying L' Hopital's Rule

$$\lim_{R\to 0}\left(\frac{1}{R}\right)\left(\frac{\partial U}{\partial R}\right)=\lim_{R\to 0}\frac{\left(\frac{\partial}{\partial R}\right)\left(\frac{\partial U}{\partial R}\right)}{\left(\frac{\partial}{\partial R}\right)(R)}=\left(\frac{\partial^2 U}{\partial R^2}\right) \qquad \ldots.(3.63)$$

In a similar manner, the second term in equation (3.27) becomes:

$$\lim_{R\to 0}\left(\frac{1}{R}\right)\left(\frac{\partial(V.R)}{\partial R}\right)=\lim_{R\to 0}\frac{\left(\frac{\partial}{\partial R}\right)\left(\frac{\partial(V.R)}{\partial R}\right)}{\left(\frac{\partial}{\partial R}\right)(R)}=2\left(\frac{\partial V}{\partial R}\right) \qquad \ldots.(3.64)$$

these equations may be written at R=0 as :

$$U\frac{\partial U}{\partial Z}\bigg|_{R=0}=\frac{-dP}{dZ}+\frac{2}{\mathrm{Re}}.\frac{\partial^2 U}{\partial R^2}\bigg|_{R=0} \qquad \ldots.(3.65)$$

$$\frac{\partial U}{\partial Z}\bigg|_{R=0}+2\frac{\partial V}{\partial R}\bigg|_{R=0}=0 \qquad \ldots.(3.66)$$

Equation (3.65) and (3.66) can be written in finite difference form as :

$$U_{i,0}\,\frac{U_{i+1,0}-U_{i,0}}{\Delta Z}=-\frac{P_{i+1}-P_i}{\Delta Z}+4\left[\frac{U_{i+1,1}-U_{i+1,0}}{(\Delta R)^2}\right] \qquad \ldots.(3.67)$$

Equation (3.67) includes the symmetry boundary condition on U at R=0 expressed in difference form as :

$$U_{i+1,1}=U_{i+1,-1}$$

And

$$\frac{U_{i+1,1}+U_{i+1,0}-U_{i,1}-U_{i,0}}{2(\Delta Z)}+\frac{2V_{i+1,1}}{\Delta R}=0 \qquad \ldots.(3.68)$$

Equation (3.68) includes the condition V(0,Z) = 0 .

Equations (3.61) and (3.62) are written for j=1(1)n and equations (3.67) and (3.68) for j=0 together constitute (*2n+2*) equations in the (*2n+2*) unknowns ($U_{i+1,j}$,$V_{i+1,j}$); and (P_{i+1}).

The system of equations may be considerably reduced in size by using the integral continuity equation . Adding the continuity equation (3.62) for J=1(1)n and equation (3.68) for J=0 together , the resulting equation can be written in the form :

$$\Delta R\left(\frac{1}{4}U_{i+1,0}+\frac{3}{4}U_{i+1,1}\right)+\sum_{j=2}^{n}R_jU_{i+1,j}=\Delta R\left(\frac{1}{4}U_{i,0}+\frac{3}{4}U_{i,1}\right)+\sum_{j=2}^{n}R_jU_{i,j} \quad \ldots.(3.69)$$

It is now convenient to rewrite equation (3.61) as:

$$\left[-\frac{V_{i,j}}{2(\Delta R)}-\frac{1}{2\,\mathrm{Re}.R_j(\Delta R)}-\frac{1}{\mathrm{Re}(\Delta R)^2}\right]U_{i+1,j-1}+\left[\frac{U_{i,j}}{\Delta Z}+\frac{2}{\mathrm{Re}(\Delta R)^2}\right]U_{i+1,j}$$
$$+\left[\frac{V_{i,j}}{2(\Delta R)}-\frac{1}{2\,\mathrm{Re}.R_j(\Delta R)}-\frac{1}{\mathrm{Re}(\Delta R)^2}\right]U_{i+1,j+1}+\frac{1}{\Delta Z}P_{i+1}=\frac{U_{i,j}^2+P_i}{\Delta Z} \quad \ldots.(3.70)$$

And equation (3.67) as:

$$\left[\frac{U_{i,0}}{\Delta Z}+\frac{4}{\mathrm{Re}(\Delta R)^2}\right]U_{i+1,0}-\left[\frac{4}{\mathrm{Re}(\Delta R)^2}\right]U_{i+1,1}+\left(\frac{1}{\Delta Z}\right)P_{i+1}=\frac{U_{i,0}^2+P_i}{\Delta Z} \quad \ldots.(3.71)$$

Equation (3.70) written for J=1(1) n , equation (3.71) for J=0 ,and equation (3.69) now comprise (n+2) linear algebraic equations in the (n+2) unknowns $U_{i+1,j}$ and P_{i+1}.

This set of equations may be written in matrix form as :

$$\begin{vmatrix}
\frac{\Delta R}{4} & \frac{3\Delta R}{4} & R_2 & R_3 & R_4 & - & - & R_{n-1} & R_n & 0 \\
\beta_0 & \Omega_0 & & & & & & & & 1/\Delta Z \\
\alpha_1 & \beta_1 & \Omega_1 & & & & & & & 1/\Delta Z \\
 & \alpha_2 & \beta_2 & \Omega_2 & & & & & & 1/\Delta Z \\
 & & \alpha_3 & \beta_3 & \Omega_3 & & & & & 1/\Delta Z \\
 & & & - & - & - & & & & - \\
 & & & & - & - & - & & & - \\
 & & & & & - & - & - & & - \\
 & & & & & & \alpha_{n-1} & \beta_{n-1} & \Omega_{n-1} & 1/\Delta Z \\
 & & & & & & & \alpha_n & \beta_n & 1/\Delta Z
\end{vmatrix}
\times
\begin{vmatrix}
U_{i+1,0} \\ U_{i+1,1} \\ U_{i+1,2} \\ U_{i+1,3} \\ U_{i+1,4} \\ - \\ - \\ - \\ U_{i+1,n} \\ P_{i+1}
\end{vmatrix}
=
\begin{vmatrix}
S \\ \Phi_0 \\ \Phi_1 \\ \Phi_2 \\ \Phi_3 \\ - \\ - \\ - \\ \Phi_{n-1} \\ \Phi_n
\end{vmatrix}
\quad \ldots.(3.72)$$

where

$$\beta_0=\frac{U_{i,0}}{\Delta Z}+\frac{4}{\mathrm{Re}(\Delta R)^2} \quad \ldots.(3.72a)$$

$$\Omega_0=-\frac{4}{\mathrm{Re}(\Delta R)^2} \quad \ldots.(3.72b)$$

$$\Phi_o=\frac{U_{i,0}^2+P_i}{\Delta Z} \quad \ldots.(3.72c)$$

$$S = \left(\frac{\Delta R}{4}\right)U_{i,0} + \left(\frac{3(\Delta R)}{4}\right)U_{i,1} + \sum_{j=2}^{n} R_J . U_{i,j}$$

….(3.72d)

And

$$\alpha_j = \frac{-V_{i,j}}{2(\Delta R)} + \frac{1}{2\,\mathrm{Re}.R_j(\Delta R)} - \frac{1}{\mathrm{Re}(\Delta R)^2} \qquad j>0 \qquad \text{….(3.72e)}$$

$$\beta_j = \frac{U_{i,j}}{\Delta Z} + \frac{2}{\mathrm{Re}(\Delta R)^2} \qquad j>0 \qquad \text{….(3.72f)}$$

$$\Omega_j = \frac{V_{i,j}}{2(\Delta R)} - \frac{1}{2\,\mathrm{Re}.R_j(\Delta R)} - \frac{1}{\mathrm{Re}(\Delta R)^2} \qquad j>0 \qquad \text{….(3.72g)}$$

$$\Phi_j = \frac{U_{i,j} + P_i}{\Delta Z} \qquad \text{….(3.72h)}$$

for n=5 the matrix becomes

$$\begin{vmatrix} \Delta R/4 & 3\Delta R/4 & R_2 & R_3 & R_4 & R_5 & 0 \\ \beta_0 & \Omega_0 & & & & & 1/\Delta Z \\ \alpha_1 & \beta_1 & \Omega_1 & & & & 1/\Delta Z \\ & \alpha_2 & \beta_2 & \Omega_2 & & & 1/\Delta Z \\ & & \alpha_3 & \beta_3 & \Omega_3 & & 1/\Delta Z \\ & & & \alpha_4 & \beta_4 & \Omega_4 & 1/\Delta Z \\ & & & & \alpha_5 & \beta_5 & 1/\Delta Z \end{vmatrix} \times \begin{vmatrix} U_{i+1,0} \\ U_{i+1,1} \\ U_{i+1,2} \\ U_{i+1,3} \\ U_{i+1,4} \\ U_{i+1,5} \\ P_{i+1} \end{vmatrix} = \begin{vmatrix} S \\ \Phi_0 \\ \Phi_1 \\ \Phi_2 \\ \Phi_3 \\ \Phi_4 \\ \Phi_5 \end{vmatrix} \qquad \text{….(3.73)}$$

The matrix of coefficients in equation (3.73) does not have the desirable tridiagonal character of the matrices. This matrix is, however, quite sparse. It would be possible to write a special computer program to solve the set (3.73) by taking full advantage of this sparseness. This would only be practical if a large number of production runs were contemplated and the savings in running time and storage space considered more important than the programming time required. As a general rule, it seems most practical to solve the set by using one of the standard routines for linear equations or matrix inversion which are available at any computer installation. A possible alternative is to solve the set by

Gaussian elimination method. This method will work effectively except for equation (3.69) [top row of equation (3.73)], which must be drastically under relaxed.

After the set (3.73) has been solved for ($U_{i+1,0}$,….,$U_{i+1,n}$) and (P_{i+1}), equation (3.62) may be employed in the form

$$V_{i+1,j+1}=\left(\frac{R_j}{R_{j+1}}\right)V_{i+1,j}-\frac{\Delta R}{2(\Delta Z)}\left[U_{i+1,j+1}-U_{i,j+1}+\left(\frac{R_j}{R_{j+1}}\right)(U_{i+1,j}-U_{i,j})\right] \qquad \ldots.(3.74)$$

which may be marched outward from the tube centerline to give the values of ($V_{i+1,1}$,….,$V_{i+1,n}$).

Another step (ΔZ) downstream may now be taken and the process repeated. This may be continued as many times until reach to (0.001)percentage error of iteration.

The proper choice of the (ΔZ) mesh size at and near the tube entrance is a very important factor in obtaining an accurate solution. The entrance itself represents a mathematical difficulty in that it behaves like a singularity. This mathematical singularity may be dealt with in the manner described in this chapter for the leading edge in the boundary layer development problem, by keeping (ΔZ) very small and hence taking a large number of steps in the region close to the entrance. As in the boundary layer case, the spread of the effect of the singularity downstream is primarily a function of how many steps are taken to reach a given (Z) position. If a large number of steps are taken to reach this value of (Z), then the effect of the singularity there tends to disappear. The effect of the singularity may thus be confined to a region arbitrarily close to the entrance.

3.3.2. Finite Difference Representation for Dimensionless Energy Equation

Equation (3.35) or (3.39) may now be expressed in an implicit finite difference form similar to that used for the momentum equation in the preceding section. This difference form is :

$$U_{i,j}\frac{\theta_{i+1,j}-\theta_{i,j}}{\Delta Z}+V_{i,j}\frac{\theta_{i+1,j+1}-\theta_{i+1,j-1}}{2(\Delta R)}$$

$$=\frac{1}{\mathrm{Pr.Re}}\left[\frac{\theta_{i+1,j+1}-2\theta_{i+1,j}+\theta_{i+1,j-1}}{(\Delta R)^2}+\frac{1}{R_j}\frac{\theta_{i+1,j+1}-\theta_{i+1,j-1}}{2(\Delta R)}\right] \quad \ldots.(3.77)$$

This equation applies for j=1(1)n

For R=0 it is again necessary to apply the limiting process as $R\to 0$ to equation (3.35) ,which results in

$$U\frac{\partial\theta}{\partial Z}\bigg|_{R=0}=\frac{2}{\mathrm{Re.Pr}}\left(\frac{\partial^2\theta}{\partial R^2}\right)\bigg|_{R=0} \quad \ldots.(3.78)$$

Expressing equation (3.78) in finite difference form yields :

$$U_{i,0}\left[\frac{\theta_{i+1,0}-\theta_{i,0}}{\Delta Z}\right]=\frac{4}{\mathrm{Re.Pr}}\left[\frac{\theta_{i+1,1}-\theta_{i+1,0}}{(\Delta R)^2}\right] \quad \ldots.(3.79)$$

Equation (3.79) includes the symmetry condition expressed as

$\theta_{i+1,1}=\theta_{i+1,-1}$ at R=0

Equation (3.77) and (3.79) may be rewritten in more useful forms as:

$$\left[\frac{-V_{i,j}}{2(\Delta R)}+\frac{1}{2\,\mathrm{Re.Pr}.R_j(\Delta R)}-\frac{1}{\mathrm{Re.Pr}(\Delta R)^2}\right]\theta_{i+1,j-1}+\left[\frac{U_{i,j}}{\Delta Z}+\frac{2}{\mathrm{Re.Pr}(\Delta R)^2}\right]\theta_{i+1,j}$$

$$+\left[\frac{V_{i,j}}{2(\Delta R)}-\frac{1}{2\,\mathrm{Re.Pr}.R_j(\Delta R)}-\frac{1}{\mathrm{Re.Pr}(\Delta R)^2}\right]\theta_{i+1,j+1}=\frac{U_{i,j}.\theta_{i,j}}{\Delta Z} \quad \ldots.(3.80)$$

And

$$\left[\frac{U_{i,0}}{\Delta Z}+\frac{4}{\mathrm{Re}.\mathrm{Pr}(\Delta R)^2}\right]\theta_{i+1,0}+\left[\frac{-4}{\mathrm{Re}.\mathrm{Pr}(\Delta R)^2}\right]\theta_{i+1,1}=\frac{U_{i,0}.\theta_{i,0}}{\Delta Z} \qquad \text{….(3.81)}$$

If the wall temperature is constant , equation (3.80) written for j=1(1)n and equation (3.81) for j=0 constitute a set of (n+1) linear algebraic equations in the (n+1) unknowns $\theta_{i+1,j}$. This set may be written in matrix form as :

$$\begin{vmatrix} \beta'_0 & \Omega'_0 & & & & & & \\ \alpha'_1 & \beta'_1 & \Omega'_1 & & & & & \\ & \alpha'_2 & \beta'_2 & \Omega'_2 & & & & \\ & & - & - & - & & & \\ & & & - & - & - & & \\ & & & & - & - & - & \\ & & & & & \alpha'_{n-1} & \beta'_{n-1} & \Omega'_{n-1} \\ & & & & & & \alpha'_n & \beta'_n \end{vmatrix} \times \begin{vmatrix} \theta_{i+1,0} \\ \theta_{i+1,1} \\ \theta_{i+1,2} \\ - \\ - \\ - \\ \theta_{i+1,n-1} \\ \theta_{i+1,n} \end{vmatrix} = \begin{vmatrix} \Phi'_0 \\ \Phi'_1 \\ \Phi'_2 \\ - \\ - \\ - \\ \Phi'_{n-1} \\ \Phi'_n \end{vmatrix} \qquad \text{….(3.82)}$$

Where

$$\beta'_0=\frac{U_{i,0}}{\Delta Z}+\frac{4}{\mathrm{Pr}.\mathrm{Re}(\Delta R)^2} \qquad \text{….(3.82a)}$$

$$\Omega'_0=-\frac{4}{\mathrm{Pr}.\mathrm{Re}(\Delta R)^2} \qquad \text{….(3.82b)}$$

$$\Phi'_0=\frac{U_{i,0}\theta_{i,0}}{\Delta Z} \qquad \text{….(3.82c)}$$

And

$$\alpha'_j=\frac{-V_{i,j}}{2(\Delta R)}+\frac{1}{2\mathrm{Re}.\mathrm{Pr}.R_j(\Delta R)}-\frac{1}{\mathrm{Re}.\mathrm{Pr}(\Delta R)^2} \qquad \text{….(3.82d)}$$

$$\beta'_j=\frac{U_{i,j}}{\Delta Z}+\frac{2}{\mathrm{Re}.\mathrm{Pr}(\Delta R)^2} \qquad (j>0) \qquad \text{….(3.82e)}$$

$$\Omega'_j=\frac{V_{i,j}}{2(\Delta R)}-\frac{1}{2\mathrm{Re}.\mathrm{Pr}.R_j(\Delta R)}-\frac{1}{\mathrm{Re}.\mathrm{Pr}(\Delta R)^2} \qquad (j>0) \qquad \text{….(3.82f)}$$

$$\Phi'_j=\frac{U_{i,j}.\theta_{i,j}}{\Delta Z} \qquad \text{….(3.82g)}$$

for n=5 the matrix becomes

$$\begin{vmatrix} \beta'_0 & \Omega'_0 & & & & \\ \alpha'_1 & \beta'_1 & \Omega'_1 & & & \\ & \alpha'_2 & \beta'_2 & \Omega'_2 & & \\ & & \alpha'_3 & \beta'_3 & \Omega'_3 & \\ & & & \alpha'_4 & \beta'_4 & \Omega'_4 \\ & & & & \alpha'_5 & \beta'_5 \end{vmatrix} \times \begin{vmatrix} \theta_{i+1,0} \\ \theta_{i+1,1} \\ \theta_{i+1,2} \\ \theta_{i+1,3} \\ \theta_{i+1,4} \\ \theta_{i+1,5} \end{vmatrix} = \begin{vmatrix} \Phi'_0 \\ \Phi'_1 \\ \Phi'_2 \\ \Phi'_3 \\ \Phi'_4 \\ \Phi'_5 \end{vmatrix} \quad \ldots.(3.83)$$

The matrix equation (3.83) is tridiagonal and the method illustrated in (Ref.[36]) is used to obtain a solution for the($\theta_{i+1,j}$'s).

For the constant heat flux case, the wall temperature ($\theta_{i+1,n+1}$) becomes an additional unknown .the necessary additional equation is supplied by the wall heat flux condition in (3.23) expressed in finite difference form as :

$$\frac{3\theta_{i+1,n+1} - 4\theta_{i+1,n} + \theta_{i+1,n-1}}{2(\Delta R)} = 1 \quad \ldots.(3.84)$$

By using the backward difference in (Ref .[36]).

This additional equation must now be added to the system of equations (3.82) and the complete set may be written in matrix form as:

$$\begin{vmatrix} \beta'_0 & \Omega'_0 & & & & & & \\ \alpha'_1 & \beta'_1 & \Omega'_1 & & & & & \\ & \alpha'_2 & \beta'_2 & \Omega'_2 & & & & \\ & & - & - & - & & & \\ & & & - & - & - & & \\ & & & & - & - & - & \\ & & & & & \alpha'_{n-1} & \beta'_{n-1} & \Omega'_{n-1} \\ & & & & & & \alpha'_n & \beta'_n & \Omega'_n \\ & & & & & & 1 & -4 & 3 \end{vmatrix} \times \begin{vmatrix} \theta_{i+1,0} \\ \theta_{i+1,1} \\ \theta_{i+1,2} \\ - \\ - \\ - \\ \theta_{i+1,n-1} \\ \theta_{i+1,n} \\ \theta_{i+1,n+1} \end{vmatrix} = \begin{vmatrix} \Phi'_0 \\ \Phi'_0 \\ \Phi'_0 \\ - \\ - \\ - \\ \Phi'_{n-1} \\ \Phi'_n \\ 2(\Delta R) \end{vmatrix} \quad \ldots.(3.85)$$

where the elements are defined as in (3.82).

The element 2(ΔR) in the last row makes the matrix in (3.85) nontridiagonal. However, the matrix may be made tridiagonal by eliminating this element. This can be accomplished by multiplying it by (α'_n), and subtracting the previous equation from it. The results are:

$$\begin{vmatrix} \beta'_0 & \Omega'_0 & & & & & & & \\ \alpha'_1 & \beta'_1 & \Omega'_1 & & & & & & \\ & \alpha'_2 & \beta'_2 & \Omega'_2 & & & & & \\ & & - & - & - & & & & \\ & & & - & - & - & & & \\ & & & & - & - & - & & \\ & & & & & \alpha'_{n-1} & \beta'_{n-1} & \Omega'_{n-1} & \\ & & & & & & \alpha'_n & \beta'_n & \Omega'_n \\ & & & & & & 0 & (-4\alpha'_n - \beta'_n) & (3\alpha'_n - \Omega'_n) \end{vmatrix} \times \begin{vmatrix} \theta_{i+1,0} \\ \theta_{i+1,1} \\ \theta_{i+1,2} \\ - \\ - \\ - \\ \theta_{i+1,n-1} \\ \theta_{i+1,n} \\ \theta_{i+1,n+1} \end{vmatrix} = \begin{vmatrix} \Phi'_0 \\ \Phi'_1 \\ \Phi'_2 \\ - \\ - \\ - \\ \Phi'_{n-1} \\ \Phi'_n \\ 2(\Delta R)\alpha'_n - \Phi'_n \end{vmatrix}$$

….(3.86)

for n=5 the matrix becomes

$$\begin{vmatrix} \beta'_0 & \Omega'_0 & & & & & \\ \alpha'_1 & \beta'_1 & \Omega'_1 & & & & \\ & \alpha'_2 & \beta'_2 & \Omega'_2 & & & \\ & & \alpha'_3 & \beta'_3 & \Omega'_3 & & \\ & & & \alpha'_4 & \beta'_4 & \Omega'_4 & \\ & & & & \alpha'_5 & \beta'_5 & \Omega'_5 \\ & & & & 0 & (-4\alpha'_5 - \beta'_5) & (3\alpha'_5 - \Omega'_5) \end{vmatrix} \times \begin{vmatrix} \theta_{i+1,0} \\ \theta_{i+1,1} \\ \theta_{i+1,2} \\ \theta_{i+1,3} \\ \theta_{i+1,4} \\ \theta_{i+1,5} \\ \theta_{i+1,6} \end{vmatrix} = \begin{vmatrix} \Phi'_0 \\ \Phi'_1 \\ \Phi'_2 \\ \Phi'_3 \\ \Phi'_4 \\ \Phi'_5 \\ 2(\Delta R)\alpha'_n - \Phi'_5 \end{vmatrix} \quad \text{….(3.87)}$$

Equation (3.87) has a tridiagonal matrix of coefficients and the method of (Ref.[36]) is used.

After the solution has been obtained another step downstream may be taken and the process is repeated .

It is of course best to obtain the velocity and temperature solutions together, solving first at each step for the velocity and then for the temperature .

3.3.3. Convergence and Stability

Convergence means that (ΔR) and (ΔZ) approach zero, and the results of finite difference technique approach the true solution. Stability means that errors at any stage of the computation are not amplified but are attenuated as the computation progresses.

The stability restrictions for this problem have been established by Bodoia, (mentioned by Hornbeck, [36]) for the incompressible boundary layer problem. The formulation is universally stable for (U ≥ 0), and if (U < 0) , then:

$$\frac{\Delta Z}{|U|(\Delta R)^2} \geq \frac{1}{2} \qquad \ldots.(3.75)$$

$$\left|V - \frac{1}{R}\right| \geq \sqrt{\frac{2|U|}{\Delta Z}} \qquad \ldots.(3.76)$$

These will , in general , be satisfied only for very small negative values of U .

The truncation error of the momentum equation is of $\sigma(\Delta Z)$ and $\sigma((\Delta R)^2)$ and that of continuity $\sigma(\Delta Z)$ and $\sigma(\Delta R)$.

The difference formulation for the energy equation is universally stable . The truncation error of the difference form of the energy equation is of $\sigma(\Delta Z)$ and $\sigma\left((\Delta R)^2\right)$.

3.3.4. Heat Transfer Calculations

3.3.4.1. Dimensionless Bulk Temperature (θ_b)

The dimensionless bulk temperature (θ_b) is calculated numerically by employing Simpson's rule:

$$\theta_b\big|_{i+1} = \frac{\Delta R}{3}\left(4 \sum_{j=1,3,5,7,\ldots}^{n} U_{i+1,j} R_j \theta_{i+1,j} + 2 \sum_{j=2,4,6,8,\ldots.}^{n-1} U_{i+1,j} R_j \theta_{i+1,j}\right) \qquad \ldots.(3.88)$$

Where n must be odd ; that is , there must be an even number of spaces across the tube radius .

for n=5 equation (3.88) becomes

$$\theta_b\big|_{i+1} = \frac{\Delta R}{3}\left(4 \sum_{j=1,3,}^{5} U_{i+1,j} R_j \theta_{i+1,j} + 2 \sum_{j=2,}^{4} U_{i+1,j} R_j \theta_{i+1,j}\right) \qquad \ldots.(3.89)$$

3.3.4.2. Local Nusselt Number (Nu_z)

The Nusselt number is given by equation (3.48). The local Nusselt number for constant wall temperature boundary condition is given by equation (3.52), which is written in a finite difference form as,

$$N_{uz} = -2\frac{\left(3\theta_{i+1,n+1} - 4\theta_{i+1,n} + \theta_{i+1,n-1}\right)}{2(\Delta R)\theta_b\big|_{i+1}} \quad \ldots.(3.90)$$

for n=5 the equation (3.90) becomes

$$N_{uz} = -2\frac{\left(3\theta_{i+1,6} - 4\theta_{i+1,5} + \theta_{i+1,4}\right)}{2(\Delta R)\theta_b\big|_{i+1}} \quad \ldots.(3.91)$$

The local Nusselt number for constant heat flux boundary condition is given by equation (3.60), which is written in a finite difference form as,

$$N_{uz} = \frac{-2}{\theta_b\big|_{i+1} - \theta_w\big|_{i+1}} \quad \ldots.(3.92)$$

3.3.5. Steps of Numerical Solution

The numerical solution steps for all equations can be summarized as follows :

1. The calculation of Z-momentum equation coefficients are obtained by using equations (3.72a),…,(3.72h).
2. The calculation of pressure difference in the axial direction (P_{i+1}) and the axial velocity component ($U_{i+1,5} \rightarrow U_{i+1,0}$) for one column are obtained by using solve equation (3.73). The nodal Gaussian-elimination method was used for doing this calculation.
3. The calculation of vertical velocity component($V_{i+1,j+1}$) for one column is obtained by using equation (3.74).
4. Steps from 1 to 3 should be repeated until reaching the fully developed region. To ensure the reaching to the fully developed region ,it must be get

constant axial velocity in z-direction. i.e. $\frac{\partial U}{\partial Z} = 0$ .the maximum error of iteration was 0.001

5. The calculation of energy equation coefficients are obtained by using equations (3.82a),…,(3.82g).
6. The calculation of temperature component ($\theta_{i+1,0} \rightarrow \theta_{i+1,5}$)for one column is obtained by using equation (3.83) for constant wall temperature and the temperature component ($\theta_{i+1,0} \rightarrow \theta_{i+1,6}$) by using equation (3.87) for constant heat flux. The nodal Gaussian-elimination method was used for doing this calculation.
7. The calculation of the dimensionless bulk temperature (θ_b)from equation (3.89).
8. The calculation of bulk temperature (Tb) for constant wall temperature (Tw=80°C) from equation (3.51) .
9. The calculation of bulk temperature(Tb) and wall temperature (Tw) for constant heat flux (q''=100W/m^2)from equations (3.58) and (3.59) respectively
10. The calculation of the local Nusselt number for constant wall temperature boundary condition is obtained by using equation (3.91), and the local Nusselt number for constant heat flux boundary condition is obtained by using equation (3.92).

3.3.6. Computer Program

The computer program was developed to calculate the velocity profile, temperature distribution, bulk temperature, and local Nusselt number. These calculations were based on the theoretical analysis presented in this chapter.

The computer program was written in QuickBasic language. The flowchart of this program was shown in figure (3-4).

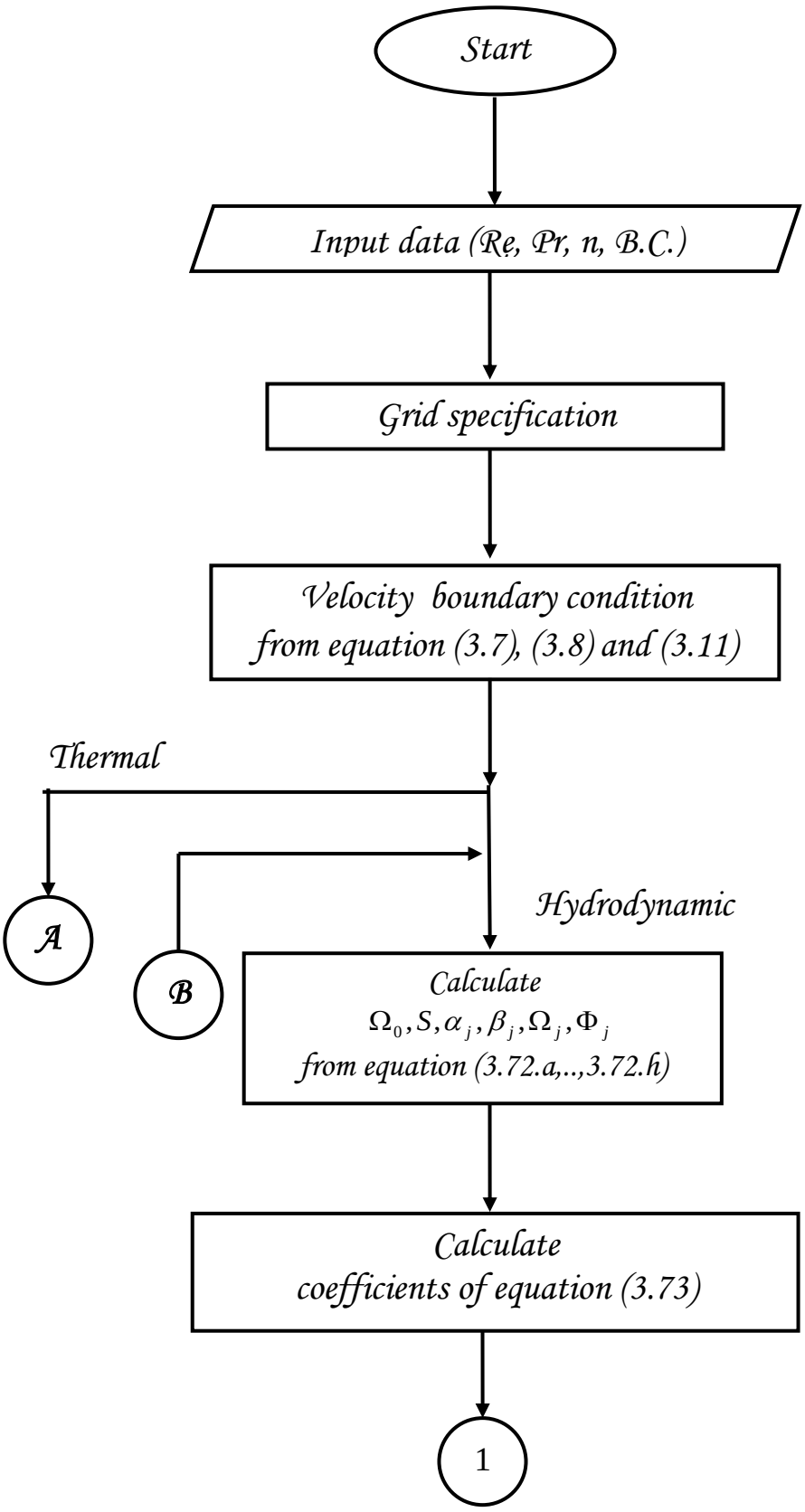

Figure (3-4) flowchart of the computer program

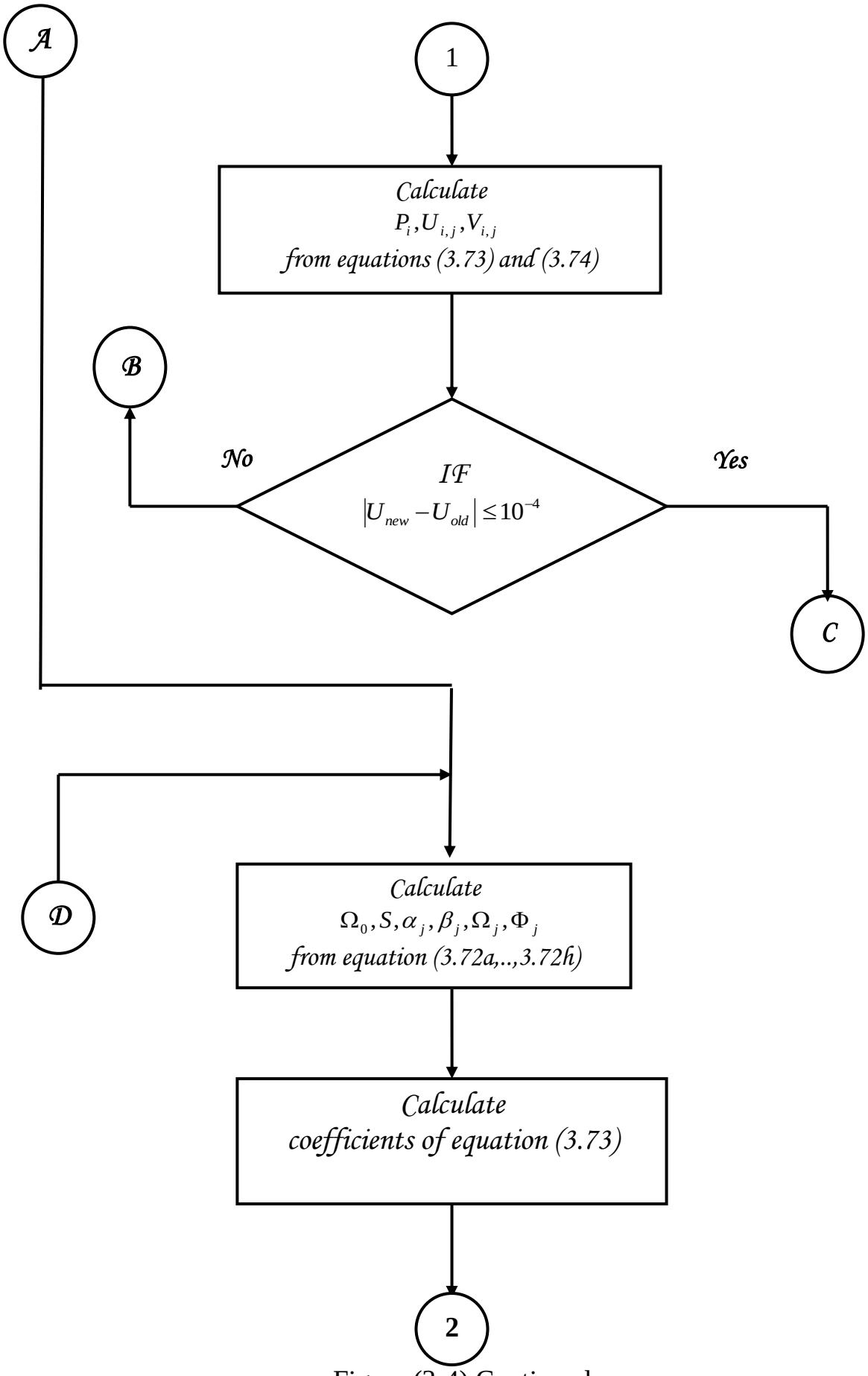

Figure (3-4) Continued

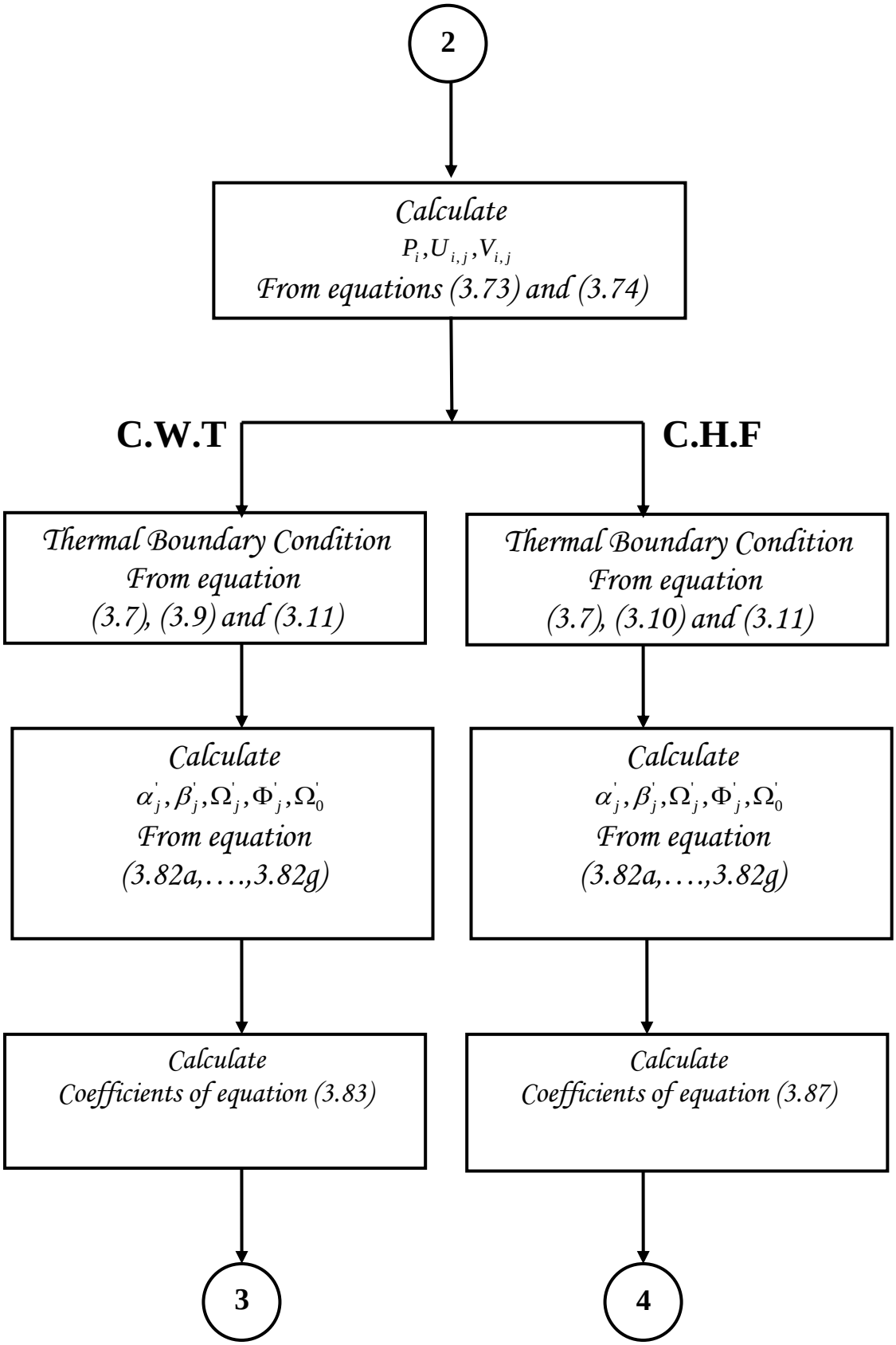

Figure (3-4) continued

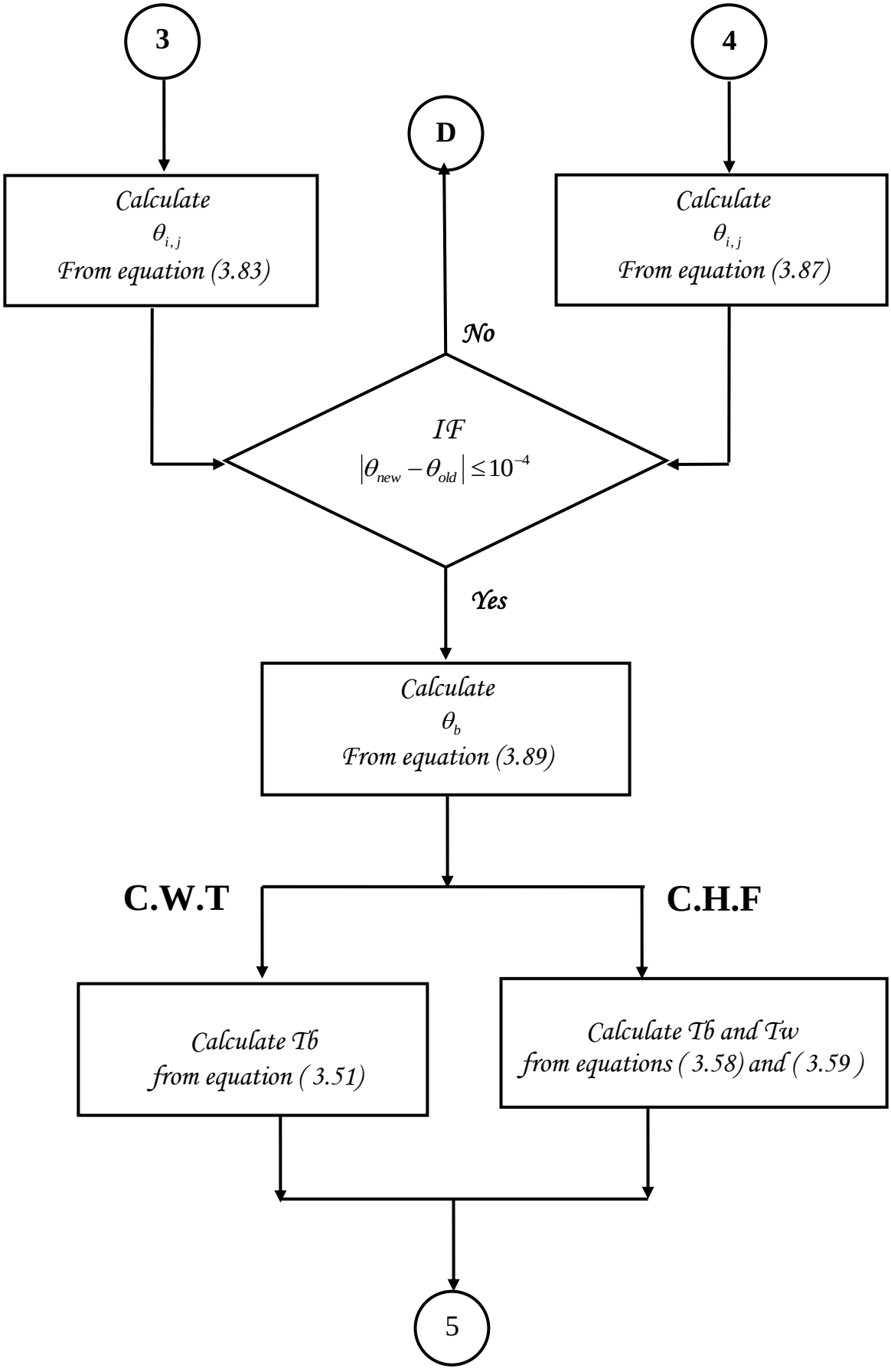

Figure (3-4) continued

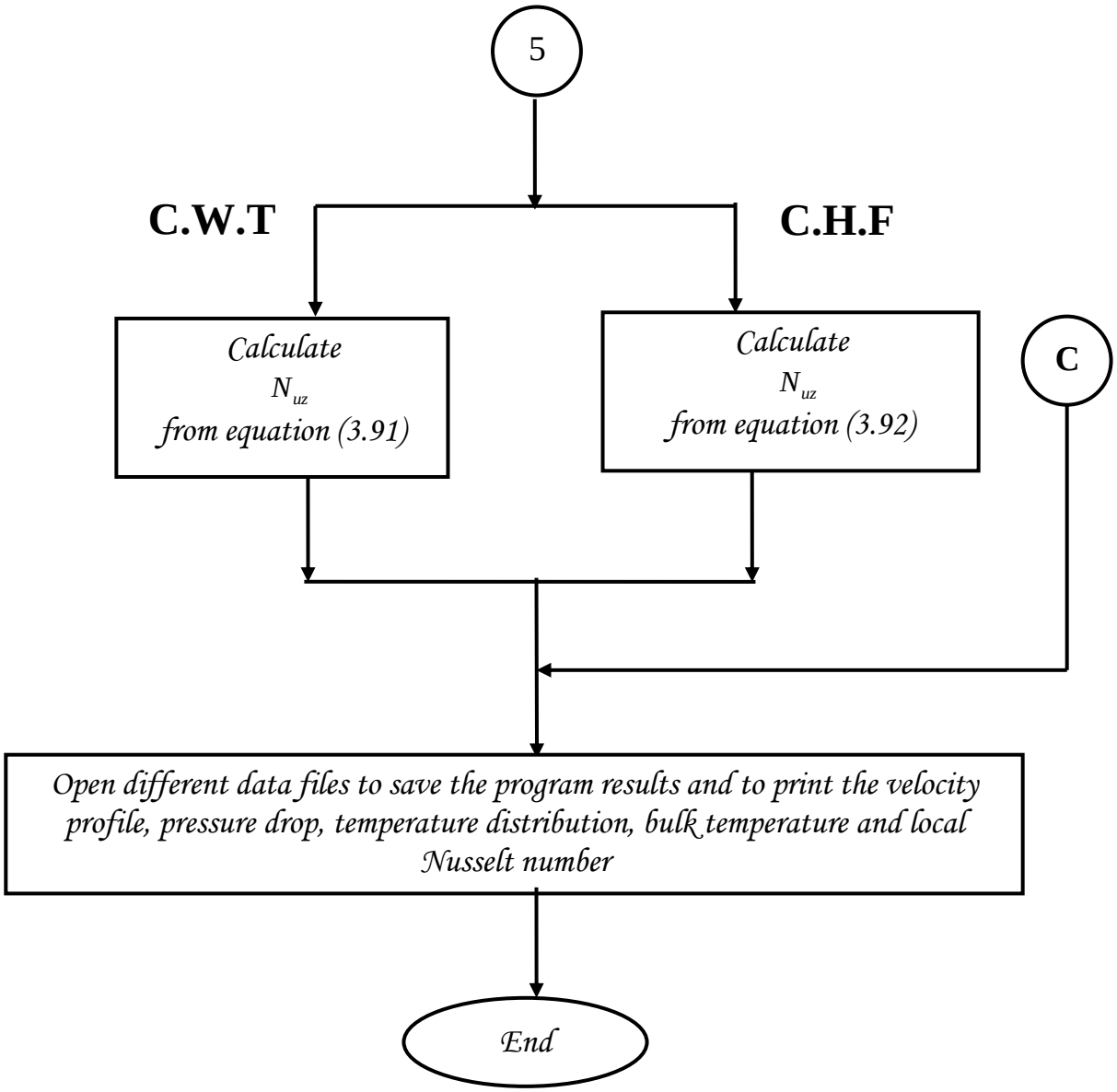

Figure (3-4) continued

Experimental Work

4.1. Introduction

The main purpose of the experimental work is to validate the investigation of the accordance between the experimental and the theoretical results. In addition the experimental work gives a clear idea and the whole information about the studied case.

In the present work, the main purpose of the experimental work is to build up and operate a simple and easy circulation loop in order to examine and study the pressure drop. These were done at the entrance region for water flow through circular tube with (d=3.125 and L=6.35 m) at different values of Reynolds number and compare it with the theoretical results. Also it has been measured the pressure drop at the fully developed regions for different values of Reynolds number within laminar and turbulent flow .

4.2. Experimental Set –up

An experimental rig was set up in the fluid mechanics laboratory at the university of Babylon. The pressure drop was measured at the entrance and fully developed region for water flow through circular tube with variation of water flow rates, which were pumping to the horizontal pipe. The experimental work on water flow facility shown in figure(4-1) as a photo graph and figure (4-2) as a schematic diagram.

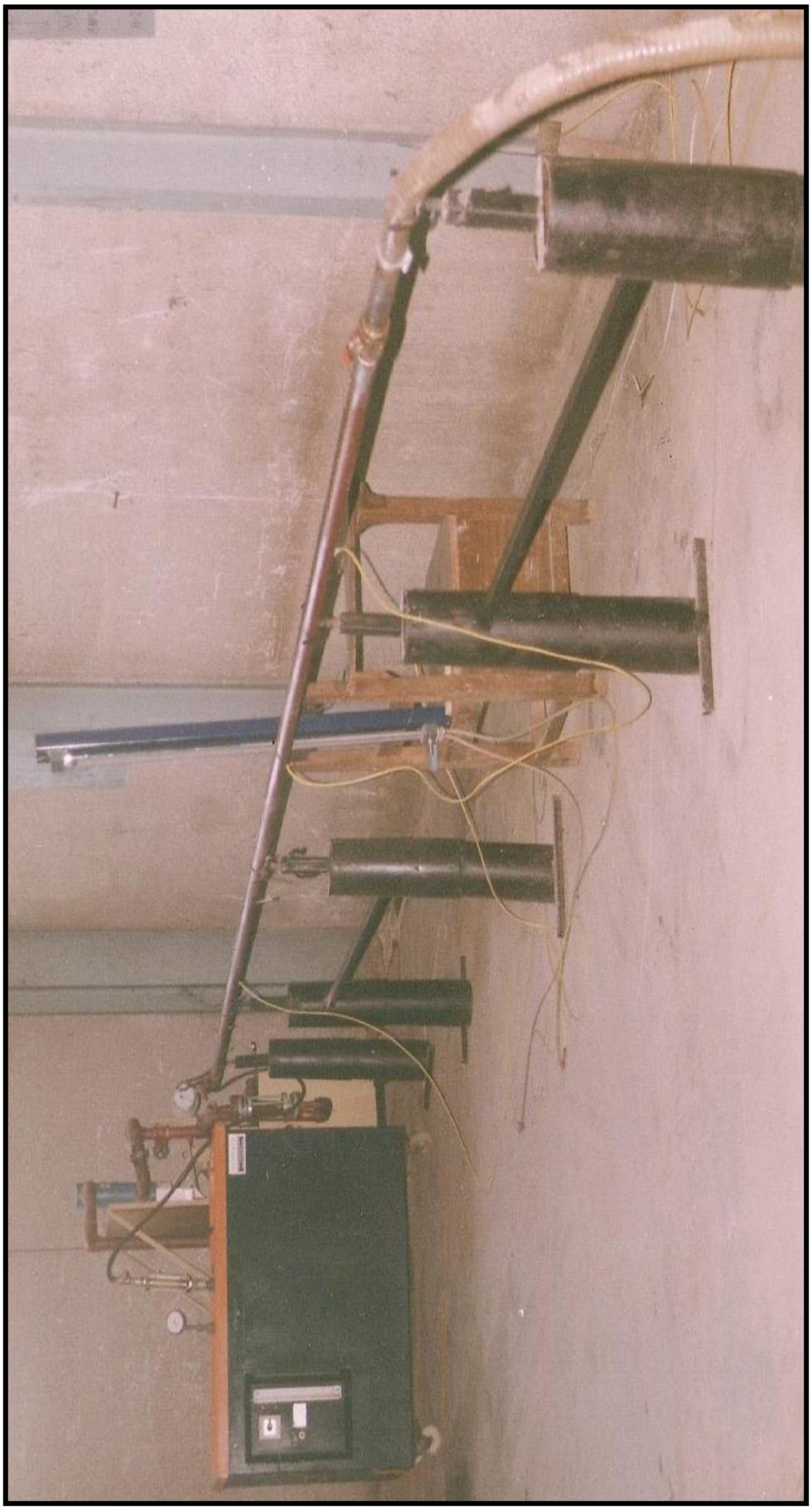

Figure (4-1) photograph for the experimental set up .

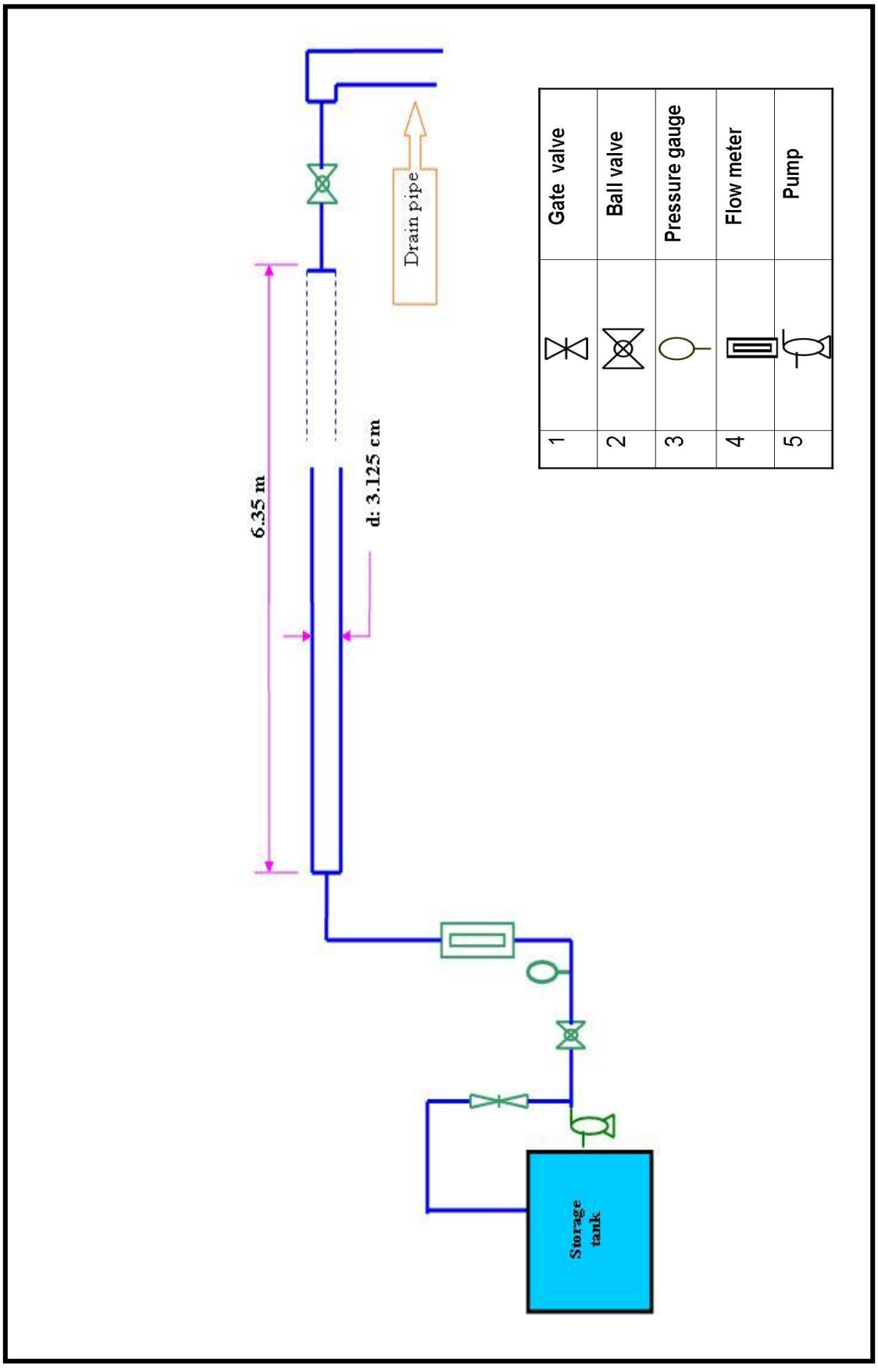

Figure (4–2) schematic diagram of the experimental setup

4.3. Equipments Used in This Technique

The flow test rig system consists of the following main parts :

1. Storage Tank

A water storage tank has a capacity of 100 liter with dimensions (65cm x 75cm x 30cm) was used to prepare the quantity of water required to flow through the used test section as shown in figure (4-3). The temperature of water in the tank will be constant by round the flow handily.

2. Pump

A centrifugal pump was used to pump the water via a flow control valve and a recycle valve so that the flow rate entering the test section can be controlled .The motor type (CMP/76 ,V=230, A=4.5 , Hz=60 and 2860 RPM) as shown in figure (4-3).

3. Flowmeter

A variable flow meter type (A1255 MK2) was used to provide the accurate measurement of the water flow rate. The actual flow rate was in the range from 1ℓ/min to 9ℓ/min as shown in figure (4-4).

4. Pressure Gauge

A pressure gauge of (0-3.5 bar) range was used to measure accurate values of pressure supply through the experiment work as shown in figure (4-5).

5. Test Section

It consist of 6.35 m of galvanized pipe of (3.125 cm diameter) as shown in figure (4-6), the reason to choose these dimensions of the used pipe was to get the suitable entrance length that was sufficient to measure the pressure drop within it . The distance between each two taps was 40 cm. In the entrance region the number of taps depended on the length of this region corresponding to each value of water flow rate and Reynolds number. While in the fully

developed region which away about 3.5 m corresponding to the maximum entrance length for laminar flow and 0.62 m for turbulent flow . The number of taps which were used in the fully developed region are four. All taps were connected with U-tube manometer to indicate the pressure losses. The properties of water through this test section at 25°C are Density (ρ) =1000 kg/m^3 , Viscosity (μ) = 8.96 x 10^{-4} kg/m.s

6. U-tube Manometer

It was used to measure the pressure drop between two points at the entrance and fully developed regions, as shown in figure (4-7). The fluid used in the manometer was air. The range of this manometer is between(0-1000)mm.

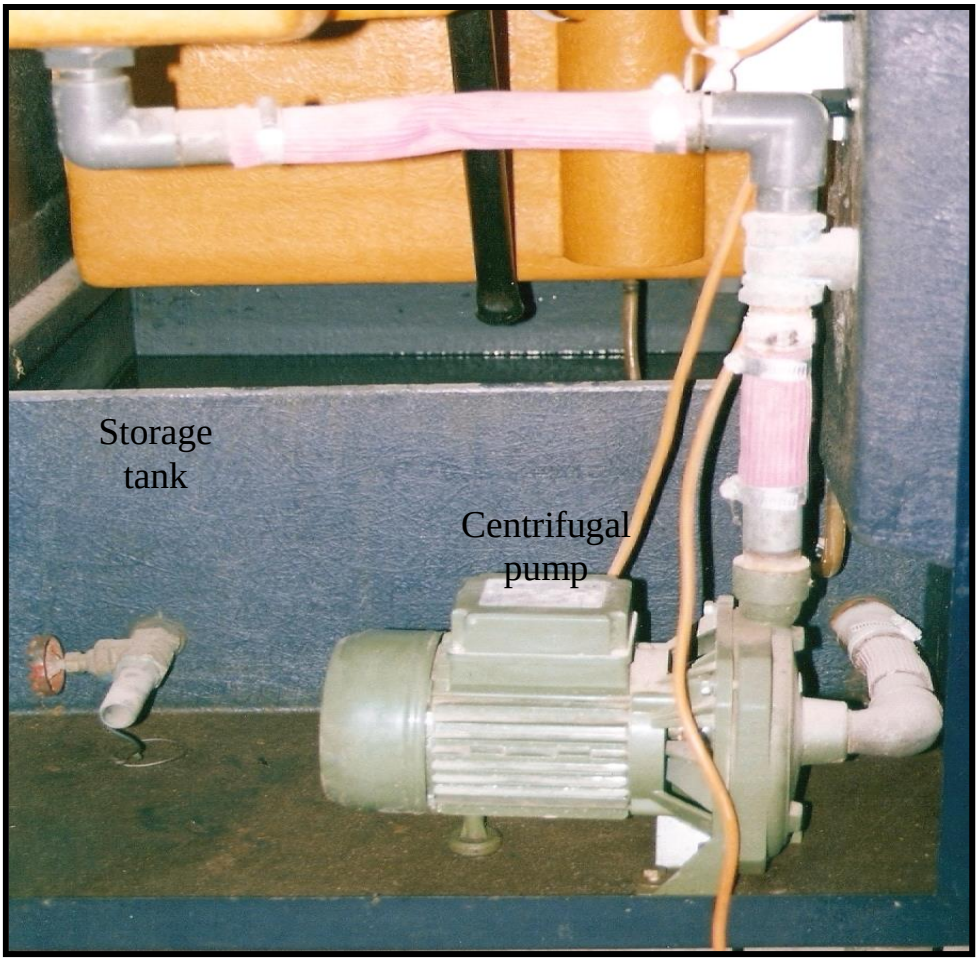

Figure (4-3) storage tank ,centrifugal pump .

Figure (4-4) water flow meter.

Figure (4-5) pressure gauge.

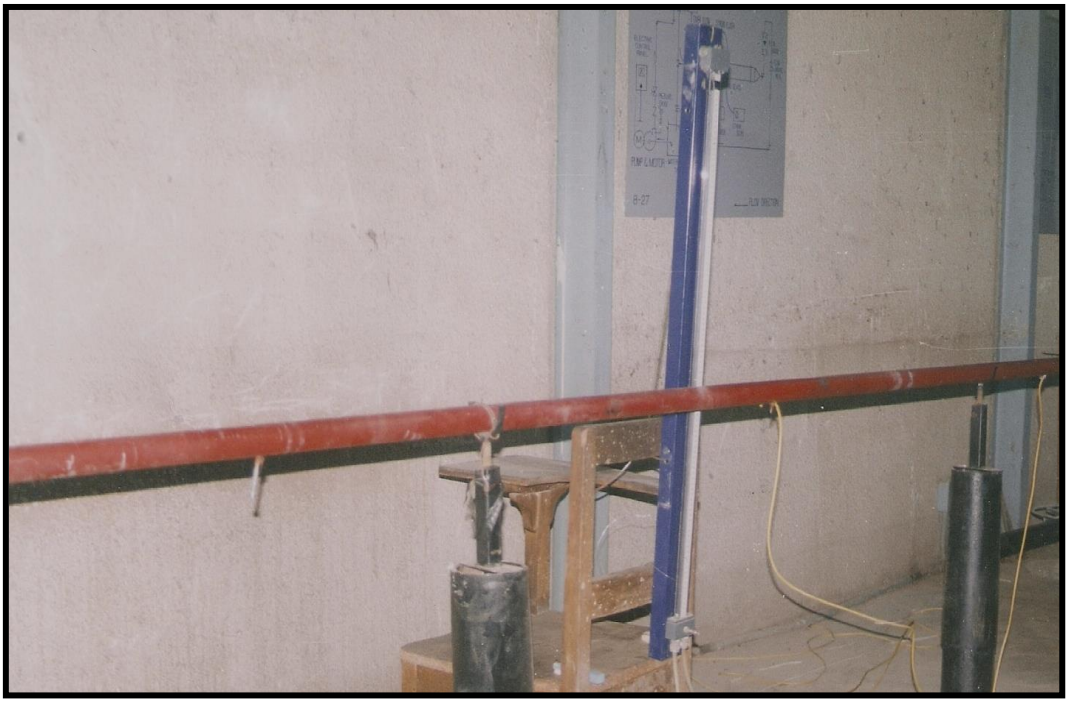

Figure (4-6) test section of the system.

.

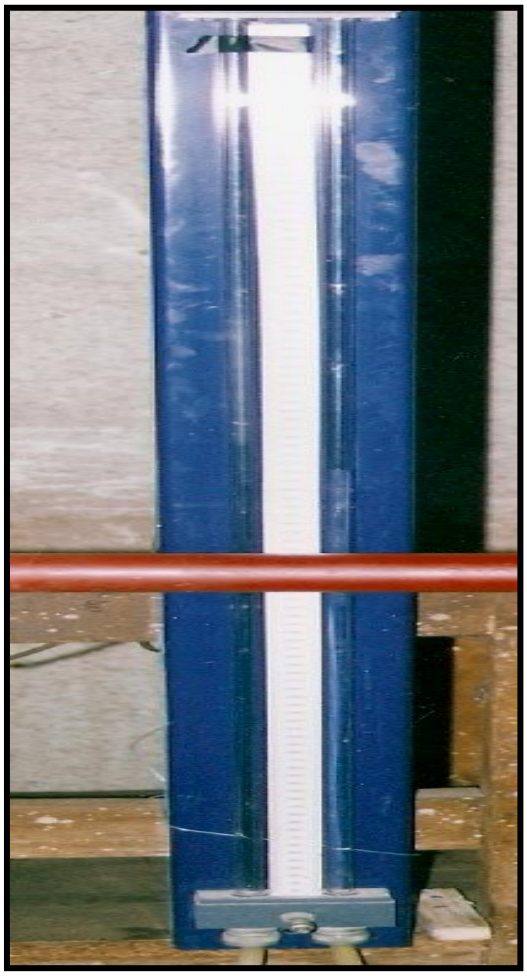

Figure (4-7) U-tube manometer

4.3. Devices Calibration

Calibration of the measuring equipments are very important in order to get the best reading accuracy for both the water flow rate and the pressure drop.

4.3.1. Water Flowmeter Calibration

The water flow meter was calibrated by measuring actual flow rate using stop watch and volumetric flask at each point of interest. These data are shown in table (4-1), allowing a calibration curve represented in figure (4-8).

Table (4-1) data of flowmeter calibration .

Flow meter readings (L/min)	1	2	3	4
Measured discharge (L/min)	1.2	2.2	3.2	4.2

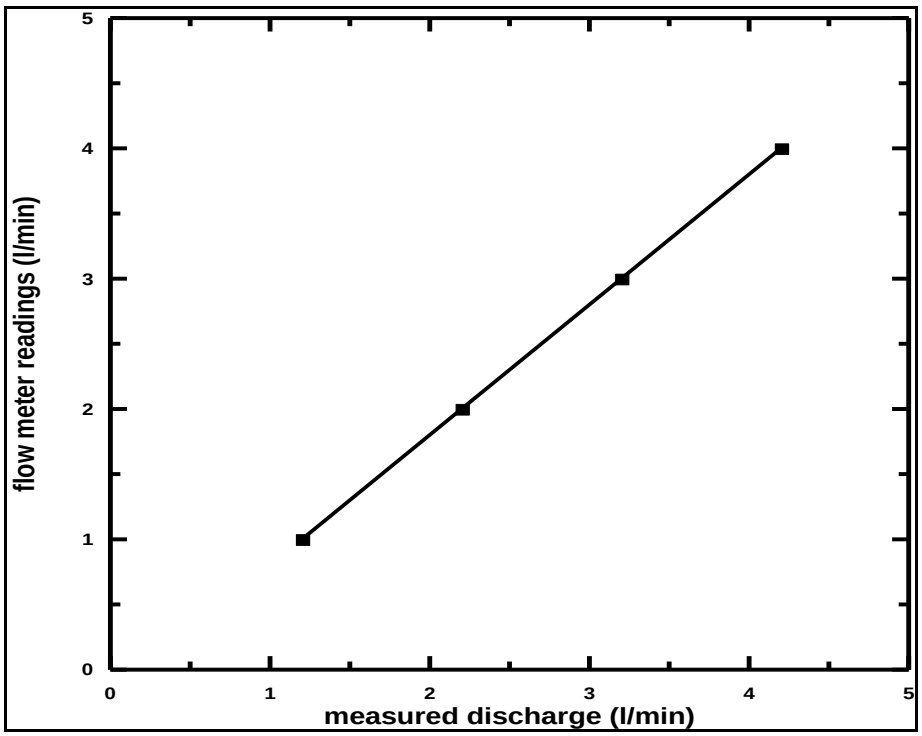

Figure (4-8) water flowmeter calibration.

So each value for water flow rate was intersecting with this curve to get the calibrated value .

4.3.2. Manometer Calibration

The manometer calibrate with a standard manometer .So the manometer readings for pressure drop comprised with standard manometer which used in another rig (Ref .44) . Figure (4-9) which represents curved calibrated for pressure taking from standard manometer. Figure (4-10) shows the calibration of the standard manometer with a pressure transducer. So each value of pressure drop was intersecting with this curve to get the calibrated value.

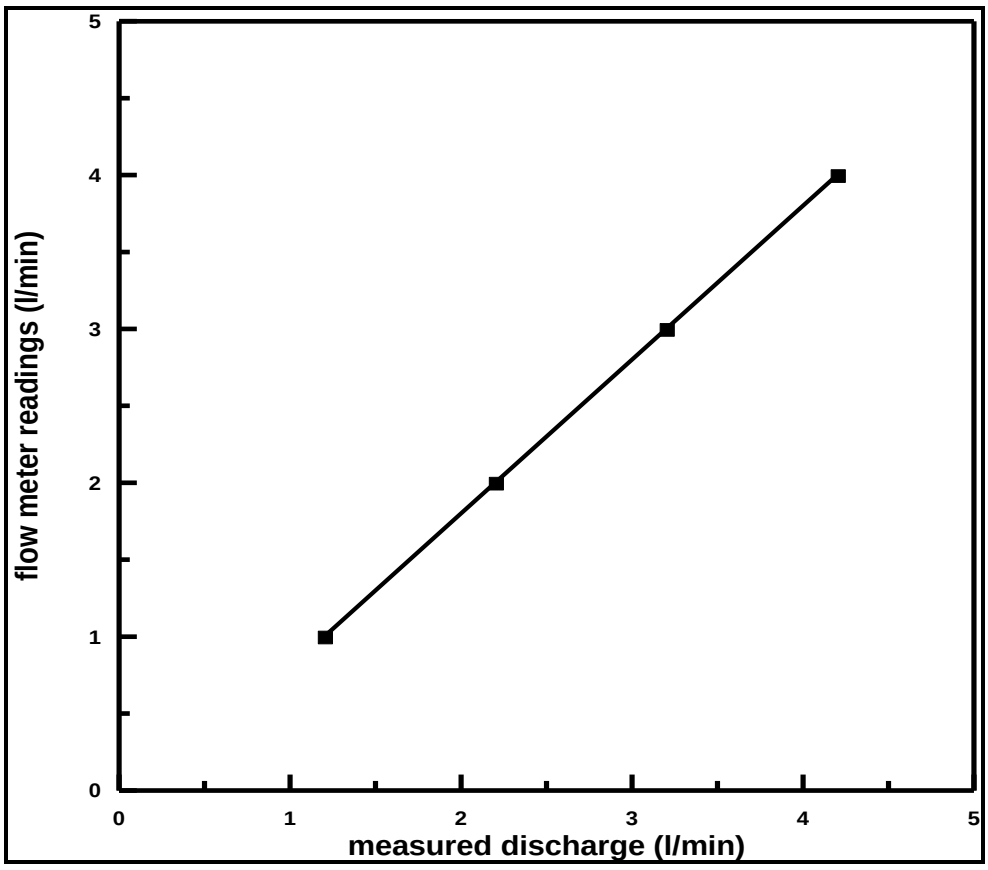

Figure (4-9) pressure manometer calibration.

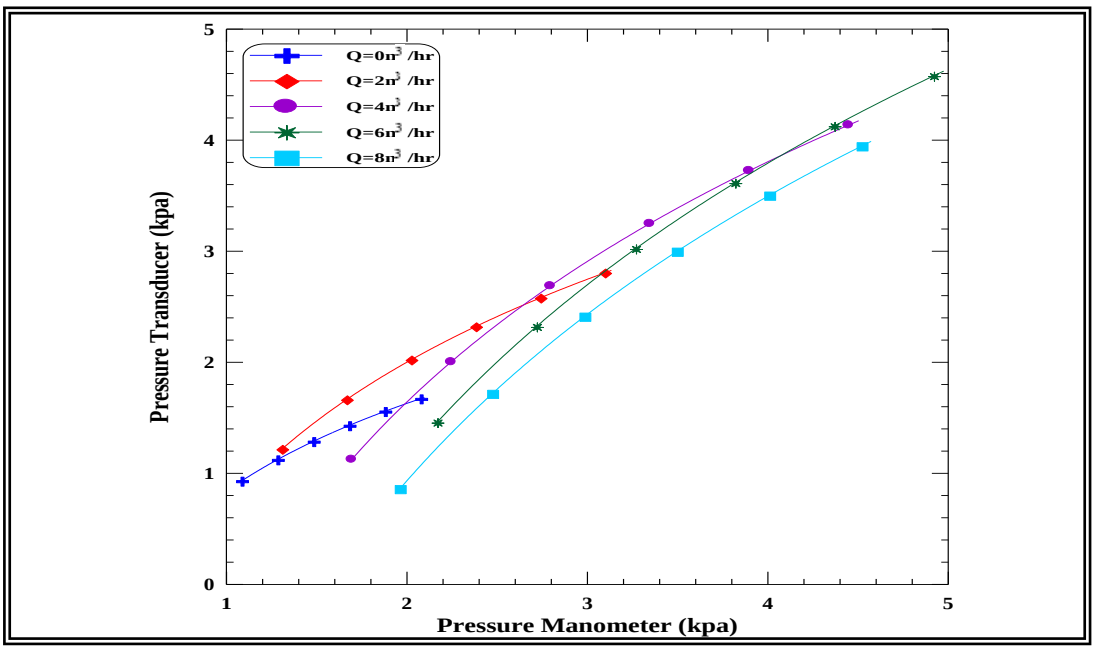

Figure (4-10) calibration of the standard manometer .

4.4. Experimental Procedure

1. After calibration process for both the water flow meter and the manometer was achieved, the water storage tank was filled with 100 litters of water. The experiments were carried out in pipe with nominal diameter of 3.125cm and length of 6.35 m . The fluid was allowed to flow through the pipe by operating the centrifugal pump. The flow rate was maintained constant by means the corresponding valves.

2. Measure the pressure drop at the entrance region for laminar water flow through the circular pipe, the number of taps used depend on the entrance region length corresponding to each value of water flow rate. The taps were fixed between the first two points on the test section for the first value of water flow rate to measure the pressure drop between them. Then taking another value of water flow rate and repeating the same procedure.

These reading were reported in table (4-2a) and (4-2b).

3. Measure the pressure drop at the entrance region for turbulent flow, the maximum entrance length for the taken water flow rates with respect to equation (4.2) is (0.62 m), since the distance between each two taps was 40 cm, so it was insufficient to measure the pressure difference along it .

4. Measure the pressure drop at the fully developed region for laminar flow. The taken region was away about 3.5m which represent the maximum entrance length corresponding to the maximum water flow rate (Q =3 L/min). So the reason to do that was to restrict our measurement in the fully developed region. Four taps were taken in this region. The first two points were connected to the manometer in order to measure the pressure difference between them. Same technique was done for the remaining points.
These reading were tabulated in table (4-3a and 4-3b).

5. Measure the pressure drop at the fully developed region for turbulent flow , the maximum entrance length corresponding to the maximum water flow rate (Q = 9 L/min) was about (o.62 m). The taken number of taps in this region was four too. The first two points were connected to the manometer to measure the pressure difference between them, and the same technique was done the remaining points.
These reading are tabulated in table (4-4 a) and (4-4 b).

4.5 Experimental Calculations

Analyzing the experimental work depends on calculation some items such as :

1. Entrance Length

Length of the pipe was based on literature concerning entry length in tubes [4]. The boundary layer was formed in the inlet of the pipe and was grown in the thickness until it fills the flow area ,or until extends to the center of the pipe. The flow is said to be fully developed when the velocity profile will not change downstream from this point .

Holman [3] has expressed the entrance length required for a fully developed velocity profile to form in laminar flow as:

$$\frac{Le}{d} = 0.05\,\mathrm{Re} \qquad \text{….(4.1)}$$

For turbulent flow, the relationship for entrance length reported by [5] as:

$$\frac{Le}{d} \cong 4.4\,Re^{\frac{1}{6}} \qquad \text{....(4.2)}$$

2. Average velocity

The water flow rate is read directly from the flow meter in l/min.The average velocity of water can be calculated from the relation as given in Ref. [4] as:

$$u = \frac{Q}{A} \qquad \text{….(4.3)}$$

Where A is the cross section area of the pipe.

3. Reynolds number

In fluid mechanics dimensionless numbers are introduced for scaling arguments and for defining the flow regime. In Newtonian Fluid Mechanics, the Reynolds number is a well-known dimensionless number. The Reynolds number appears because of writing the equations of motion in dimensionless

form. It shows up as the ratio of inertia forces versus viscous forces, [4] and at high Reynolds numbers, inertia plays a non-negligible role as:

$$\mathrm{Re} = \frac{\rho.u.d}{\mu} \qquad \text{....(4.4)}$$

4. Friction factor

Determination of the friction factor first requires a value for the head loss to be obtained . The head loss represents the conversion of mechanical energy to unwanted thermal energy . The thermal energy was generated as the flow interacts with the surface of the pipe producing heat and thus producing a pressure loss in the pipe .The pressure loss for the experiment was determined through the use of a manometer. The manometer reading was a direct measurement of the head loss that occurred between the two points of interest.

Therefore, An energy balance was shown below in equation (4.5) as mentioned in Ref.[37] for the determination of the head loss via energy per unit weight of flowing liquid between two locations of piping

$$\left(\frac{p_1}{\rho.g} + \frac{u_1^2}{2g} + z_1\right) - \left(\frac{p_2}{\rho.g} + \frac{u_2^2}{2g} + z_2\right) = H_l \qquad \text{….(4.5)}$$

The above equation can be simplified for the horizontal pipe $(z_1 = z_2)$ and for a pipe of constant diameter ($u_1 = u_2$) .At steady state flow rate, thus reducing the head loss to the change in pressure due to the frictional effects from the pipe wall was explained by Ref.[3] as :

$$H_l = \frac{\Delta P}{\rho.g} \qquad , \; H_l = f\,\frac{L}{D}\frac{u^2}{2g} \qquad \text{….(4.6)}$$

So

$$f = \frac{\Delta P}{\frac{1}{2}\rho.u^2}\frac{D}{L} \qquad \text{….(4.7)}$$

In the above , f is the Moody or Darcy friction factor . Measurements of the relation between the pressure drop and the flow rate were called "gross-flow measurements".

For a fully developed laminar flow , the theoretical Darcy friction factor was reported by Ref. [3] as :

$$f_{laminar} = \frac{64}{\mathrm{Re}} \qquad \text{….(4.8)}$$

It is noted that the friction coefficient ,also called Fanning friction factor was defined by Ref. [43] as

$$C_f = \frac{\tau_w}{0.5\rho.u^2} \qquad \text{….(4.9)}$$

For fully developed laminar circular pipe flow [43],

$$C_f = \frac{f}{4} = \frac{16}{\mathrm{Re}} \qquad \text{….(5.10)}$$

After transition to turbulence at a certain Reynolds number, a Newtonian solvent follows the empirical Blasius friction law for a smooth pipe [3] as:

$$f_{turbulent} = \frac{0.316}{\mathrm{Re}0.25} \qquad \text{….(4.11)}$$

These calculation has been done for both laminar and turbulent flow in tables (4-5) and (4-6) respectively.

Table (4-2a) experimental measurements of pressure drop (mm) at the entrance region of laminar water flow .

Q l/min	ΔP_1 mm	ΔP_2 mm	ΔP_3 mm	ΔP_4 mm	ΔP_5 mm	ΔP_6 mm	ΔP_7 mm
1	0.5	1					
1.4	1	2.5	3				
1.8	1.5	3	3.5	4			
2.2	2	3.5	4	4.5	5		
2.6	2.5	4	5.5	6	7.5	8	
3	3	5	6.5	7.5	8	9.5	10.5

Table (4-2b) experimental calculations of pressure drop (pa) at the entrance region of laminar water flow .

Q l/min	ΔP_1 pa	ΔP_2 pa	ΔP_3 pa	ΔP_4 pa	ΔP_5 pa	ΔP_6 pa	ΔP_7 pa
1	5	10					
1.4	10	25	30				
1.8	15	30	35	40			
2.2	20	35	40	45	50		
2.6	25	40	55	60	75	80	
3	30	50	65	75	80	95	105

Table (4-3 a) experimental measurements of pressure drop (mm) at the fully developed region of laminar water flow .

Q l/min	$\Delta P'$ mm	$\Delta P''$ mm	$\Delta P'''$ mm
1	1	0.5	0.5
1.4	2	2	1.5
1.8	3	2.5	2.5
2.2	4	4.5	3.5
2.6	5	5.5	5
3	7	7.5	6.5

Table (4-3 b) experimental calculations of pressure drop (pa) at the fully developed region of laminar water flow .

Q l/min	$\Delta P'$ pa	$\Delta P''$ pa	$\Delta P'''$ pa
1	10	5	5
1.4	20	20	15
1.8	30	25	25
2.2	40	45	35
2.6	50	55	50
3	70	75	65

Table (4-4 a) experimental measurements of pressure drop (mm) at the fully developed region of turbulent water flow .

Q l/min	$\Delta P'$ mm	$\Delta P''$ mm	$\Delta P'''$ mm
5	8.5	8	8
6	9	9.5	9
7	9.5	10	9
8	11.5	11	10.5
9	12	12.5	11.5

Table (4-4 b) experimental calculations of pressure drop (pa) at the fully developed region of turbulent water flow .

Q l/min	$\Delta P'$ pa	$\Delta P''$ pa	$\Delta P'''$ pa
5	85	80	80
6	90	95	90
7	95	100	90
8	115	110	105
9	120	125	115

Table (4-5) experimental calculations for laminar water flow.

Q l/min	u m/s	Re	f	Le m
1	0.0217	758.8	0.084	1.18
1.4	0.0304	1060.26	0.060	1.65
1.8	0.039	1360.2	0.047	2.1
2.2	0.0478	1667.1	0.038	2.6
2.6	0.0565	1970.5	0.032	3.08
3	0.065	2267	0.028	3.5

Table (4-6) experimental calculations for turbulent water flow.

Q l/min	u m/s	Re	f	Le m
5	0.108	3766.7	0.0403	0.54
6	0.130	4534	0.038	0.56
7	0.152	5301.3	0.037	0.57
8	0.174	6068.6	0.0358	0.58
9	0.196	6836	0.0347	0.62

Results and Discussion

PART-I

5.1 Theoretical Investigation

5.1.1 General

This part presents the results obtained from theoretical work which include dimensionless velocity profile, dimensionless axial velocity, dimensionless pressure drop, dimensionless temperature distribution, dimensionless bulk temperature, bulk temperature and local Nusselt number for two cases of heating, constant wall temperature and constant heat flux. It has been selected three values of Reynolds number (Re=500),(Re=1000) and (Re=2000) and three values of Prandtl number (Pr=1), (Pr=2.5) and (Pr=5) for both cases of heating.

Results of the theoretical work include the following parameters:

5.1.2 Hydrodynamics Parameters

5.1.2.1 Dimensionless Velocity Profile Development

Figures (5-1a), (5-1b)and (5-1c) show the dimensionless velocity profiles which represent the developing stages of the hydrodynamic boundary layer for different Reynolds numbers at the entrance region of the circular tube. Assuming uniform velocity ($U=U_o=1$) over its inlet section. The dimensionless velocity at the walls equals zero, because of adhesion, and increase as moving far away from the wall until it reaches maximum velocity at the center of the tube.

The dimensionless velocity component of fluid in z-direction (U), must then increasing gradually until it reaches the fully developed region. Figure (5-1 a) at Re=500 shows that the boundary layer reaches the fully developed region at approximately (Le/2a=25) ,Figure (5-1 b) at Re=1000 shows that the boundary layer reaches the fully developed region at approximately (Le/2a=50). Figure(5-1 c) at Re=2000 shows that the boundary layer reaches the fully developed region at approximately (Le/2a=100).

So it can be concluded that the boundary layer was developed faster for lower Reynolds number ,i.e, the hydrodynamic entrance length increases with increasing of Reynolds number. The dimensionless velocity profiles become fully developed at approximately :

$$\frac{L_e}{2a} = 0.05\,\mathrm{Re}$$

In the fully developed region the dimensionless vertical velocity component (V) is zero .The gradient of the dimensionless axial velocity component $\left(\frac{\partial U}{\partial Z}\right)$ are everywhere zero , where the boundary layer reaches to its final form at this point . Hence the dimensionless axial velocity component depends only on (R),then U(Z,R)=U(R).

Therefore, the shape of the boundary layer becomes constant after a certain distance from the entrance. This distance was called the hydrodynamic entrance length (Le), it denotes the starting of the fully developed region . The velocity distribution becomes parabolic over the section of the tube . So ,the flow field is similar for all studied cases.

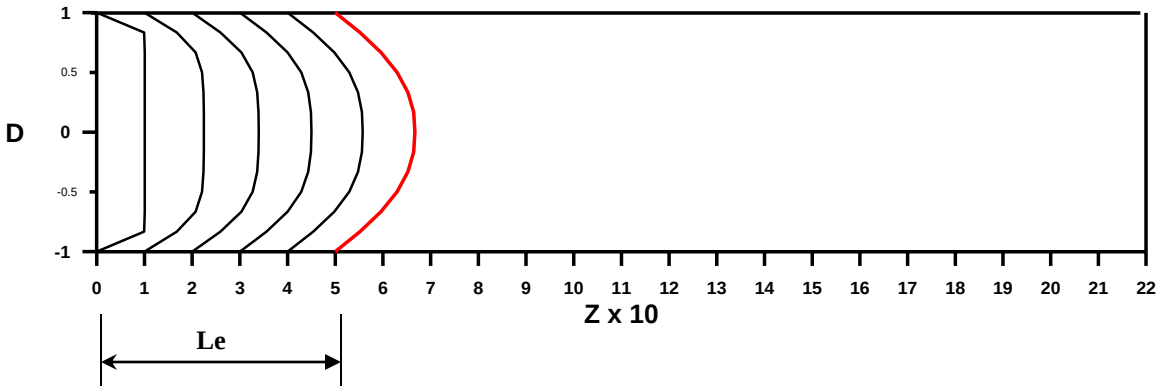

a) Re =500 Le/2a = 0.05 x 500 = 25

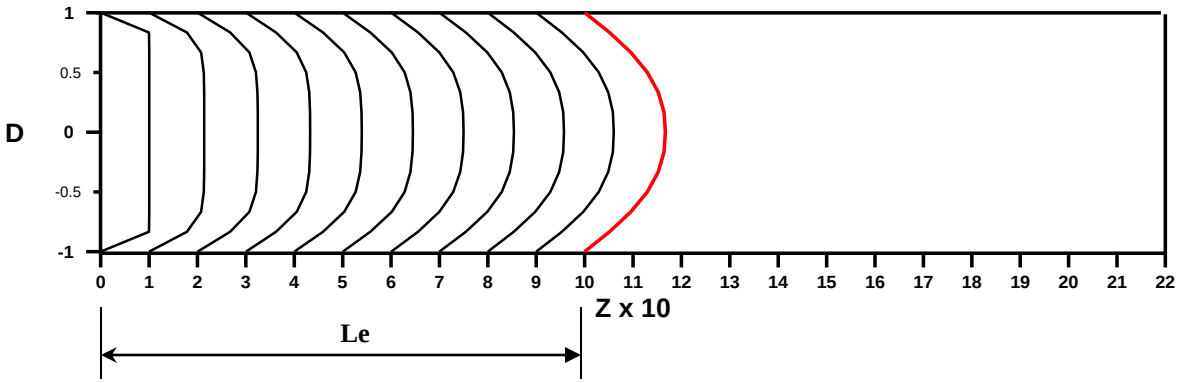

(b) Re =1000 Le/2a = 0.05 x 1000 = 50

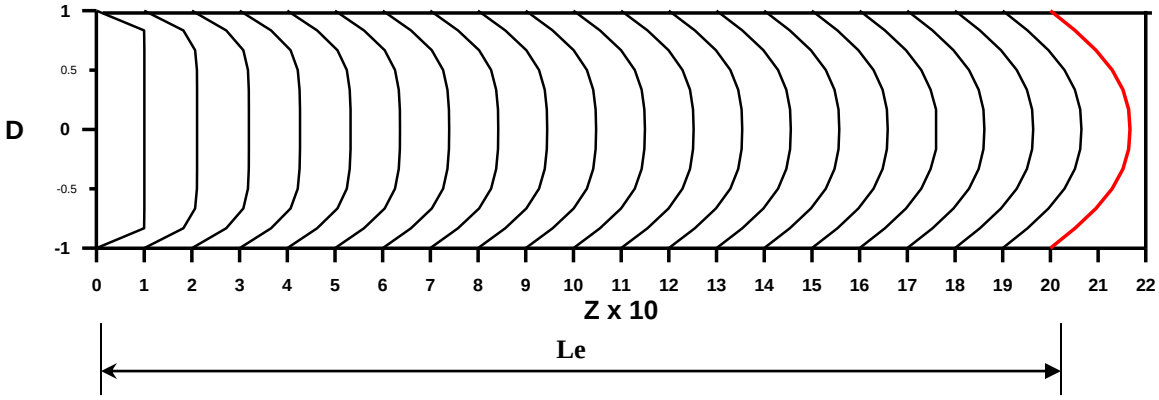

(c) Re =2000 Le/2a = 0.05 x 2000 = 100

Figure (5-1) hydrodynamic dimensionless velocity profile development through circular tube for different Reynolds numbers.

Figure (5-2) shows the dimensionless velocity profiles in the developing and fully developed region for the three values of Reynolds numbers . In developing region ,for each value of Reynolds number the dimensionless velocity at the wall equals zero and increases with moving far away from the wall until it reaches a maximum value at the centerline of the tube. The maximum velocity increases with decreasing Reynolds number but the velocity near the wall increases with increasing Reynolds number. In other hand it can be seen that the relative boundary layer thickness decreases with increasing Reynolds number ,this is due to decreasing of friction factor.

In the fully developed region the velocity at the wall equals zero and increases gradually until it reach a maximum value at the centerline of the tube. The dimensionless velocity profile in the fully developed region is the same for each value of Reynolds number ,i.e. the velocity profiles in the fully developed region is independent of Reynolds number.

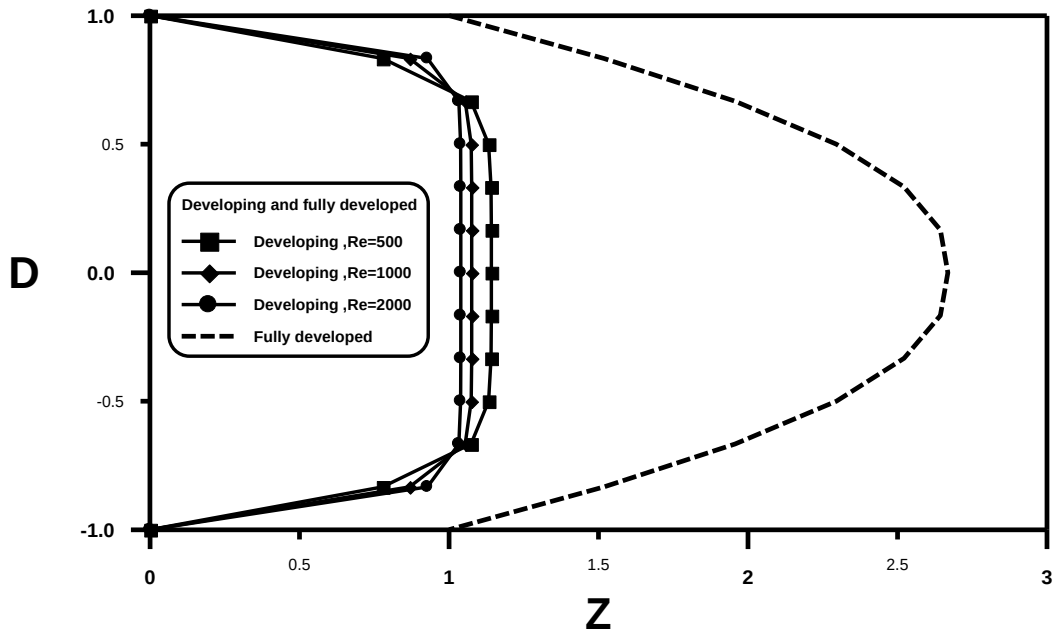

Figure (5-2) developing and fully developed dimensionless velocity profile through circular tube for different Reynolds numbers.

5.1.2.2 Dimensionless Axial Velocity

Figure (5-3) shows the dimensionless axial velocity at the entrance region of circular tube at (R=0) for three values of Reynolds numbers. For each value of Reynolds number, it can be seen that the dimensionless central velocity has an initial value of (U=1) at (Z=0) where ($U = U_0$),and then increases with increasing (Z) until it has a maximum value of (U=1.67) at the fully developed region. It can be noted that for Re=500 the dimensionless central velocity reaches to this maximum value at approximately (Le/2a=25),for Re=1000 it reaches at approximately (Le/2a=50) while for Re=2000 it reaches to this value at approximately (Le/2a=100). So it can be concluded that ,at minimum Reynolds number the dimensionless central velocity reaches to a maximum value faster than that at maximum Reynolds number depending on the value of entrance length with respect to equation (1.1) due to increasing of friction factor.

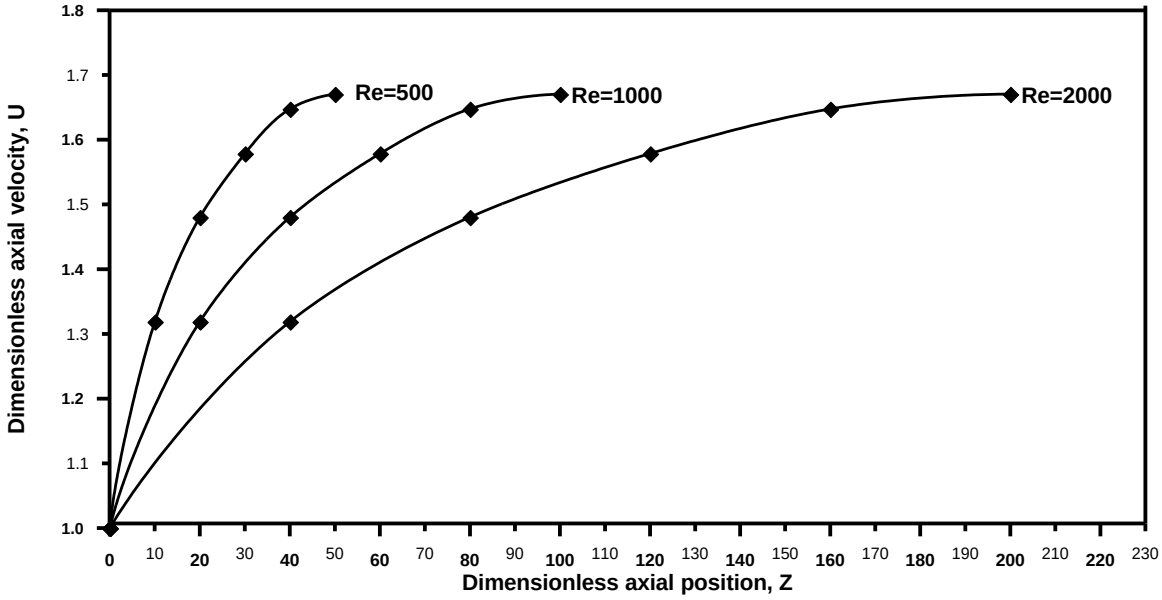

Figure (5-3) dimensionless axial velocity through circular tube for different Reynolds numbers.

5.1.2.3 Dimensionless Pressure Drop

Figure (5-4) shows the dimensionless pressure drop (P) through the entrance region of circular tube for three values of Reynolds number . For each value of Reynolds number, the dimensionless pressure drop starts from a value of zero at the inlet section of the tube where ($P = P_o$) and then increases until it have a maximum value at the fully developed region depending on the dimensionless hydrodynamic entrance length (Le/2a) which increase with increasing the Reynolds number with respect to (equation 1.1). This increase is due to decreasing of local pressure (p) with respect to increasing of friction factor(equation 4.8).

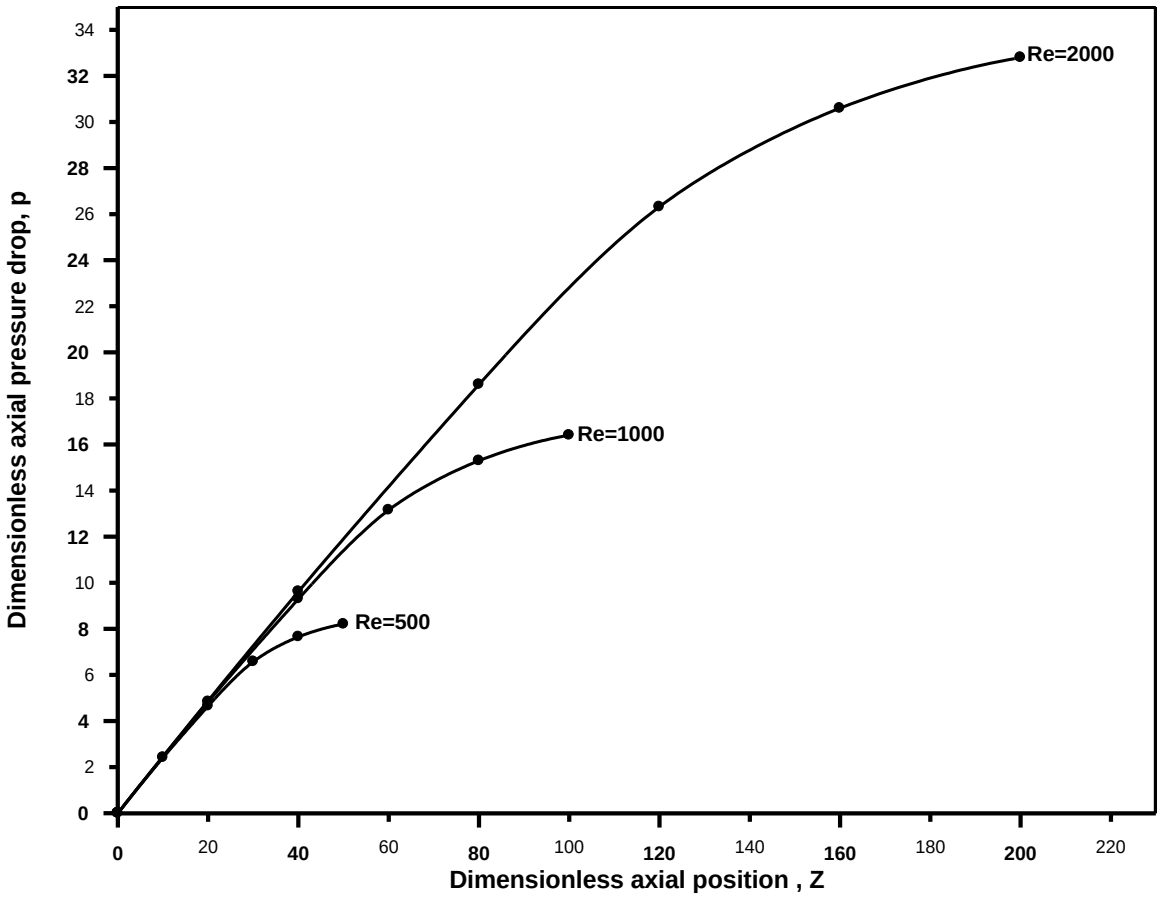

Figure (5-4) axial dimensionless pressure drop through circular tube for different Reynolds numbers.

5.1.3 Thermal Parameters

5.1.3.1 Dimensionless Temperature Distribution

A- At Constant Wall Temperature ($\theta = \frac{T - T_w}{T_o - T_w}$ **)**

All figures from (5-5a) to (5-7c) show the dimensionless temperature distribution for constant wall temperature boundary condition. These were manifested stages of developing of the thermal boundary layer for different Reynolds numbers (Re=500), (Re=1000) and (Re=2000), and for different Prandtl numbers (Pr=1), (Pr=2.5) and (Pr=5) at the entrance region of the circular tube .

The dimensionless temperature in the inlet section is uniformly distributed over its section and that its magnitude is ($\theta=\theta_o=1$).

The dimensionless temperature at the walls equals zero where (T=Tw) but increases as moving far away from the tube surface , until it approaches the maximum value at the centerline of the tube.

Where $\Pr = \frac{\nu}{\alpha} =$ kinematics viscosity / thermal diffusivity ,so as (α) increase ,Prandtl number will decrease , so the temperature profile will reach to the fully develop region faster .This can be noted as analyzing figures (5-5a) to (5-7c) .Figures (5-5 a) to (5-5 c) show the dimensionless temperature distribution at (Re=500)and different Prandtle numbers ,it can be noted that the thermal boundary layer approaches to the fully developed region faster as Prandtl number decreasing ,and the same is true for figure (5-6) at (Re=1000) and (5-7) at (Re=2000).

In other hand ,if we compare these figures ,it can be noted that the thermal boundary layer approaches faster to the fully developed region as decreasing of Reynolds number, this is due to increasing of friction factor which leads to decreasing of mean velocity (u) .

So , it can be concluded that the shape of the thermal boundary layer will be fixed after a certain distance from the entrance, which is called the thermal entry length(Le_t). It was noted that the thermal entrance length increases with increasing of Reynolds and Prandtl numbers. The temperature distribution becomes fully developed at approximately :

$$\frac{L_{et}}{2a} = 0.05\,\mathrm{Re}\,.\,\mathrm{Pr}$$

In the fully developed region the gradient of the dimensionless temperature $\left(\frac{\partial\theta}{\partial Z} = 0\right)$,this is because the value of fluid temperature reaches to the value of the wall temperature. However, the flow field is similar for all studied cases.

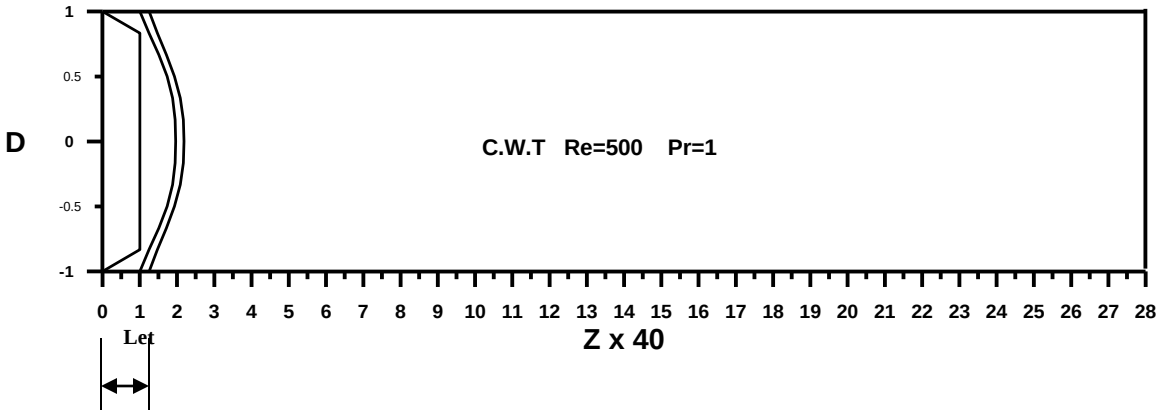

(a) Pr=1 Let/2a=0.05 x 500 x 1=25

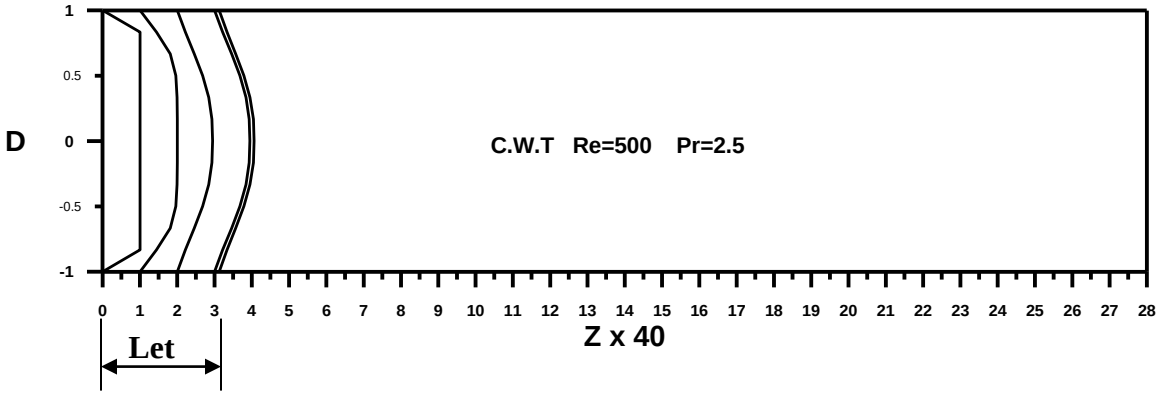

(b) Pr=2.5 Let/2a=0.05 x 500 x 2.5=62.5

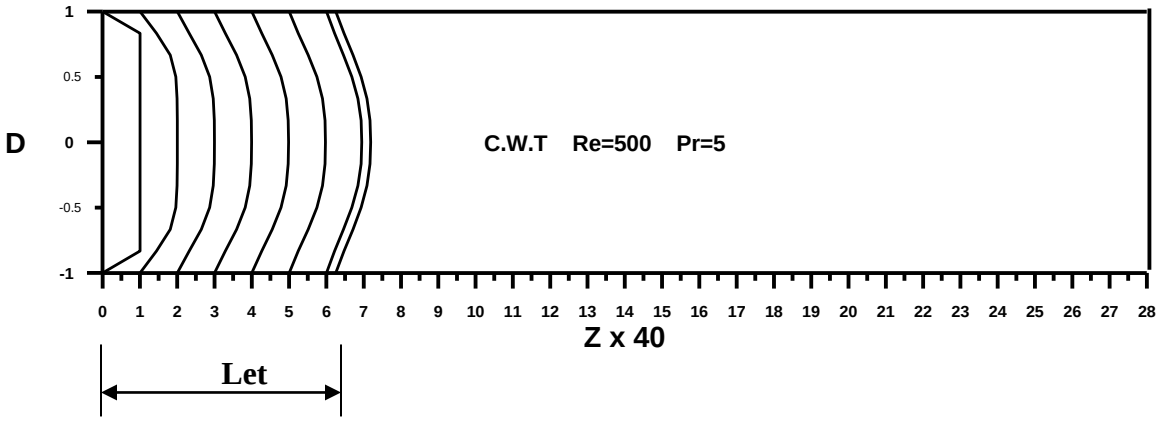

(c) Pr=5 Let/2a=0.05 x 500 x 5=125

Figure (5-5) dimensionless thermal temperature distribution development through circular tube for constant wall temperature ,Re=500 , different Prandtl number.

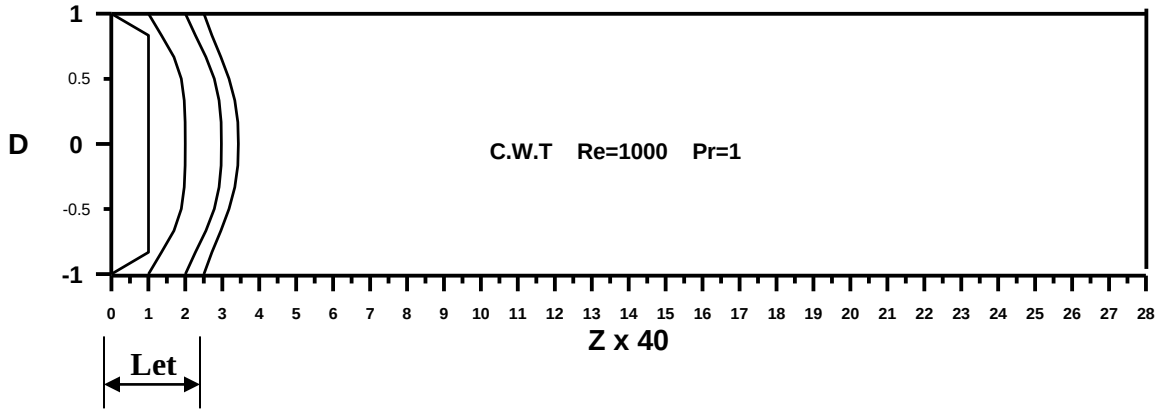

(a) Pr=1 Let/2a=0.05 x 1000 x 1=50

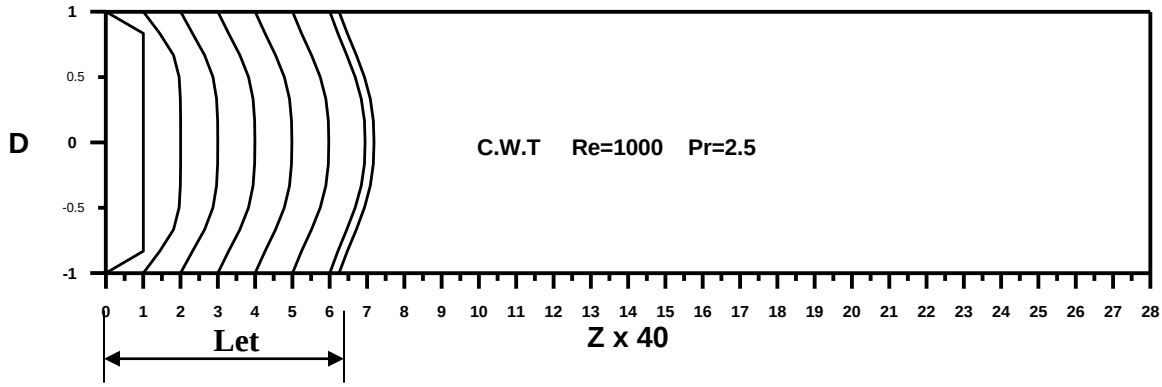

(b) Pr=2.5 Let/2a=0.05x1000x2.5=125

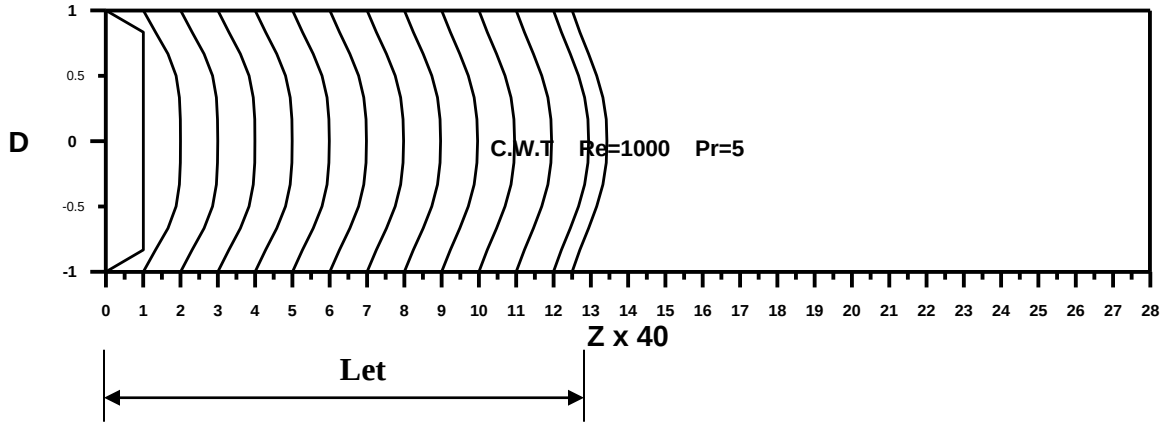

(c) Pr=5 Let/2a=0.05 x 1000 x 5=250

Figure (5-6) dimensionless thermal temperature distribution development through circular tube for constant wall temperature ,Re=1000, different Prandtl number

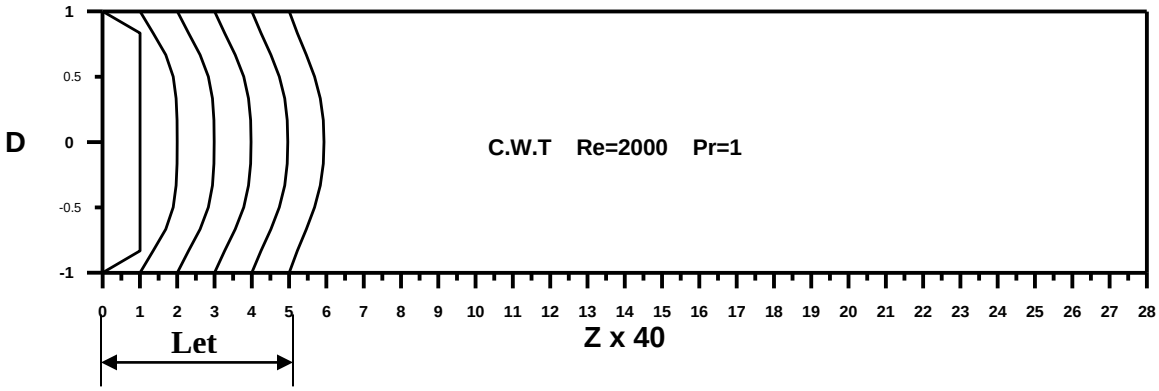

(a) Pr=1 Let/2a=0.05 x 2000 x 1=100

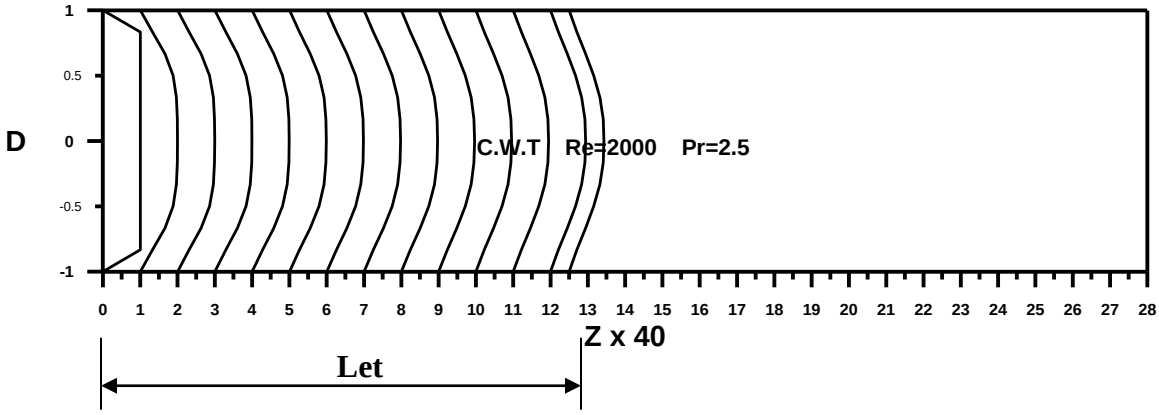

(b) Pr=2.5 Let/2a=0.05 x 2000 x 2.5=250

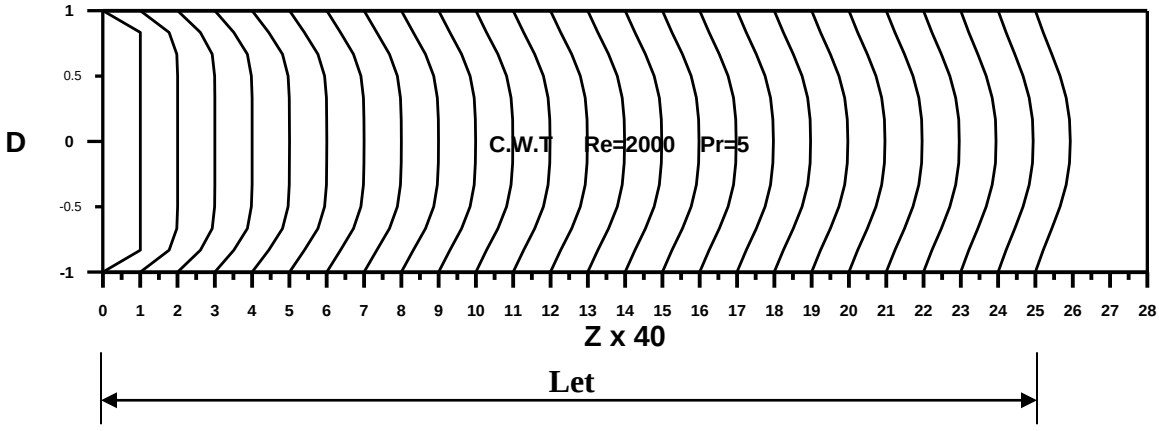

(c) Pr=5 Let/2a=0.05 x 2000 x 5=500

Figure (5-7) dimensionless thermal temperature distribution development through circular tube for constant wall temperature ,Re=2000, different Prandtl number

Figures (5-8), (5-9)and (5-10) show the developing and fully developed dimensionless temperature distribution through circular tube for constant wall temperature boundary condition and different Prandtl numbers. Figure (5-8) at Reynolds number (Re=500), figure (5-9) at Reynolds number (Re=1000)and figure (5-10) at Reynolds number (Re=2000).

In developing region the dimensionless temperature at the walls equals zero where (T=Tw) and increases as moving far away from the tube surface until it reach its maximum value at the centerline of the tube. The maximum dimensionless temperature increases with increasing Prandtl number. The dimensionless temperature near the wall increases with increasing Prandtl and Reynolds numbers.

In fully developed region the dimensionless temperature at the wall equals zero and increases gradually until it reach its maximum value at the centerline of the tube.

Dimensionless temperature distribution in fully developed region is parabolic for constant wall temperature. All values of Reynolds and Prandtl numbers have the same dimensionless temperature distribution in fully developed region because the thermal boundary layer reach to its final form at this region where the fluid temperature reaches to a value equal approximately to the value of the wall temperature . So the temperature distribution in fully developed region is independent of Reynolds and Prandtl numbers.

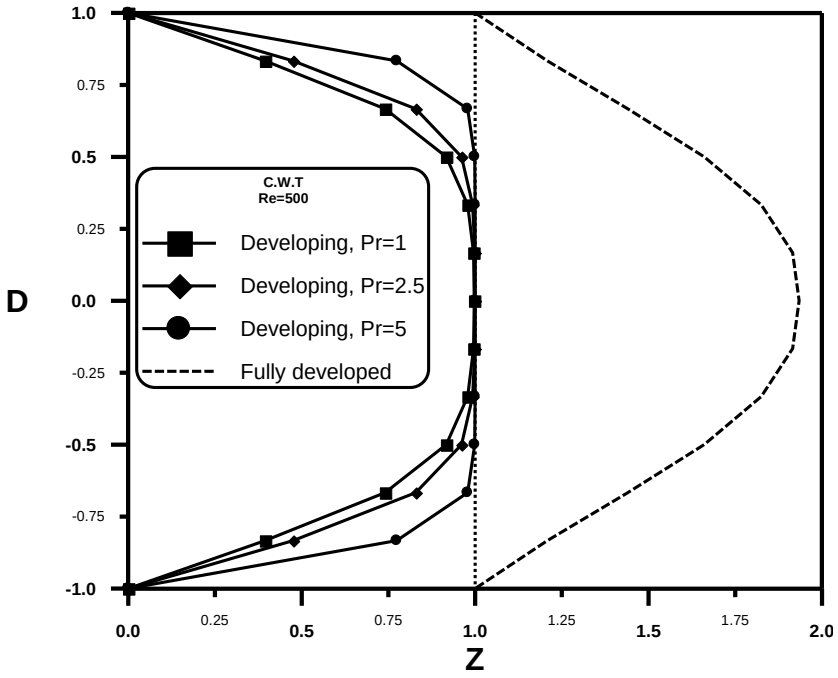

Figure (5-8) developing and fully developed dimensionless temperature distribution through circular tube for constant wall temperature ,Re=500, different Prandtl number.

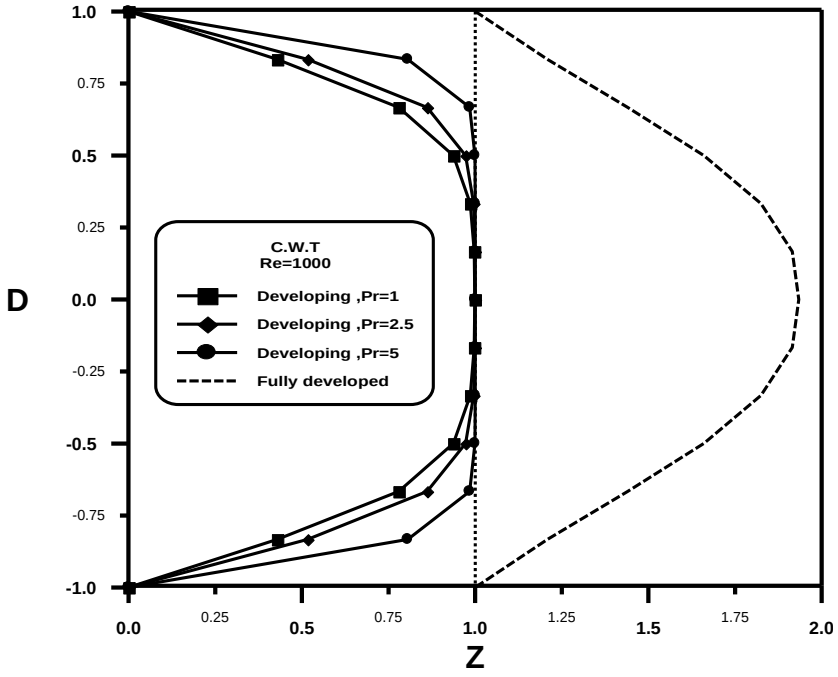

Figure (5-9) developing and fully developed dimensionless temperature distribution through circular tube for constant wall temperature ,Re=1000, different Prandtl number.

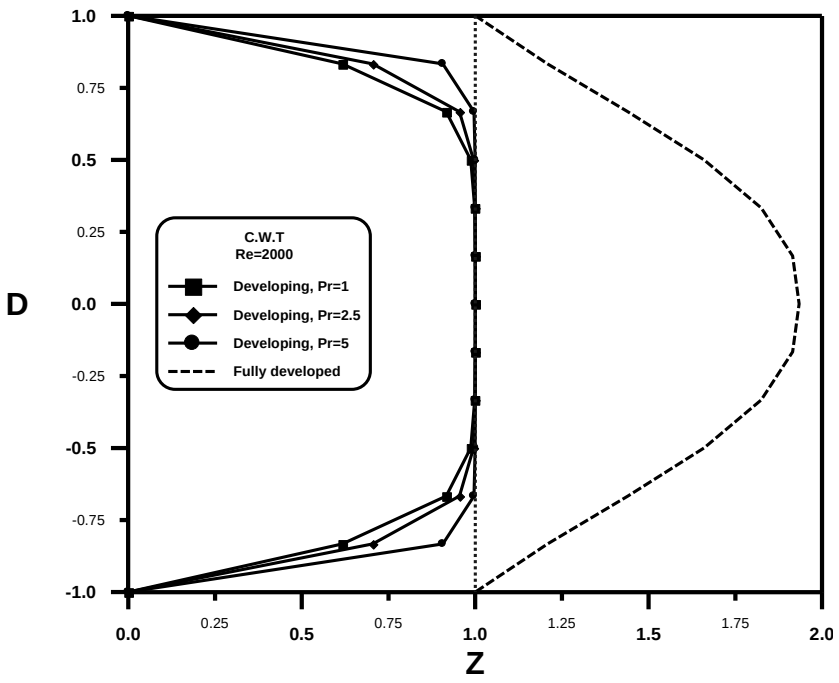

Figure (5-10) developing and fully developed dimensionless temperature distribution through circular tube for constant wall temperature ,Re=2000 , different Prandtl number.

Figures (5-11), (5-12)and (5-13) show the developing and fully developed dimensionless temperature distribution through circular tube for constant wall temperature boundary condition and different Reynolds numbers, figure (5-11) at Prandtl number (Pr=1), figure (5-12) at Prandtl number (Pr=2.5) and figure (5-13) at Prandtl number (Pr=5).

In developing region the dimensionless temperature at the walls equals zero and increases gradually until it reaches maximum value at the centerline of the tube, the maximum dimensionless temperature depend on Reynolds and Prandtl numbers .The dimensionless temperature for constant wall temperature near the wall increases with increasing Prandtl and Reynolds numbers. For higher Reynolds(must Re < 2300 for laminar flow) and Prandtl numbers the dimensionless temperature distribution is flatter than that for lower Reynolds and Prandtl numbers ,this is

because of the longer thermal entry length for the former which need more distance to reach to the parabolic fully developed profile.

In fully developed region the dimensionless temperature at the wall equals zero and increases until the maximum dimensionless temperature at the centerline of the tube. Dimensionless temperature distribution is parabolic for constant wall temperature. All values of Reynolds and Prandtl numbers have the same dimensionless temperature distribution in fully developed region (the temperature distribution in fully developed region is independent on Reynolds and Prandtl numbers).

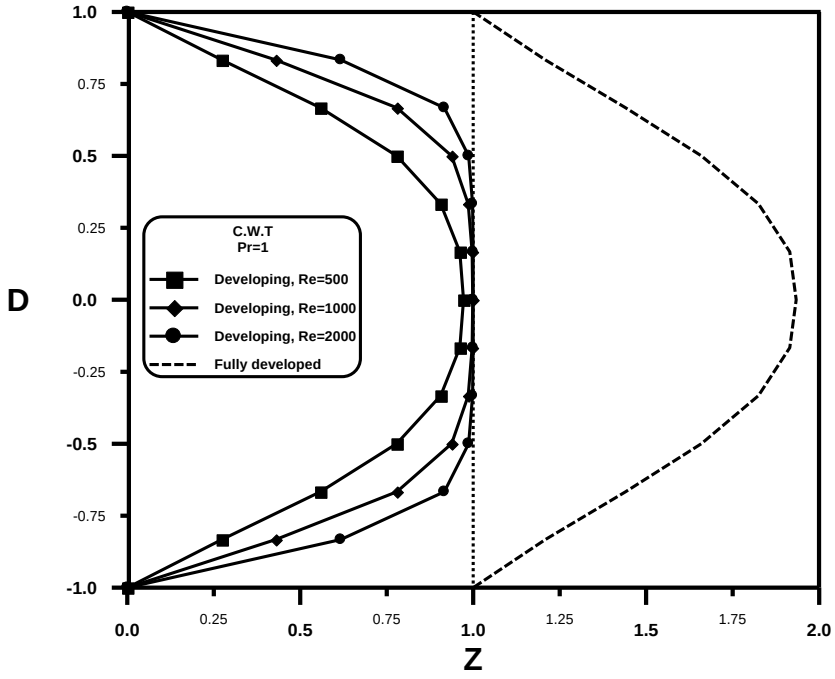

Figure (5-11) developing and fully developed dimensionless temperature distribution through circular tube for constant wall temperature ,Pr=1 , different Reynolds number

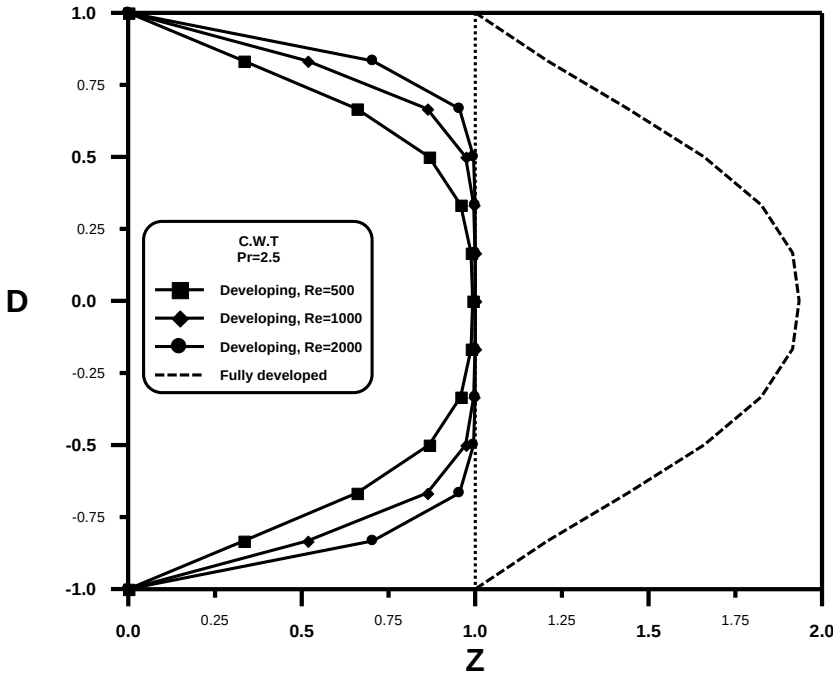

Figure (5-12) developing and fully developed dimensionless temperature distribution through circular tube for constant wall temperature Pr=2.5 , different Reynolds number

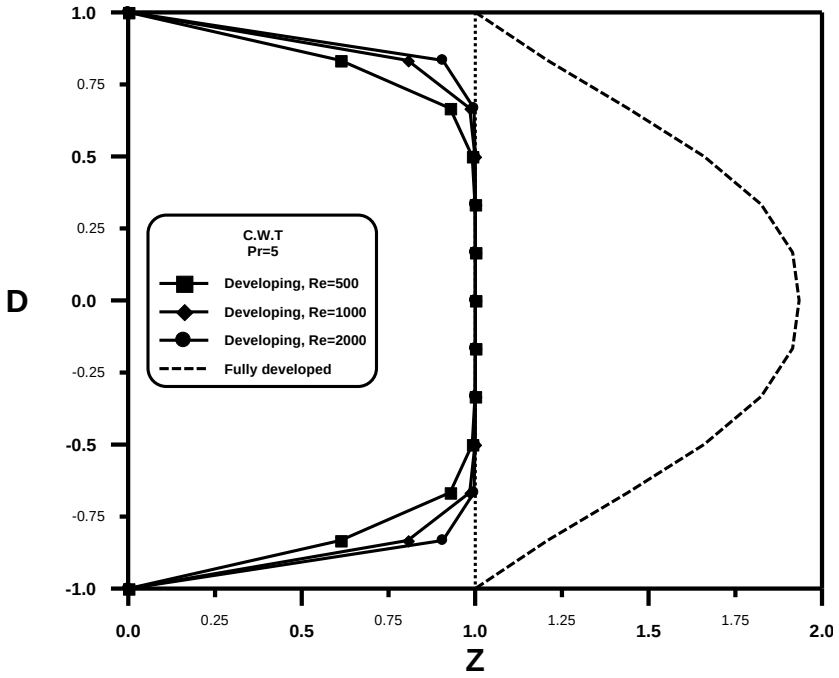

Figure (5-13) developing and fully developed dimensionless temperature distribution through circular tube for constant wall temperature , Pr=5 , different Reynolds number

B – At Constant Heat Flux ($\theta = \frac{k}{q''a}(T - T_o)$)

All figures from (5-14a) to (5-16c) show the dimensionless temperature distribution for constant heat flux boundary condition. These were manifest stages of developing of the thermal boundary layer for different Reynolds and Prandtl numbers at the entrance region of the circular tube .

The dimensionless temperature at the inlet section is zero over its section where (T=To).

The dimensionless temperature at the walls equals maximum value due to the effect of heat flux but decreases gradually with moving far away from the surface until it approaches minimum value at the centerline of tube.

Where $\Pr = \frac{\nu}{\alpha} =$ kinematics viscosity / thermal diffusivity ,so as (α) increase ,Prandtl number will decrease , so the temperature profile will reach to the fully develop region faster .This can be noted as analyzing figures (5-14a) to (6-16c). Figures (5-14 a) to (5-14 c) show the dimensionless temperature distribution at (Re=500)and different Prandtle numbers ,it can be noted that the thermal boundary layer approaches to the fully developed region faster as Prandtl number decreasing ,and the same is true for figure (5-15) at (Re=1000) and (5-16) at(Re=2000).

In other hand ,if we compare these figures we can noted that the thermal boundary layer approaches faster to the fully developed region as decreasing of Reynolds number.

The shape of the thermal boundary layer will be fixed after a certain distance from the entrance. This distance is called the thermal entry length(Le_t). It was noted that the thermal entrance length increases with increasing of Reynolds and Prandtl numbers. It can be seen that the thermal boundary layer is developed faster for lower

Reynolds and Prandtl numbers. The temperature distribution becomes fully developed at approximately :

$$\frac{L_{et}}{2a} = 0.05\,\mathrm{Re}.\mathrm{Pr}$$

In the fully developed region the gradient of the dimensionless temperature $\left(\frac{\partial \theta}{\partial Z} = 0\right)$, because the fluid temperature reaches to a value close to the wall temperature. However the flow field is similar for all studied cases.

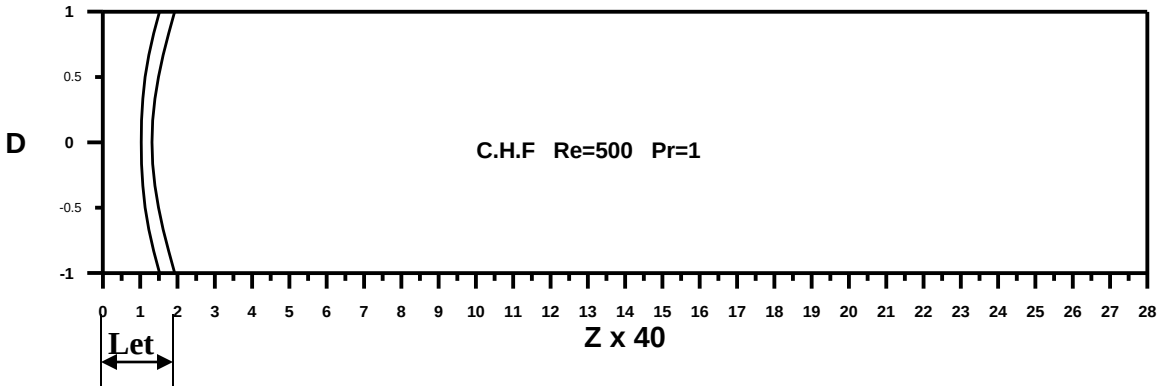

(a) Pr=1 Let/2a=0.05 x 500 x 1=25

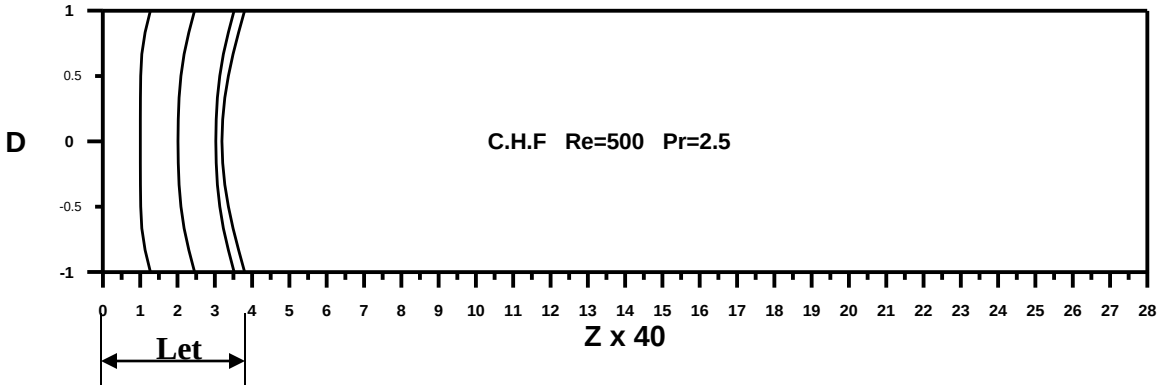

(b) Pr=2.5 Let/2a=0.05 x 500 x 2.5=62.5

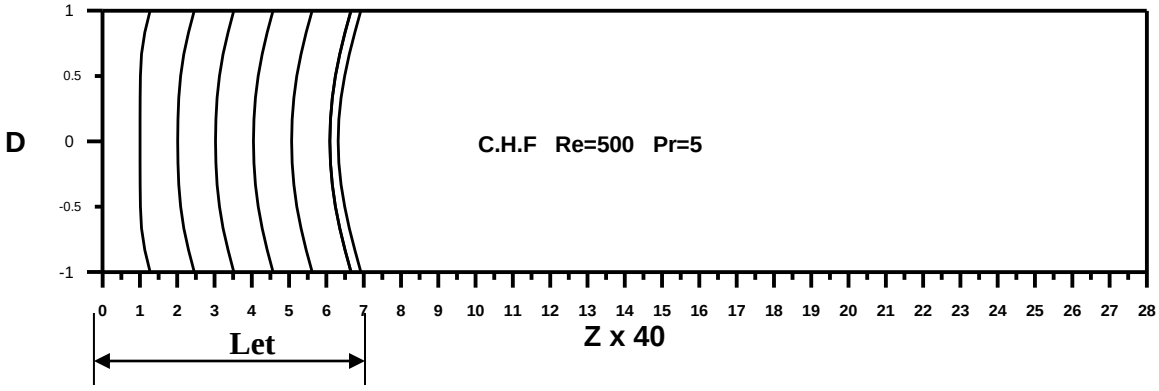

(c) Pr=5 Let/2a=0.05 x 500 x 5=125

Figure (5-14) thermal temperature distribution development through circular tube for constant heat flux ,Re=500 ,
different Prandtl number

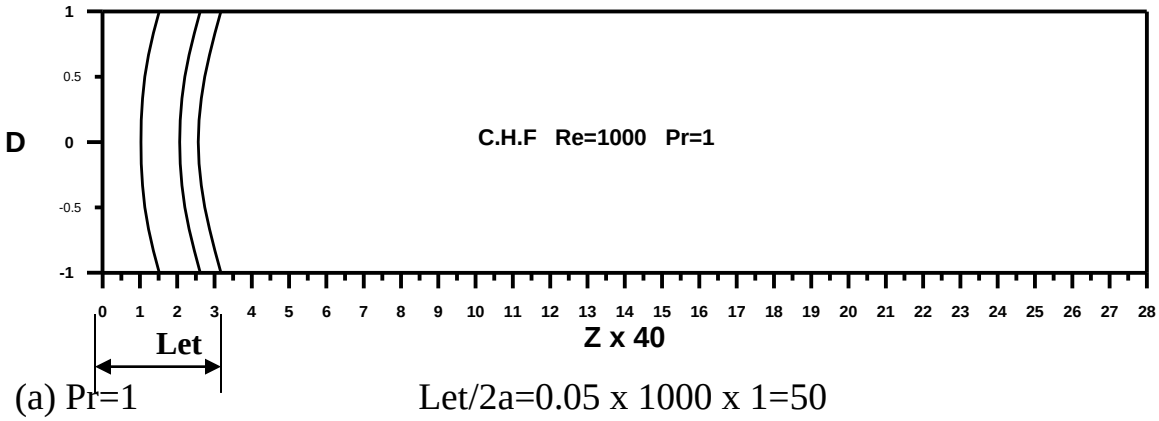

(a) Pr=1 Let/2a=0.05 x 1000 x 1=50

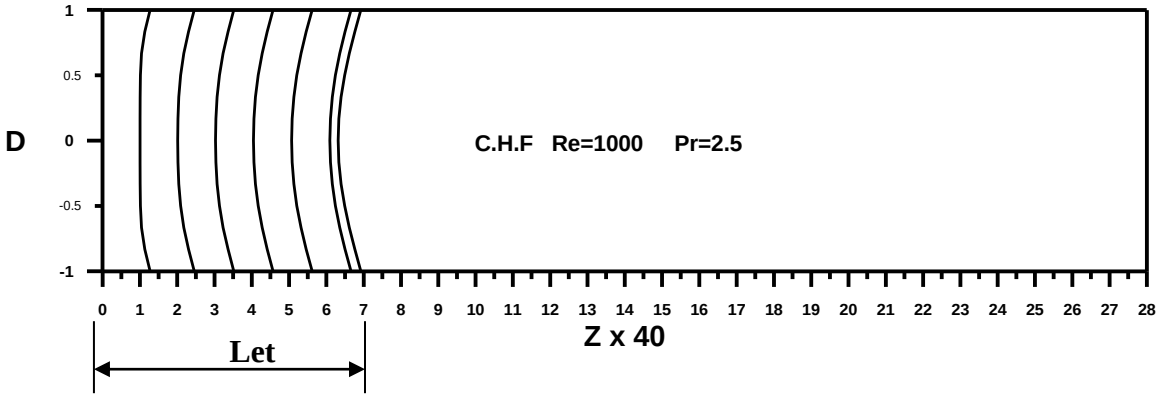

(b) Pr=2.5 Let/2a=0.05 x 1000 x 2.5=125

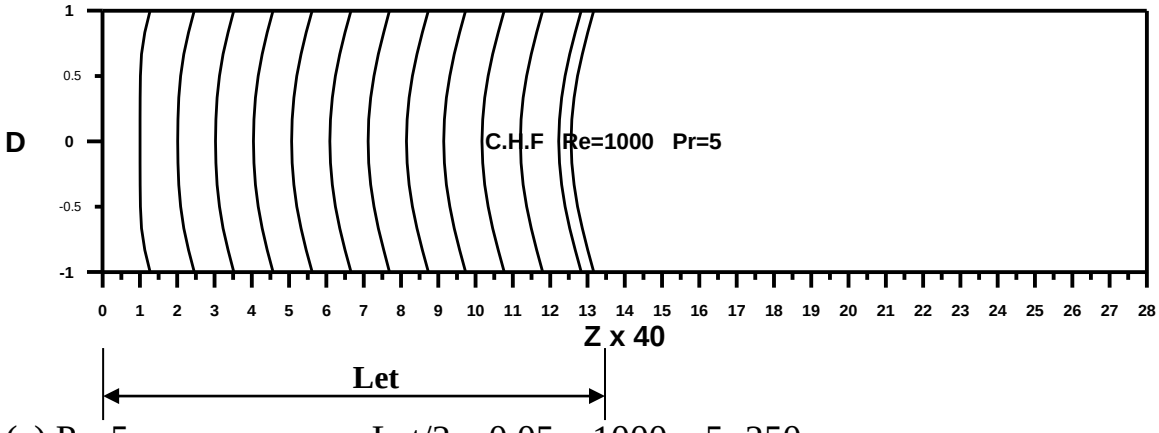

(c) Pr=5 Let/2a=0.05 x 1000 x 5=250

Figure (5-15) thermal temperature distribution development through circular tube for constant heat flux ,Re=1000 ,
different Prandtl number

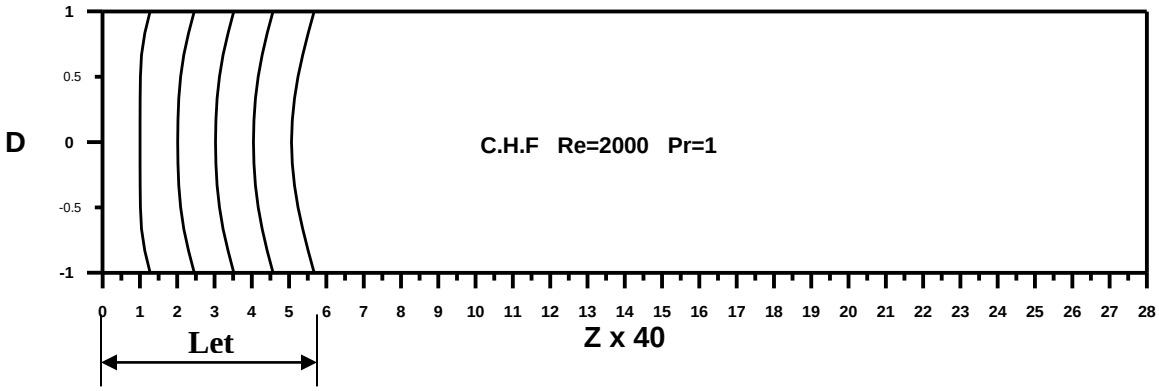

(a) Pr=1 Let/2a=0.05 x 2000 x 1=100

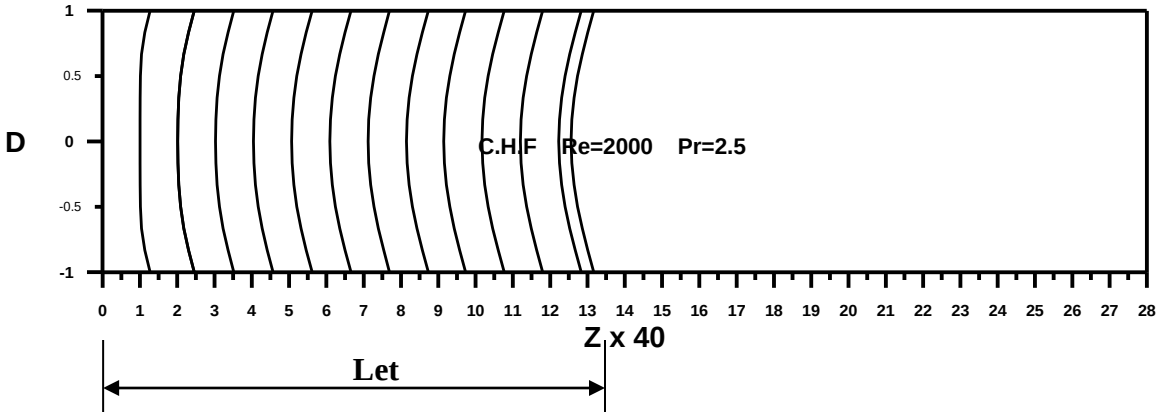

(b) Pr=2.5 Let/2a=0.05 x 2000 x 2.5=250

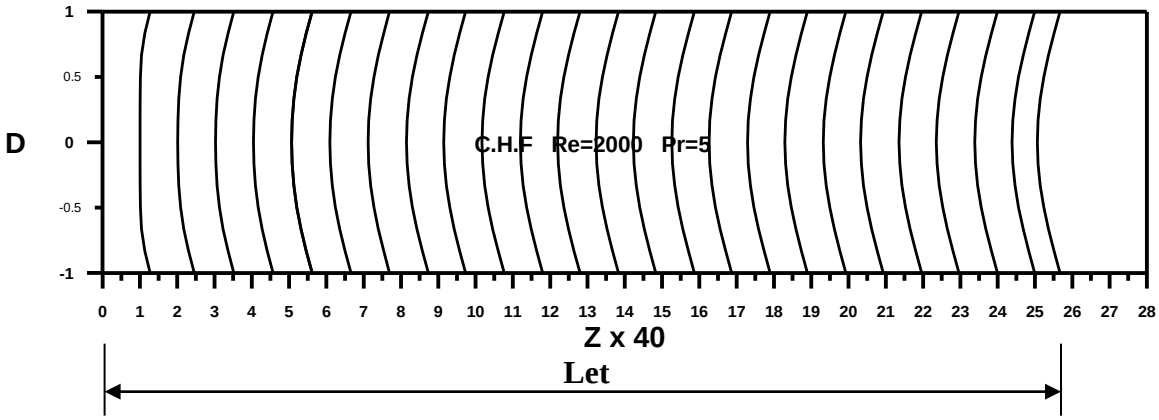

(c) Pr=5 Let/2a=0.05 x 2000 x 5=500

Figure(5-16) thermal temperature distribution development through circular tube for constant heat flux ,Re=2000 , different Prandtl number.

Figures (5-17), (5-18) and (5-19) show the developing and fully developed dimensionless temperature distribution through circular tube for constant heat flux boundary condition. These figures are for different Prandtl numbers (Pr=1), (Pr=2.5) and (Pr=5).

In developing region the dimensionless temperature at the walls equals maximum value due to the effect of heat flux and decreases with moving far away from the surface until it approaches minimum value at the centerline of the tube. For developing region the change of dimensionless temperature usually occurs near the wall.

In the fully developed region the dimensionless temperature start maximum value at the wall and decreases until the minimum value of dimensionless temperature at the centerline of the tube. In the fully developed region all figures have same dimensionless temperature distribution because the thermal boundary layer reach to its final form at this region where the fluid temperature reaches to a value equal approximately to the value of the wall temperature . So the dimensionless temperature distribution in fully developed region is independent of Reynolds and Prandtl numbers.

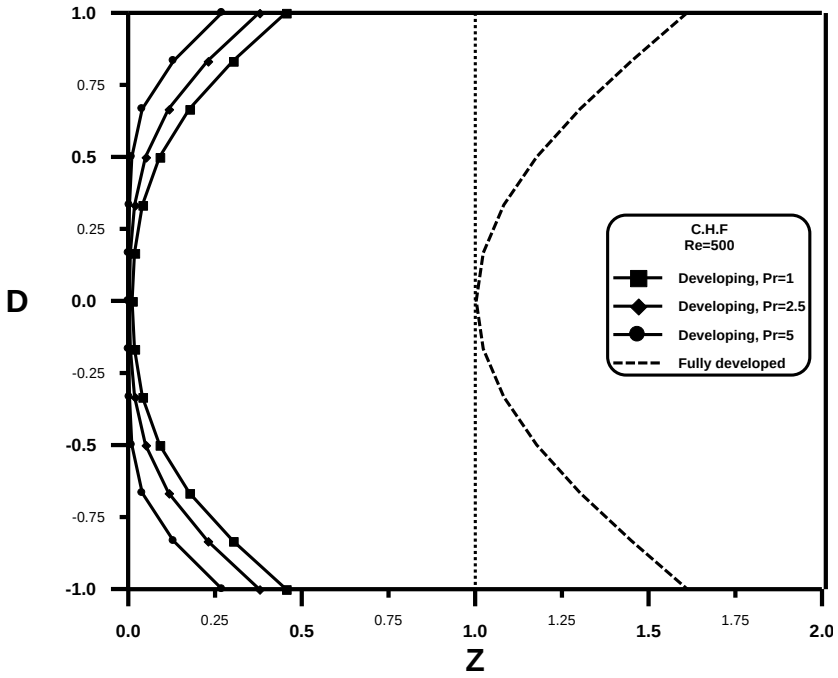

Figure (5-17) developing and fully developed dimensionless temperature distribution through circular tube for constant heat flux ,Re=500 ,different Prandtl number

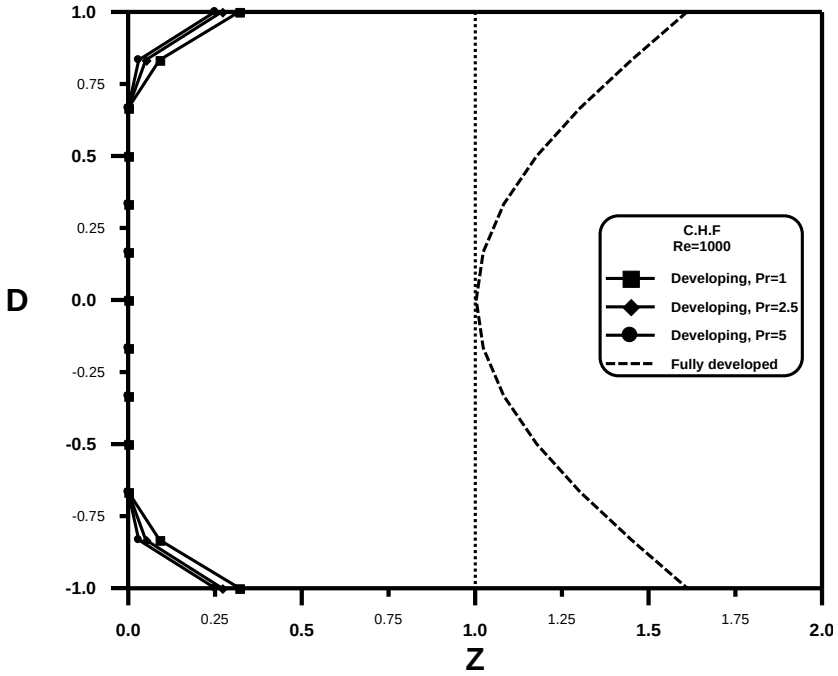

Figure (5-18) developing and fully developed dimensionless temperature distribution through circular tube for constant heat flux ,Re=1000 ,different Prandtl number

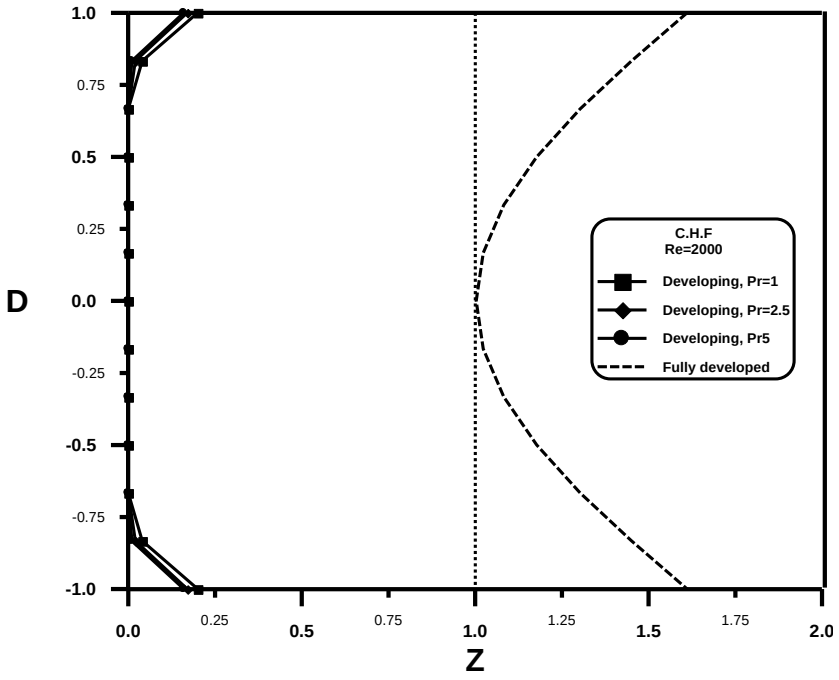

Figure (5-19) developing and fully developed dimensionless temperature distribution through circular tube for constant heat flux ,Re=2000 ,different Prandtl number

Figures (5-20), (5-21) and (5-22) show the developing and fully developed dimensionless temperature distribution for constant heat flux boundary condition and different Reynolds numbers and different Prandtl numbers .

In developing region the dimensionless temperature at the walls equals maximum value due to the effect of heat flux and decreases with moving far away from the surface until it reaches minimum value at the centerline of the tube. For developing region the change of dimensionless temperature usually occurs near the wall.

In the fully developed region the dimensionless temperature start maximum value at wall and decreases until it approaches its minimum value at the centerline of the tube, this is because the surface of the tube has a maximum temperature due to the effect of the heat flux . In the fully developed region all figures have same

dimensionless temperature distribution (the dimensionless temperature distribution in fully developed region is independent of Reynolds and Prandtl numbers).

It can be concluded that the shape of the developing and fully developed dimensionless temperature distribution θ(Z,R) differs according to whether a constant wall temperature or constant heat flux is maintained, where $\theta(Z,R)=\frac{T-T_w}{T_o-T_w}$ for constant wall temperature equals zero at the walls of the tube where (T=Tw) and increases gradually as moving far away from the tube surface until it approaches the maximum value at the centerline of the tube, while $\theta(Z,R)=\frac{k}{q''a}(T-T_o)$ for constant heat flux equals maximum value at the surface of the tube due to the effect of heat flux but decreases gradually as moving far away from the surface until it approaches minimum value at the centerline of tube.

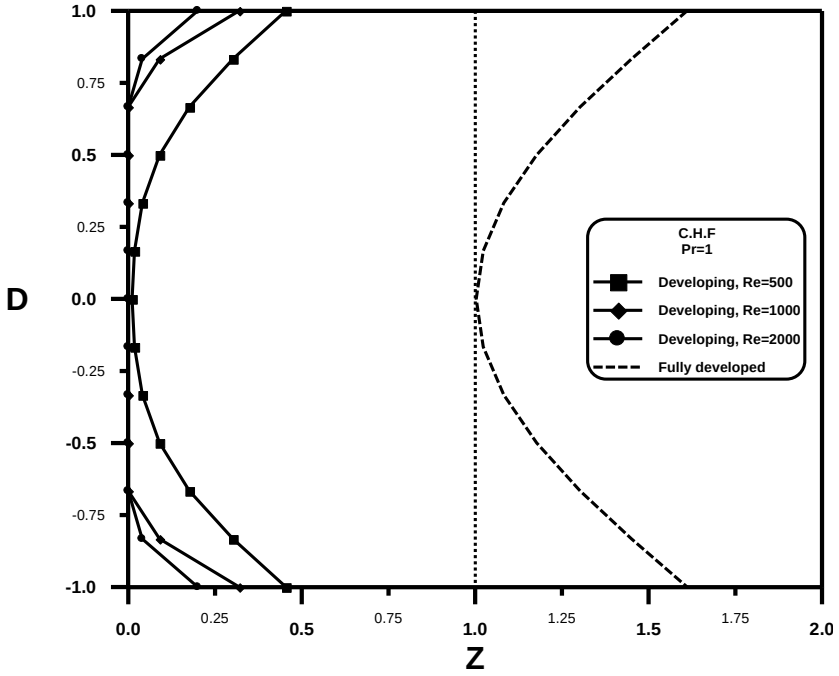

Figure (5-20) developing and fully developed dimensionless temperature distribution through circular tube for constant heat flux , Pr=1 ,different Reynolds number

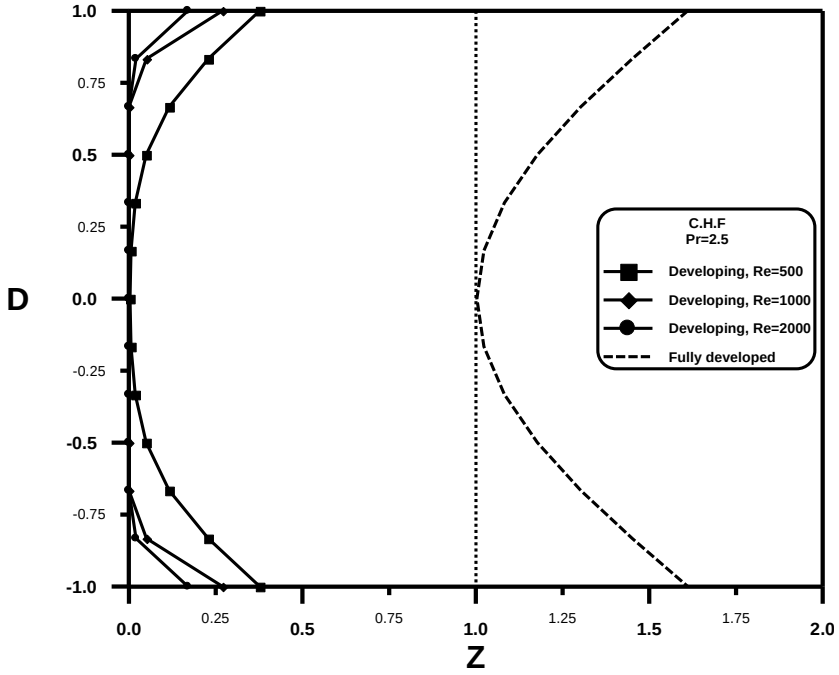

Figure (5-21) developing and fully developed dimensionless temperature distribution through circular tube for constant heat flux ,Pr=2.5 ,different Reynolds number

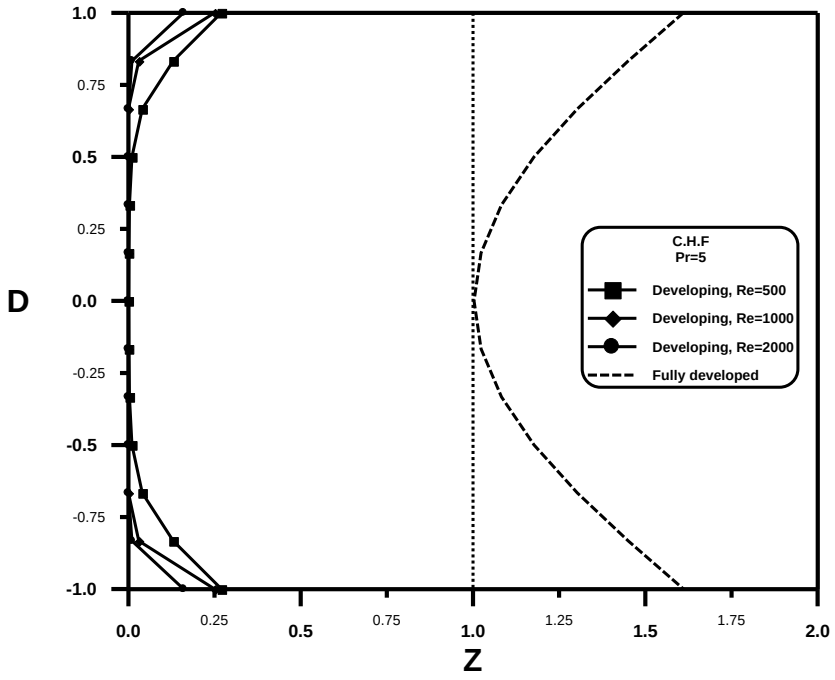

Figure (5-22) developing and fully developed dimensionless temperature distribution through circular tube for constant heat flux ,Pr=5
,different Reynolds number

5.1.3.2 Dimensionless Bulk Temperature (θ_b)

A- At Constant Wall Temperature ($\theta_b = \frac{T_b - T_w}{T_o - T_w}$)

Figures (5-23), (5-24) and (5-25) show the dimensionless bulk temperature in developing region for constant wall temperature boundary condition and different Prandtl numbers. At the inlet section of the tube where ($T = T_o$) the dimensionless bulk temperature have a maximum value of one, and this value decreases with increasing the axial distance from inlet. For low Prandtl number the dimensionless bulk temperature is faster reach to the minimum value (approximately 0.1).This is due to the small thermal entry length .As comparing these figures, it can be noted that The thermal entry length increasing with increasing of Reynolds number with respect to (equation 1.5). So it can be concluded that the dimensionless bulk temperature depends on Prandtl, Reynolds number and the dimensionless axial distance (Z).

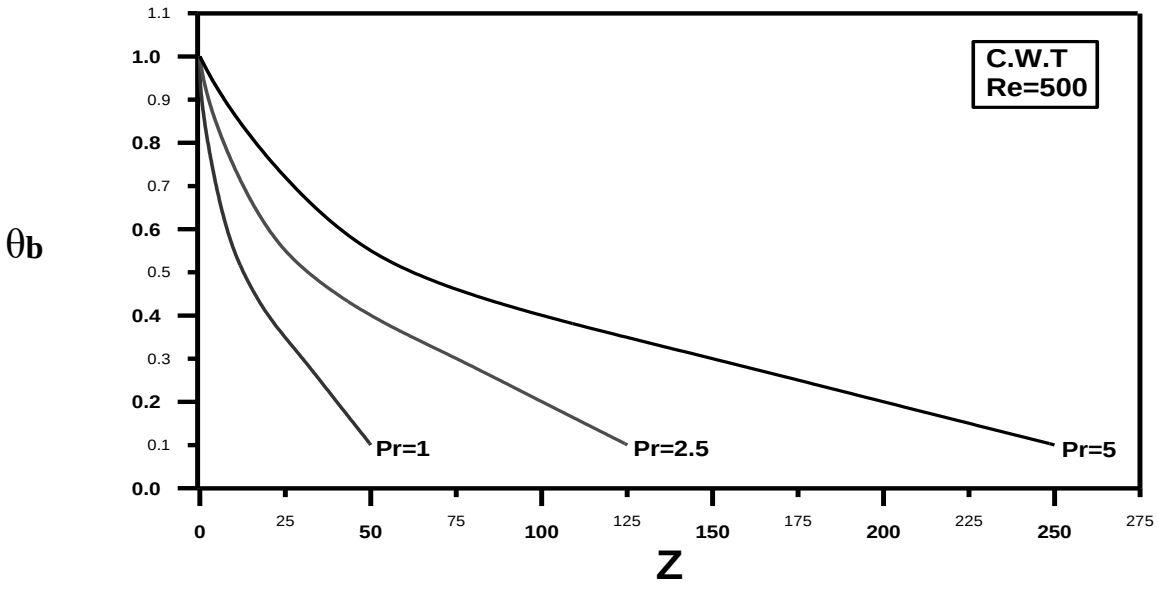

Figure (5-23) dimensionless bulk temperature through circular tube for constant wall temperature ,Re=500 ,different Prandtl number.

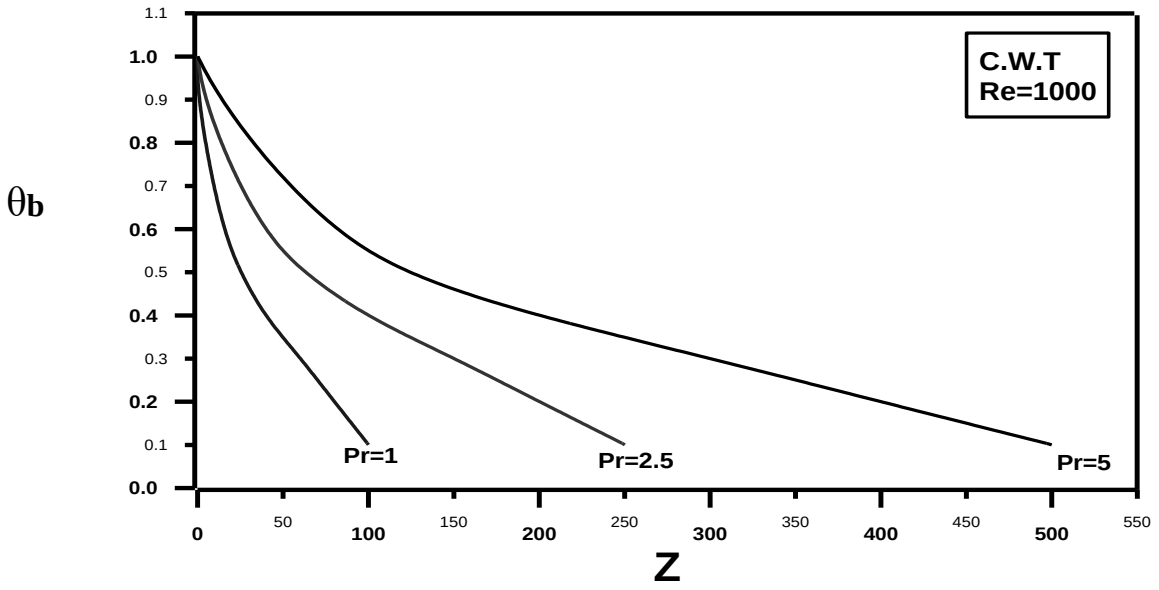

Figure (5-24) dimensionless bulk temperature through circular tube for constant wall temperature Re=1000,different Prandtl number.

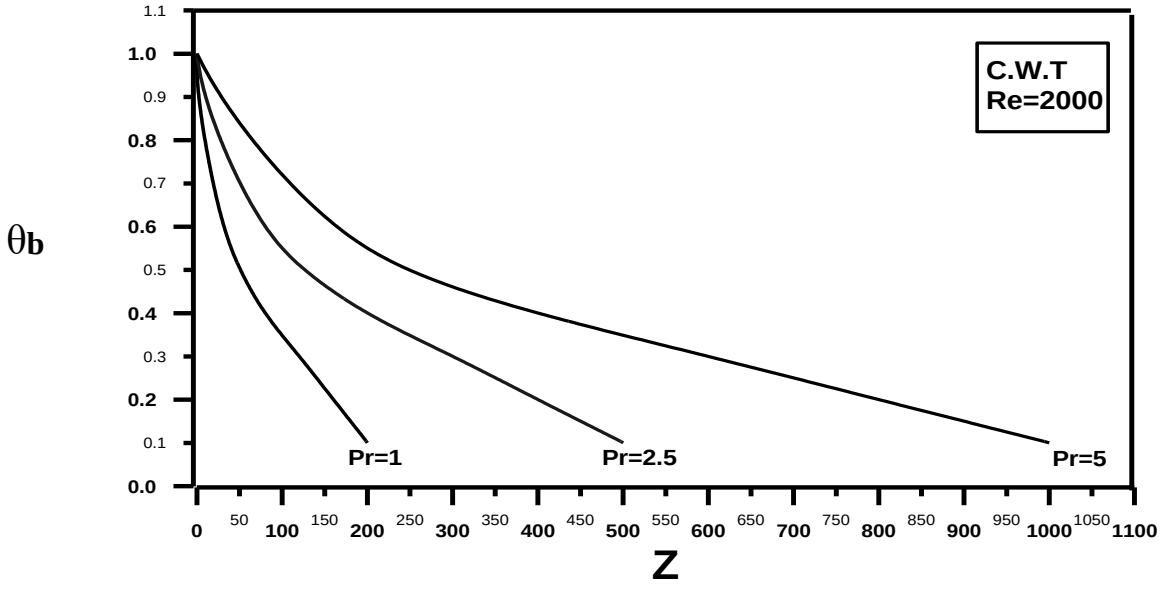

Figure (5-25) dimensionless bulk temperature through circular tube for constant wall temperature ,Re=2000 ,different Prandtl number.

B- At Constant Heat Flux ($\theta_b = \frac{k}{q.a}(T_b - T_o)$)

Figures (5-26), (5-27) and (5-28) show the dimensionless bulk temperature in developing region for constant heat flux boundary condition and different Prandtl numbers. At the inlet section of the tube where($T = T_o$) the dimensionless bulk temperature have a minimum value equals to zero and increases with increasing axial distance from inlet and reaches maximum value of approximately (0.92) at the thermally fully developed region. For low Prandtl number the dimensionless bulk temperature is faster reach to the maximum value. This is due to small thermal entry length. As comparing these figures, it can be noted that The thermal entry length increasing with increasing of Reynolds number with respect to (equation 1.5). So it can be concluded that the dimensionless bulk temperature depends on Prandtl, Reynolds number and the dimensionless axial distance (Z).

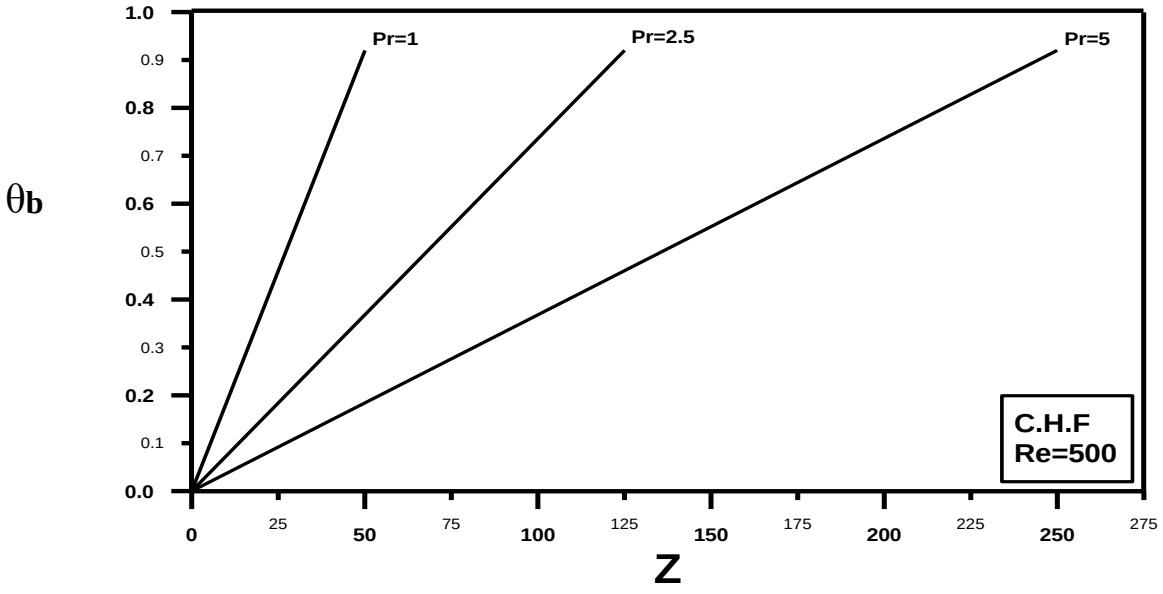

Figure (5-26) dimensionless bulk temperature through circular tube for constant heat flux , Re=500 , different Prandtl number

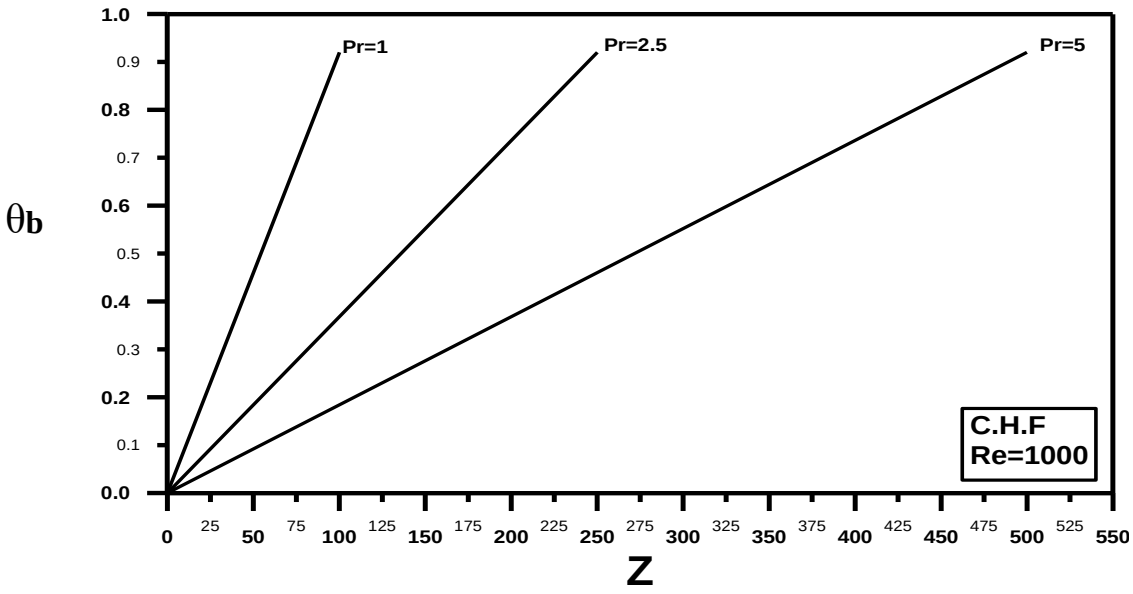

Figure (5-27) dimensionless bulk temperature through circular tube for constant heat flux ,Re=1000 ,
different Prandtl number.

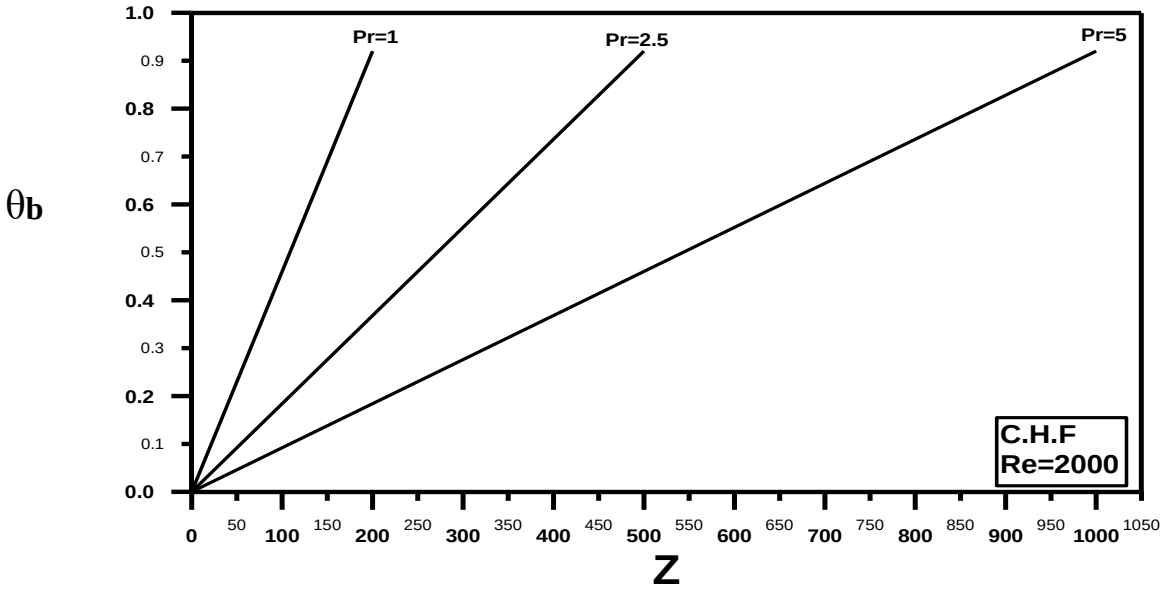

Figure (5-28) dimensionless bulk temperature through circular tube for constant heat flux Re=2000,
different Prandtl number.

5.1.3.3 Bulk temperature (Tb)

A- At Constant Wall Temperature

Figures (5-29),(5-30) and (5-31) show the axial temperature distribution for heat transfer through circular tube of (d=2cm) at constant wall temperature(Tw=80ºC) and different Reynolds and Prandtl numbers. The bulk temperature at the inlet section of the tube has a minimum value approximately ($T = T_o = 30^o C$) and then increase with increasing axial distance from inlet and reaches maximum value of approximately (T_b=72$^o C$). For low Reynolds and Prandtl number the bulk temperature is faster reach to the maximum value due to small thermal entry length. As comparing these figures, it can be noted that the thermal entry length increasing with increasing of Reynolds and Prandtl numbers with respect to equation (1.5). The bulk temperature depends on Prandtl, Reynolds number, and the axial distance (z).

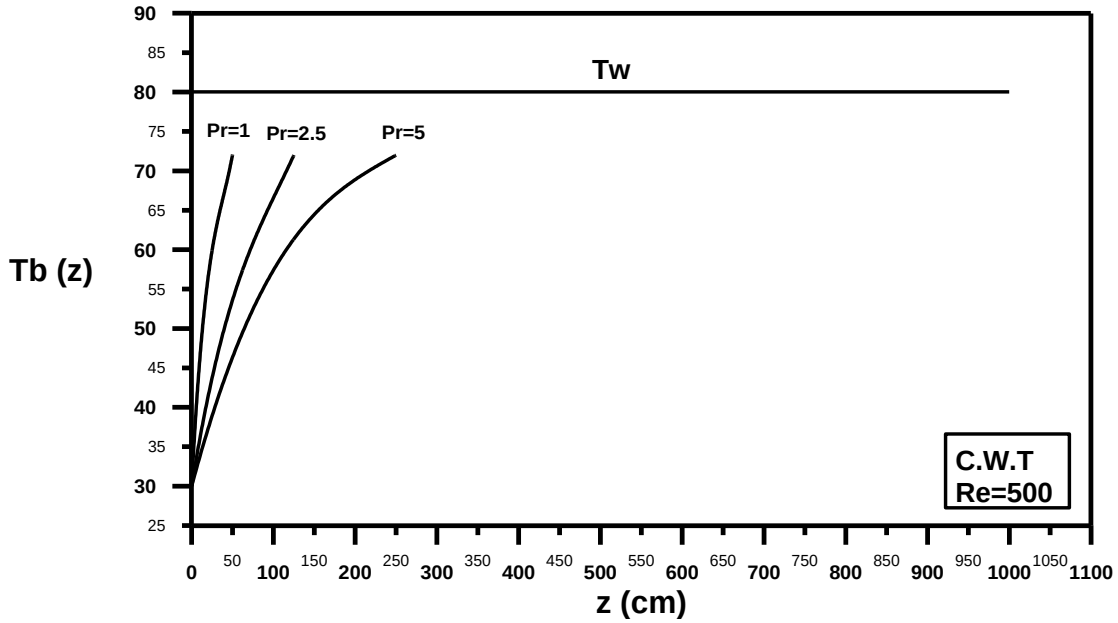

Figure (5-29) axial temperature representation for heat transfer through circular tube (d=2 cm) for constant wall temperature
Tw=80 ºC ,Re=500, different Prandtl number

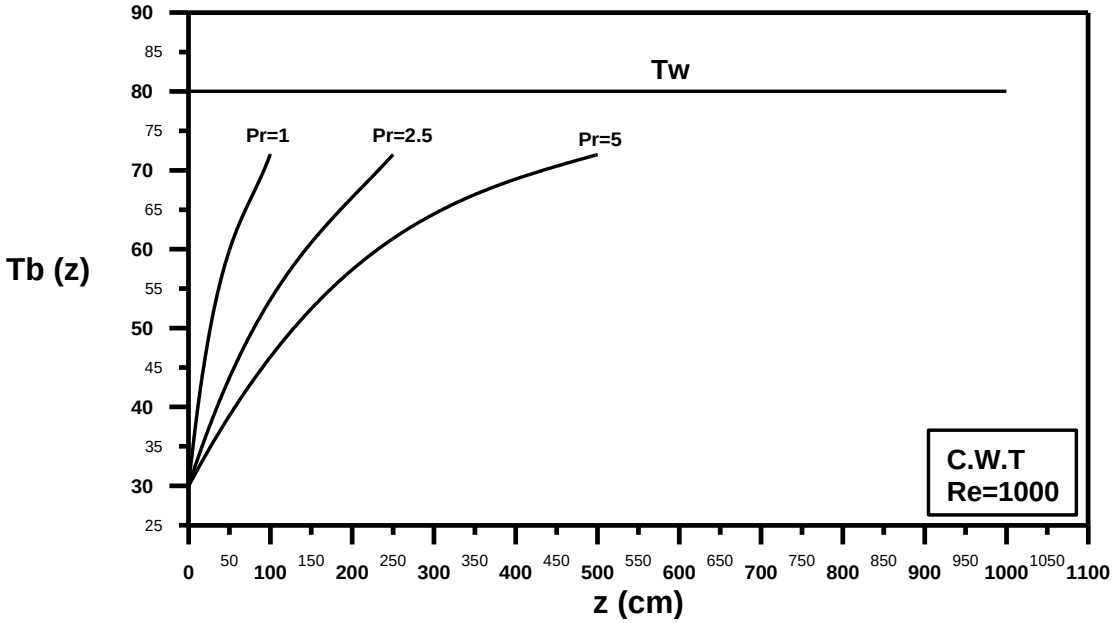

Figure (5-30) axial temperature representation for heat transfer through circular tube (d=2cm) for constant wall temperature
Tw=80 ºC ,Re=1000,different Prandtl number.

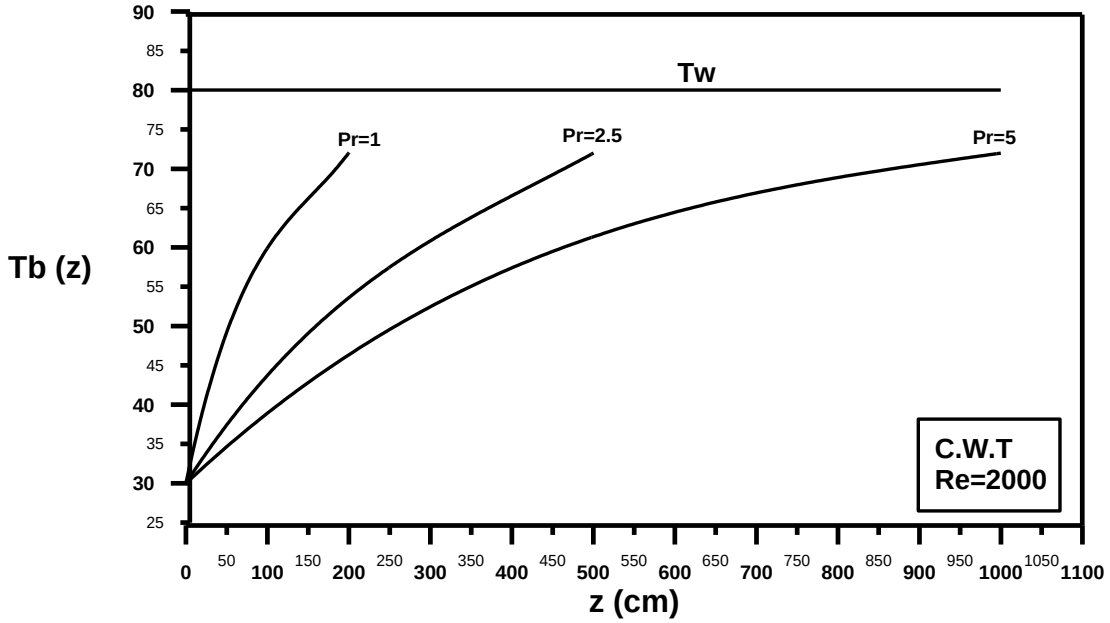

Figure (5-31) axial temperature representation for heat transfer through circular tube(d=2 cm) for constant wall temperature
Tw=80 ºC ,Re=2000,different Prandtl number.

B- At Constant Heat Flux

Fgures from (5-32a) to (5-34c) show the axial temperature distribution for heat transfer through circular tube of (d=2 cm) at constant heat flux ($q''=100 W/m^2$) for different Reynolds numbers and Prandtl numbers. .At the inlet section of the tube the wall temperature (Tw) have a minimum value of approximately (Tw=35 ºC) and increase with increasing the axial distance from inlet until it has a maximum value of approximately (Tw=96 ºC) while the bulk temperature (T_b) start from a minimum value of(T_b=30 ºC) at the inlet section of the tube and increase with increasing axial distance from inlet until it have a maximum value of (T_b=88 ºC).

For lower Reynolds and Prandtl numbers both wall temperature and bulk temperature are faster reach to the maximum value due to smaller thermal entry length. So the wall temperature and the bulk temperature are depending on Prandtl, Reynolds number, and the axial distance (z).

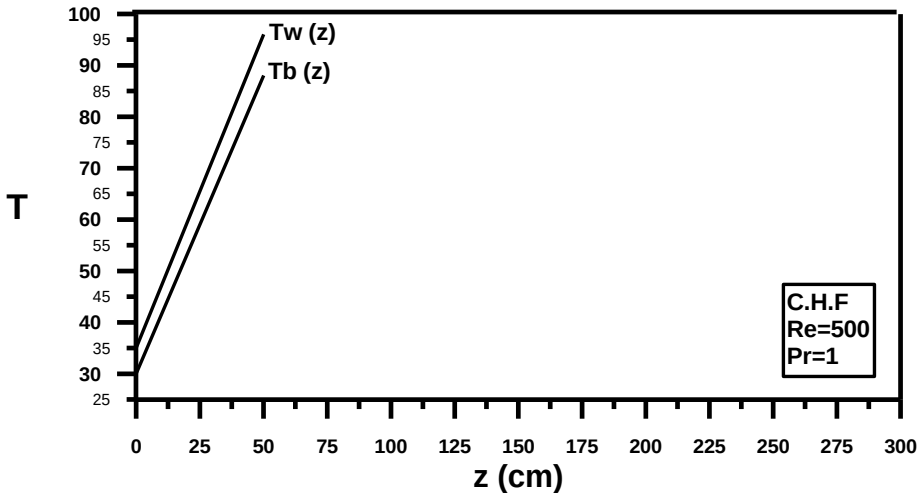

(a) Pr=1

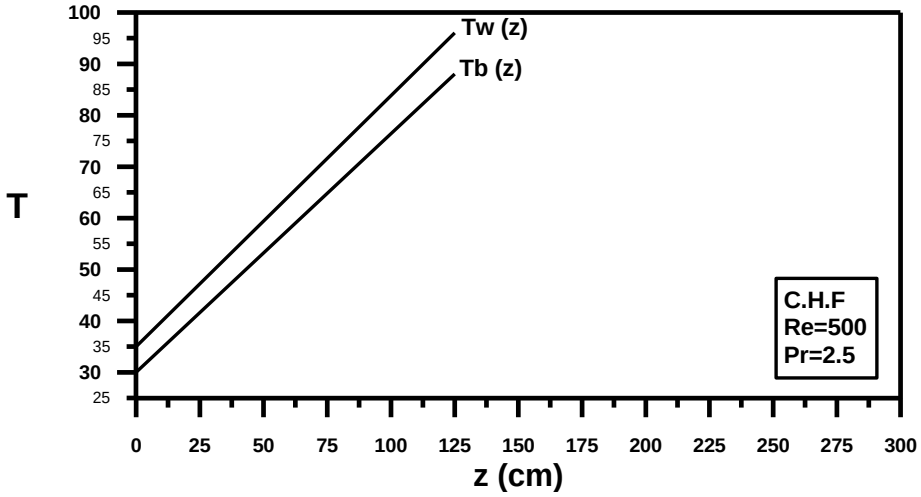

(b) Pr=2.5

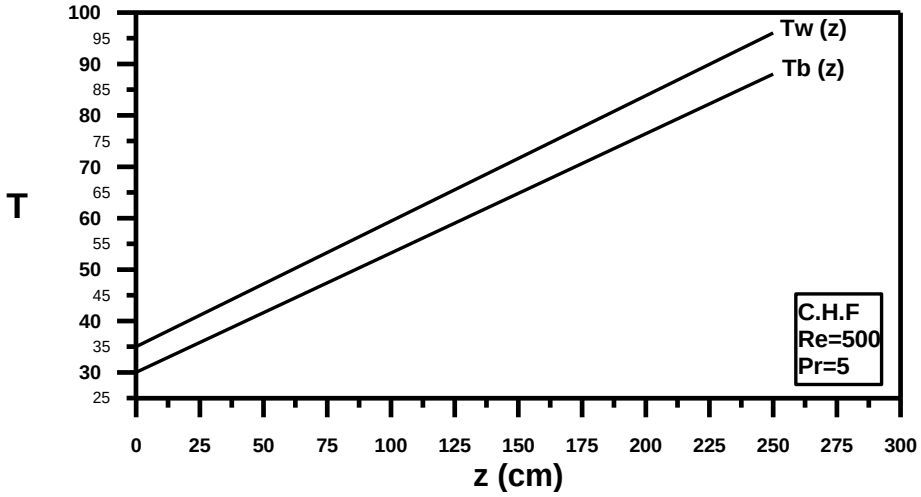

(c) Pr=5

Figure (5-32) axial temperature distribution for heat transfer through circular tube(d=2 cm) for constant heat flux

$q'' = 100 W/m^2$

Re=500,different Prandtle number

(a) Pr=1

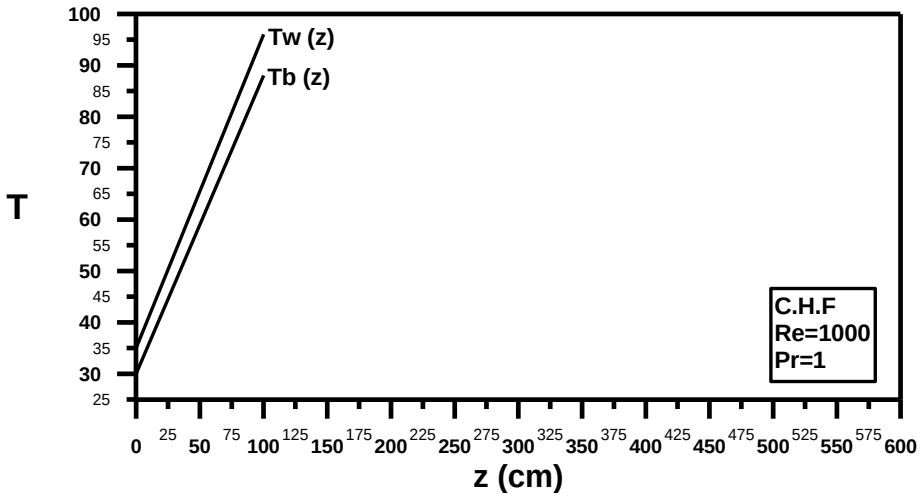

(b) Pr=2.5

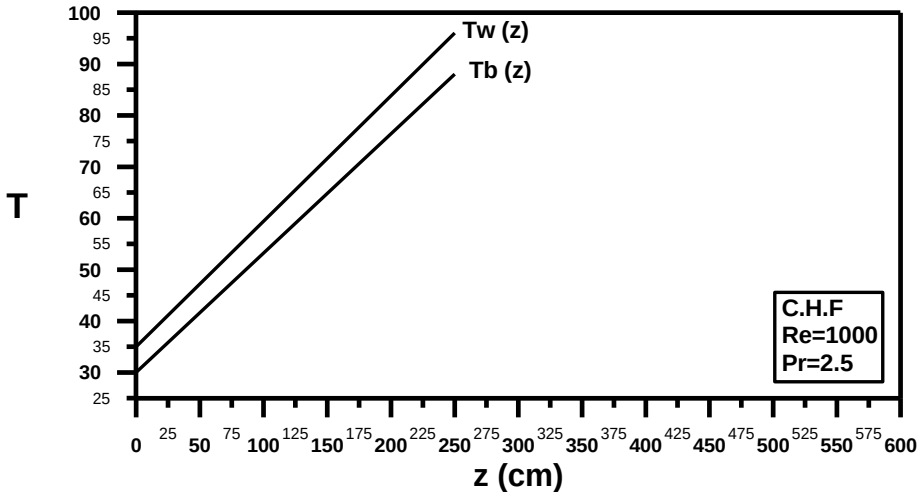

(c) Pr=5

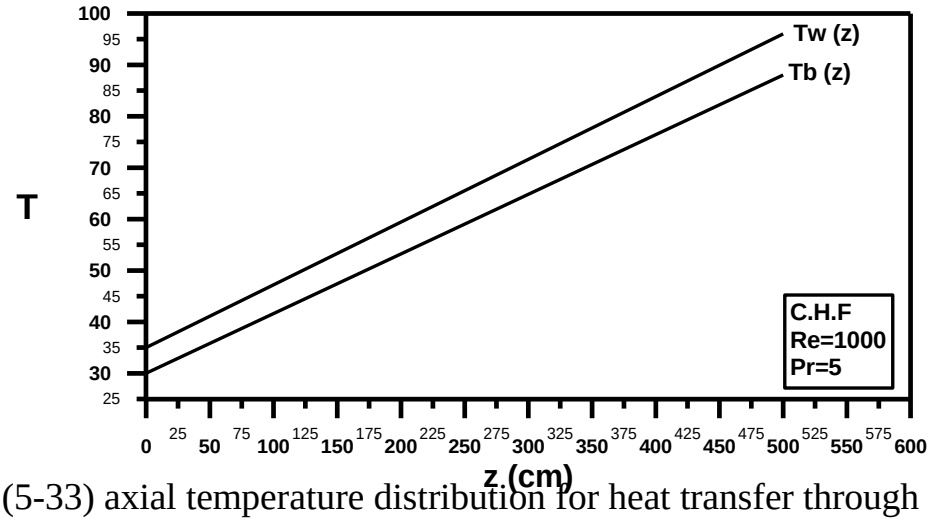

Figure (5-33) axial temperature distribution for heat transfer through circular tube(d=2 cm) for constant heat flux

$q'' = 100 W/m^2$

Re=1000, different Prandtle number

(a) Pr=1

(b) Pr=2.5

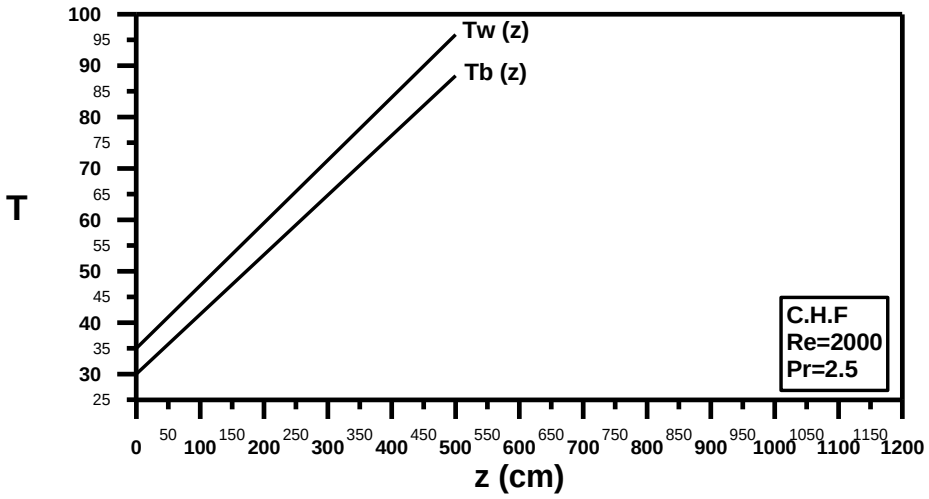

(c) Pr=5

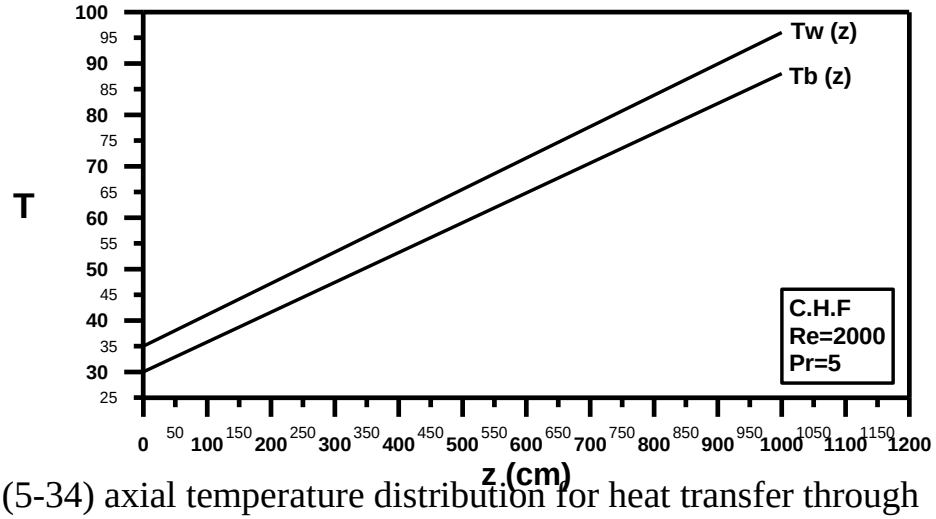

Figure (5-34) axial temperature distribution for heat transfer through circular tube(d=2 cm) for constant heat flux

$q'' = 100 W/m^2$

Re=2000, different Prandtle number

5.1.3.4 Local Nusselt Number (Nu_z)

A –At Constant Wall Temperature

Figures (5-35), (5-36) and (5-37) show the axial development of local Nusselt number at the entrance region of circular tube with Reynolds numbers (Re=500), (Re=1000) and (Re=2000), for constant wall temperature boundary condition. Figure (5-35) at Prandtl number (Pr=1), figure (5-36) at Prandtl number (Pr=2.5) and figure (5-37) at Prandtl number (Pr=5).

In these figures, Nusselt number has a maximum value at the start of entrance region (first step)of approximately (12.2) and then decreases gradually until it has a minimum value of approximately (4.23) where it close to the thermal fully developed region. The boundary layer thickness is zero at the start of entrance region, hence, there is no resistance against heat transfer which leads to raise the heat transfer coefficient value to maximum. So the heat transfer coefficient decreases as the boundary layer begins the process of developing until it reaches a constant value. The length at which the thermal boundary layer is fully developed increases with increasing Reynolds and Prandtl numbers. For low Reynolds and Prandtl numbers the local Nusselt number reaches faster the minimum value (small thermal entry length $\frac{L_{et}}{2a} = 0.05\,\mathrm{Re}.\mathrm{Pr}$). As comparing these figures, it can be noted that The thermal entry length increasing with increasing of Reynolds number with respect to equation (1.5) .So it can be concluded that the local Nusselt number depends on Prandtl number, Reynolds number, and the dimensionless axial distance from inlet.

Figure (5-35) local Nusselt number through circular tube for constant wall temperature Pr=1, different Reynolds number.

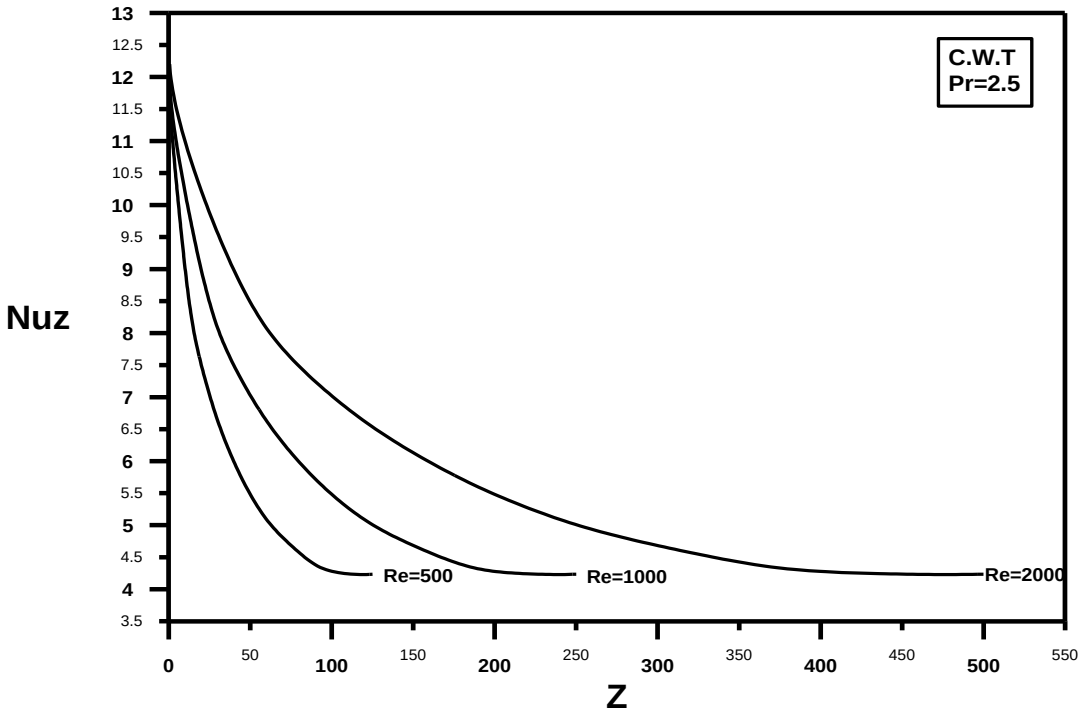

Figure (5-36) local Nusselt number through circular tube for constant wall temperature ,Pr=2.5 ,different Reynolds number.

Figure (5-37) local Nusselt number through circular tube for constant wall temperature ,Pr=5 ,different Reynolds number.

B- At Constant Heat Flux

Figures (5-38), (5-39) and (5-40) show the axial development of local Nusselt number at the entrance region of circular tube. These figures are with different Reynolds numbers and Prandtle numbers for constant heat flux boundary condition. In these figures, Nusselt number has a maximum value at the start of entrance region (first step) and then decreases gradually until it will be close to thermal fully developed region. The boundary layer thickness is zero at the start of entrance region. Hence, there is no resistance against heat transfer which leads to raise the heat transfer coefficient value to maximum. So the heat transfer coefficient decreases as the boundary layer begins the process of developing until it reaches a constant value. The length at which the thermal boundary layer is fully developed increases with increasing Reynolds and Prandtl numbers.

For Constant Heat Flux boundary condition, the maximum Nusselt number is (14.8), but the minimum value of Nusselt number is (4.3) for all Reynolds and Prandtl numbers.

As comparing these figures, it can be noted that the thermal entry length increasing with increasing of Reynolds number with respect to (equation 1.5) .So it can be concluded that the local Nusselt number depends on Prandtl number, Reynolds number, and the axial distance from inlet. i.e., for low Reynolds and Prandtl numbers the local Nusselt number is faster reach to the minimum value (small thermal entry length $\frac{L_{et}}{2a} = 0.05\,\mathrm{Re}.\mathrm{Pr}$).

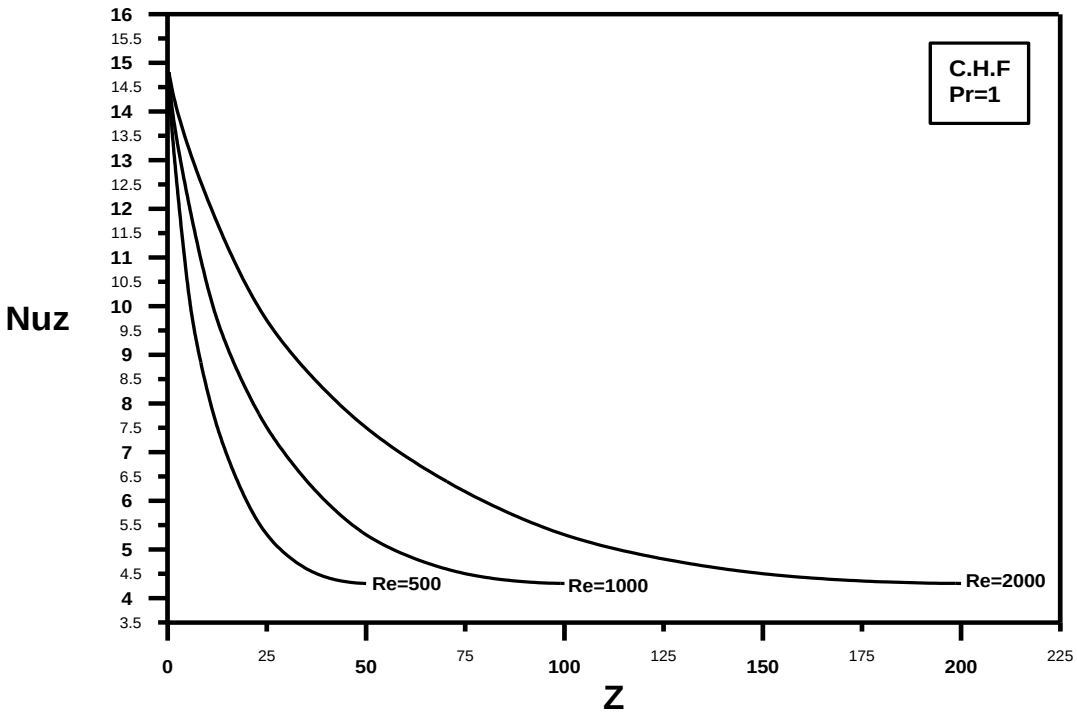

Figure (5-38) local Nusselt number through circular tube for constant heat flux, Pr=1 ,different Reynolds number

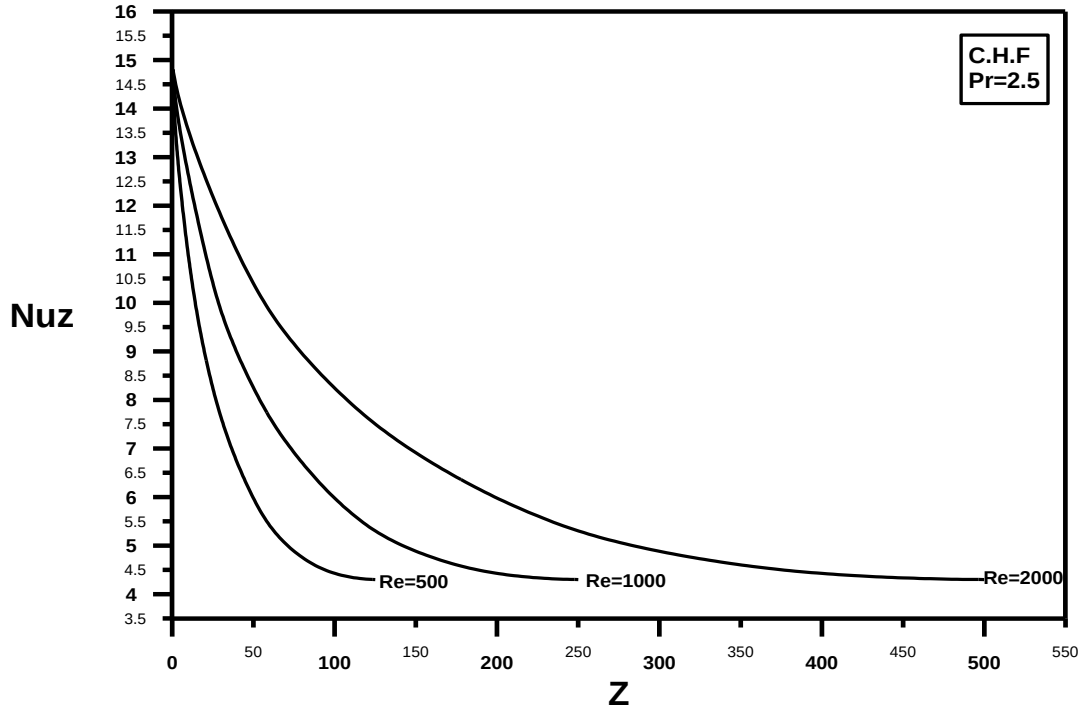

Figure (5-39) local Nusselt number through circular tube for constant heat flux, Pr=2.5 ,different Reynolds number

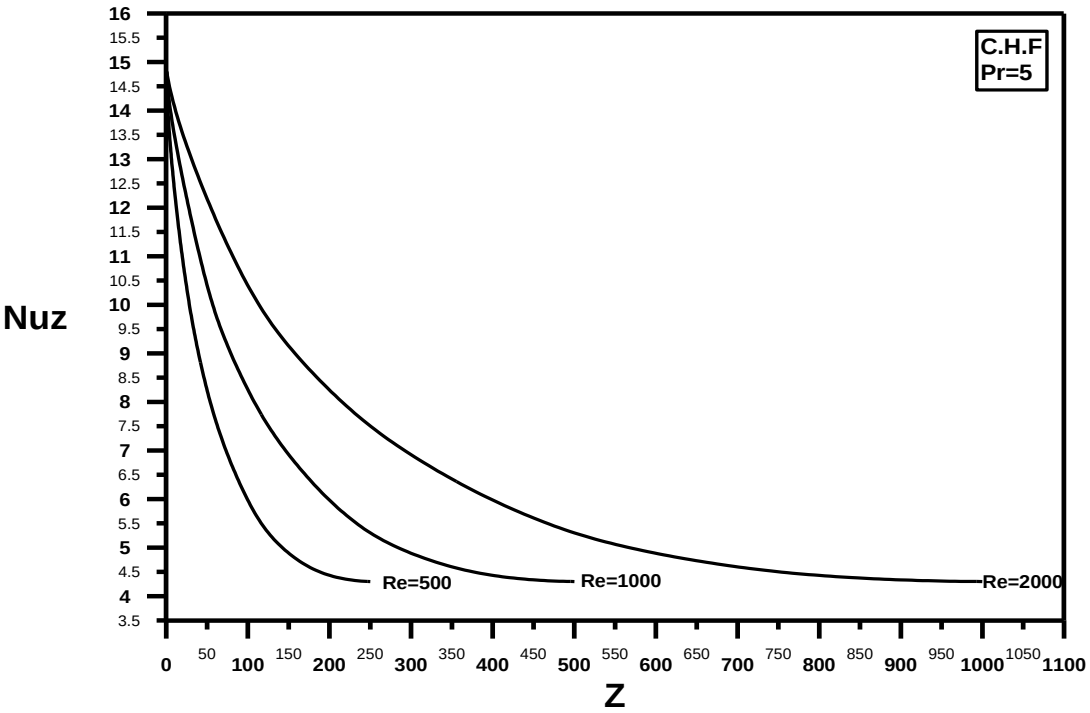

Figure (5-40) local Nusselt number through circular tube for constant heat flux, Pr=5 ,different Reynolds number

It is noted that the local Nusselt number for the constant heat flux case is greater than the local Nusselt number for constant wall temperature case, however, the flow field is similar for all studied cases (same Reynolds and Prandtl numbers).

Results of prediction model appear to be in excellent agreement with the correlation related to the references [1], [2], [3] and [4] .

A comparison of local Nusselt number of the present work for both cases of heating with a previous work is shown in table (5-1) below.

Table (5-1) Comparison the Nusselt number with previous work

Reference	Local Nusselt number (Nu_z)			
	Constant wall temperature		Constant heat flux	
	maximum	minimum	maximum	minimum
Kays [1]	12.8	3.6	12	4.36
Holman [3]	12.8	3.6	14.6	4.364
Desmond[43]	12.86	3.66	12	4.36
Present work	12.2	4.23	14.8	4.3

Also table (5-2) shows the convergence behavior of the dimensionless central axial velocity between the present work (numerical solution) and Ref.[33] which used the (GITT) analytically to solve the problem. These data are shown in figure (5-41), there is (∓ 0.03)percentage error between them.

Table (5-2) Convergence behavior of the dimensionless central axial velocity between the present work and Ref.[33]

Z	Present work	Shirly and Joao
0.0005	1.1	1.08
0.00105	1.127	1.155
0.00125	1.233	1.166
0.005	1.41	1.363
0.012	1.61	1.607
0.0125	1.661	1.612
0.013	1.661	1.612
0.014	1.668	1.618

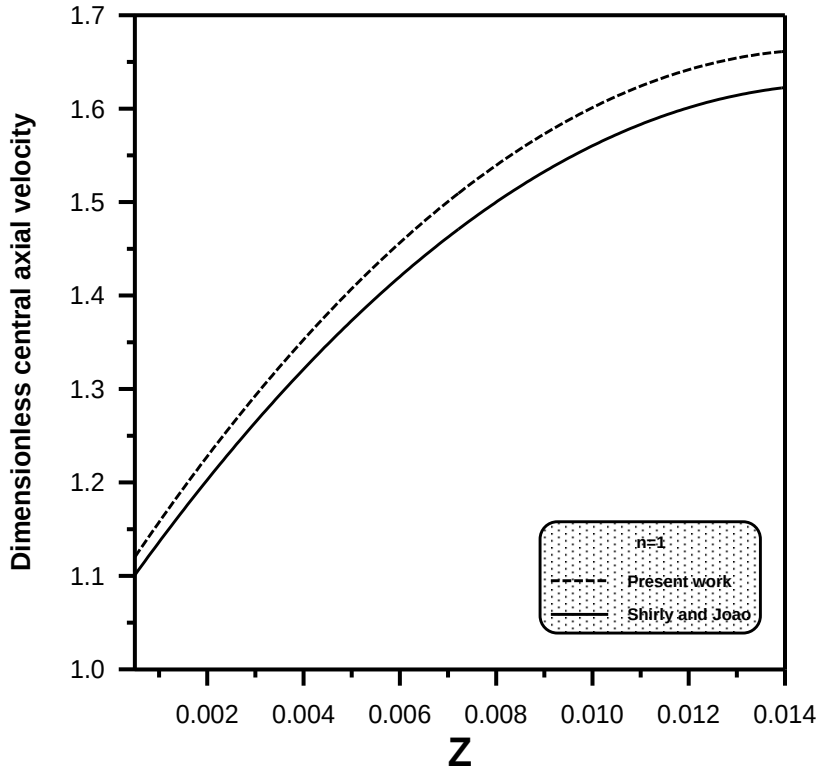

Figure (5-41) convergence behavior of the dimensionless central axial velocity between the present work and Ref. [33]

PART-II

5.2. Experimental Investigation

5.2.1 General

The main results in experimental work which represents the pressure drop at the entrance region for water flow through circular tube with (d=3.125cm and L=6.35 m) at different values of Reynolds number and compare it with the theoretical results, also the pressure distribution at the fully developed regions for different values of Reynolds number within laminar and turbulent flow .

6.2.2 Developing region

Figure (5-42) shows the pressure gradient (dp/dz) with respect to axial distance (z) at the entrance region of laminar water flow through circular pipe of diameter (d=3.125 cm) for different values of Reynolds numbers. It can be seen that the pressure drop increases with increasing axial distance (z) until it has approximately a maximum value at the fully developed region of the pipe for each value of Reynolds number. This increase is due to decreasing of local pressure (p) with respect to increasing of friction factor [equation 4.8].

Figures (5-43),(5-44) and (5-45) show comparisons of the experimental pressure drop and theoretical pressure drop with percentage error (∓ 0.04) for ($p_o = 1.9 bar$) and ($u_o = 0.04 m/s$) for three values of Reynolds number ,it is noted that there is a good convergent between them. Figure (5-45) shows that there is un intersection between the experimental and theoretical results at higher pressure drop ,i.e., there is a convergence between them.

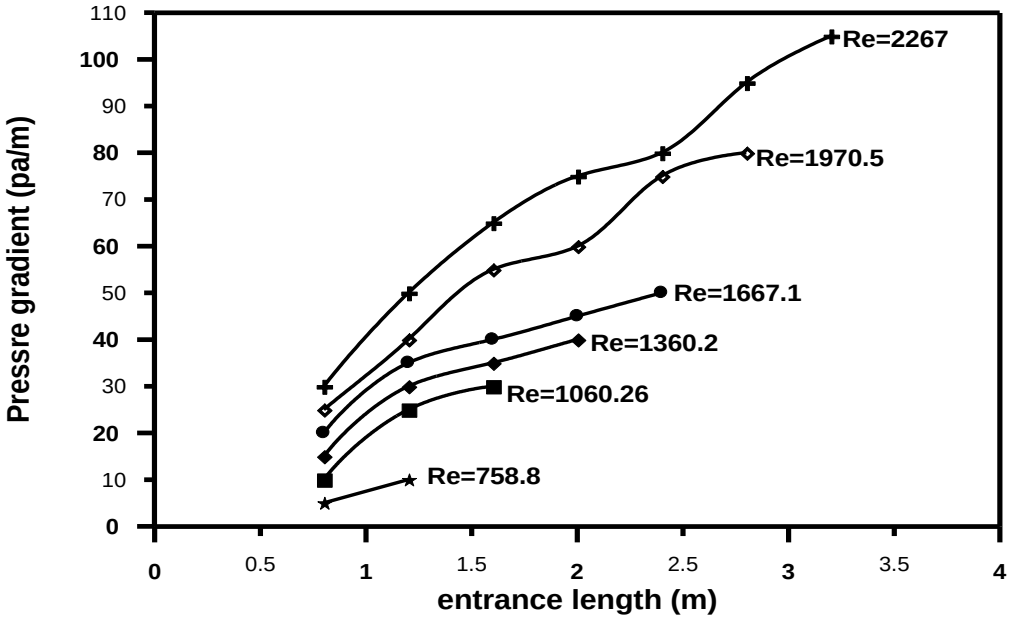

Figure (5-42) experimental pressure distribution through the entrance region of (d=3.125 cm) circular pipe at different Reynolds number.

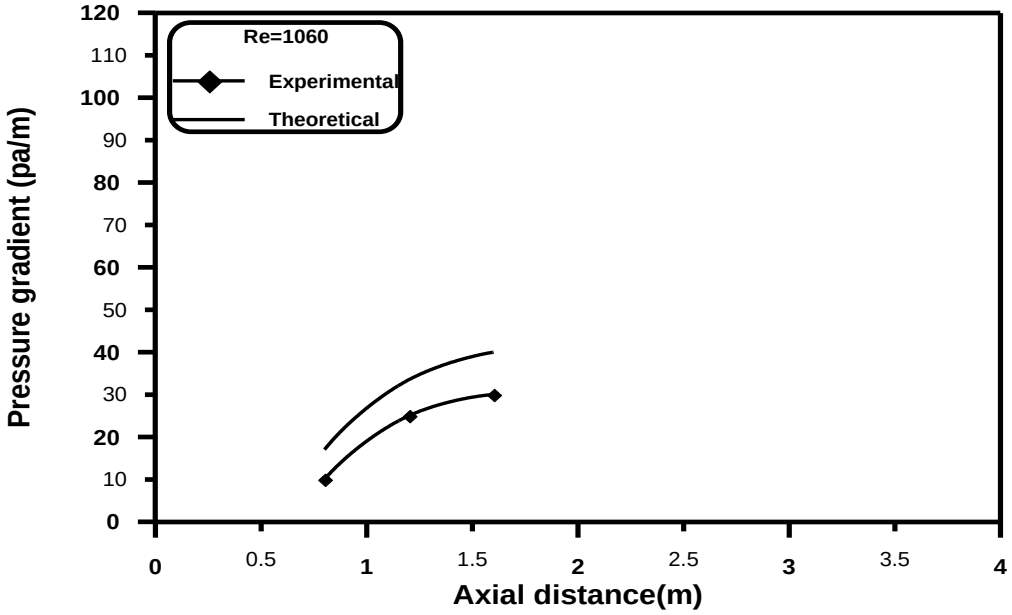

Figure (5-43) comparison of experimental pressure drop with theoretical pressure drop, Re=1060.

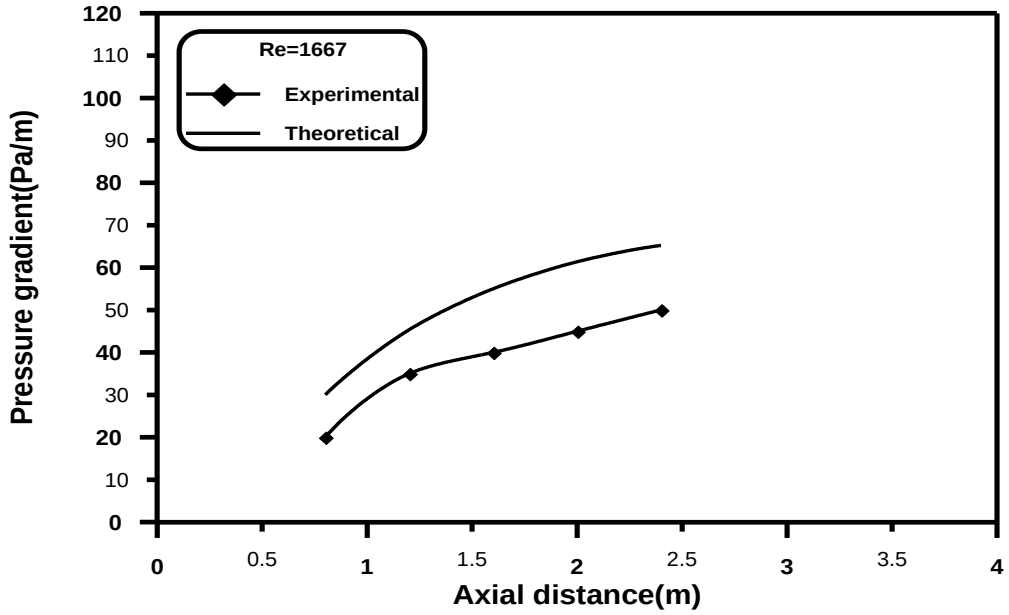

Figure (5-44) comparison of experimental pressure drop with theoretical pressure drop, Re=1667.

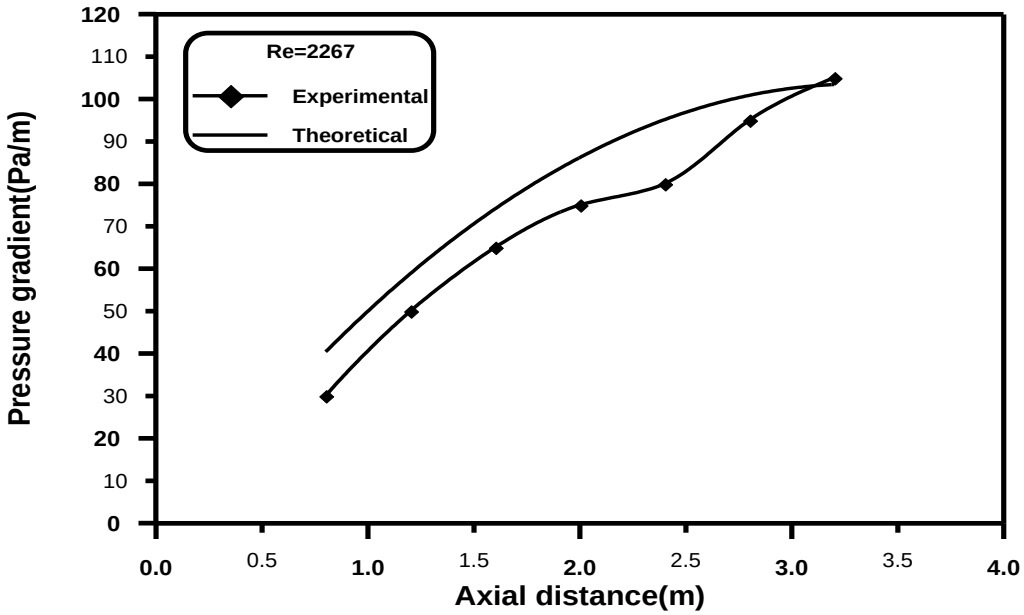

Figure (5-45) comparison of experimental pressure drop with theoretical pressure drop, Re=2267.

5.2.3 Fully Developed Region

Figures (5-46)and (5-47) show the pressure gradient (dp/dz) with respect to axial distance (z) through the fully developed region of laminar and turbulent water flow respectively through circular pipe(d=3.125 cm) for different values of Reynolds number. It can be seen that the pressure gradient remains approximately constant .

Figures (5-48) and (5-49) show that the water flow rate is inversely proportional with friction factor for laminar and turbulent flow respectively.

Figures (5-50) and (5-51) show that the water flow rate is directly proportional with Reynolds number for laminar and turbulent flow respectively, this is due to the increase of water mean velocity.

Figures (5-52), and (5-53) show the relation of friction factor for laminar and turbulent flow respectively with different values of Reynolds number). It is shown that, the friction factor decreases with increasing Reynolds number with respect to equations (4.8 and 4.11) respectively .

Figure (5-54) shows the relation of friction factor for both laminar and turbulent flow on the same curve with different values of Reynolds number). It is noted that, the gradient of friction factor for laminar flow is more than that for turbulent flow because of the lower limit of Reynolds number for laminar flow($758 \rightarrow 2267$) than that for turbulent flow ($3766 \rightarrow 6836$).

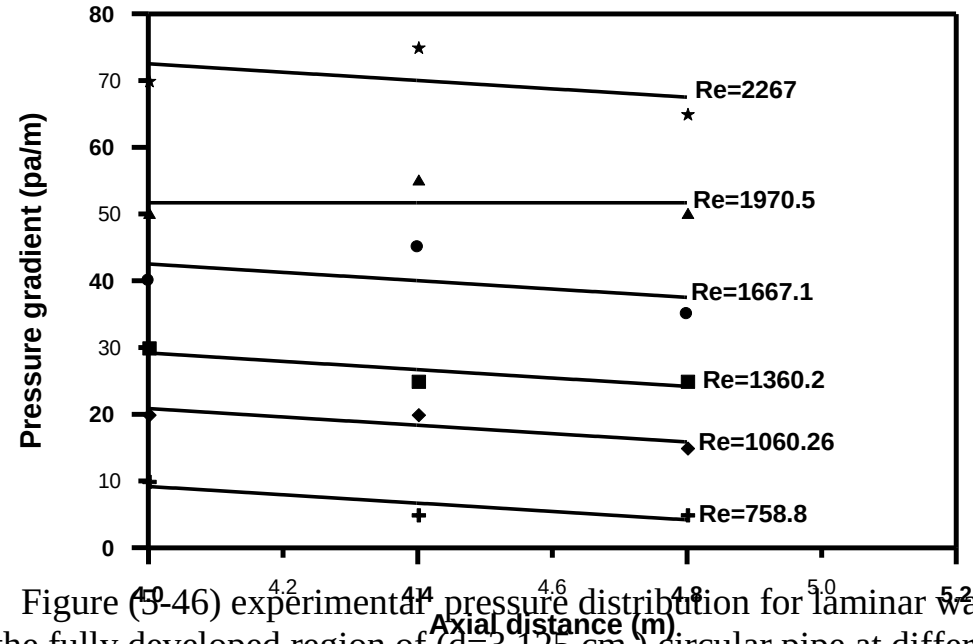

Figure (5-46) experimental pressure distribution for laminar water flow at the fully developed region of (d=3.125 cm) circular pipe at different Reynolds number.

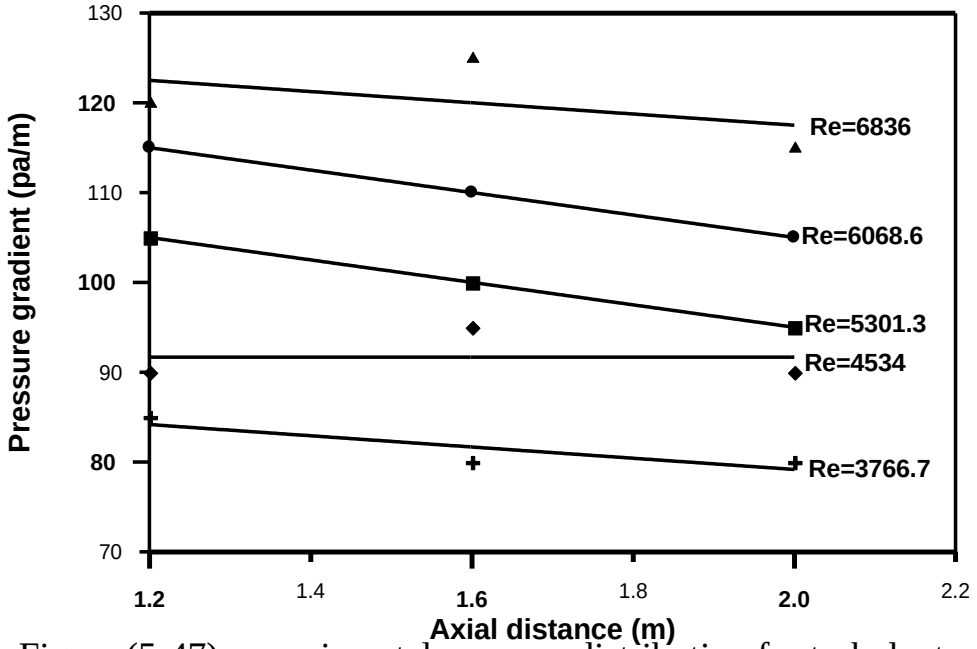

Figure (5-47) experimental pressure distribution for turbulent water flow at the fully developed region of (d=3.125 cm) circular pipe at different Reynolds numbers.

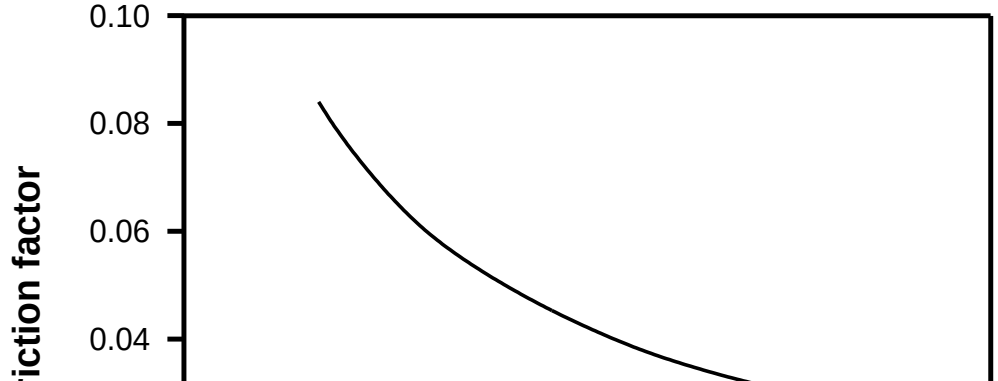

Figure (5-48) the relation between friction factor and laminar water flow rate.

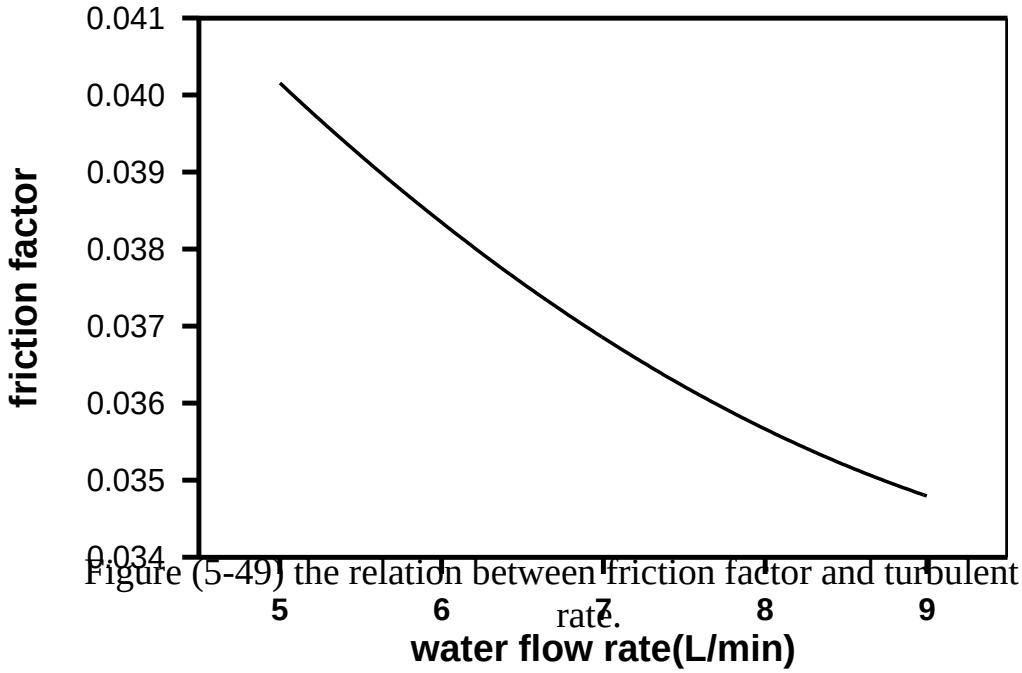

Figure (5-49) the relation between friction factor and turbulent water flow rate.

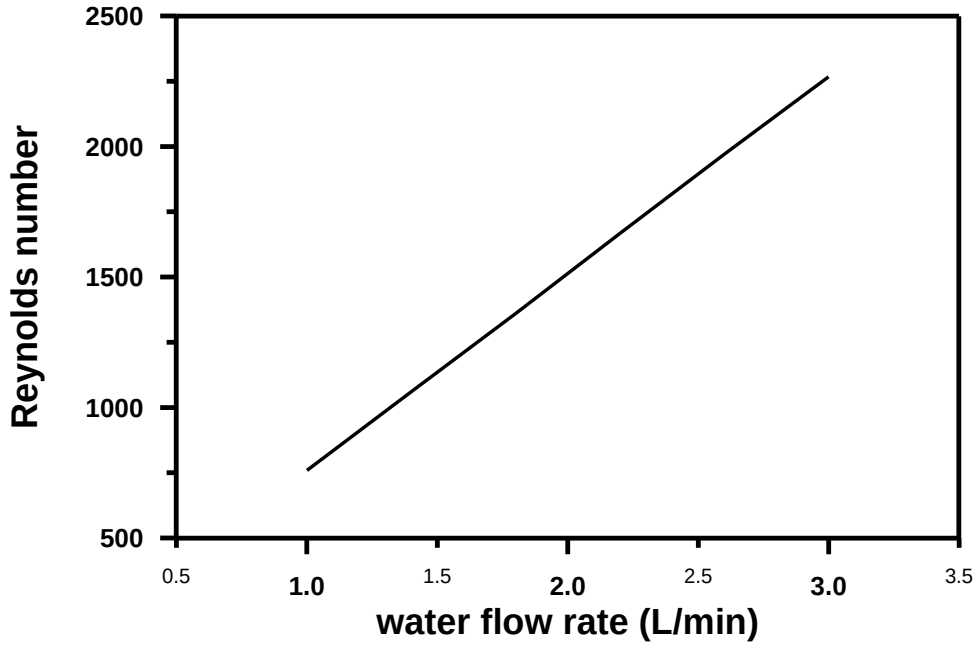

Figure (5-50) the relation between Reynolds number and laminar water flow rate.

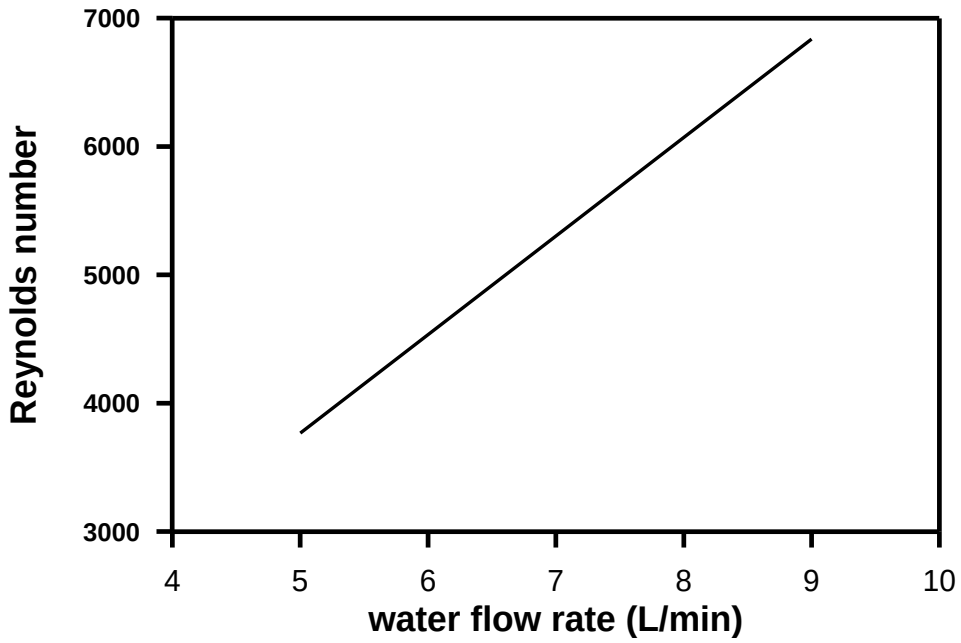

Figure (5-51) the relation between Reynolds number and turbulent water flow rate.

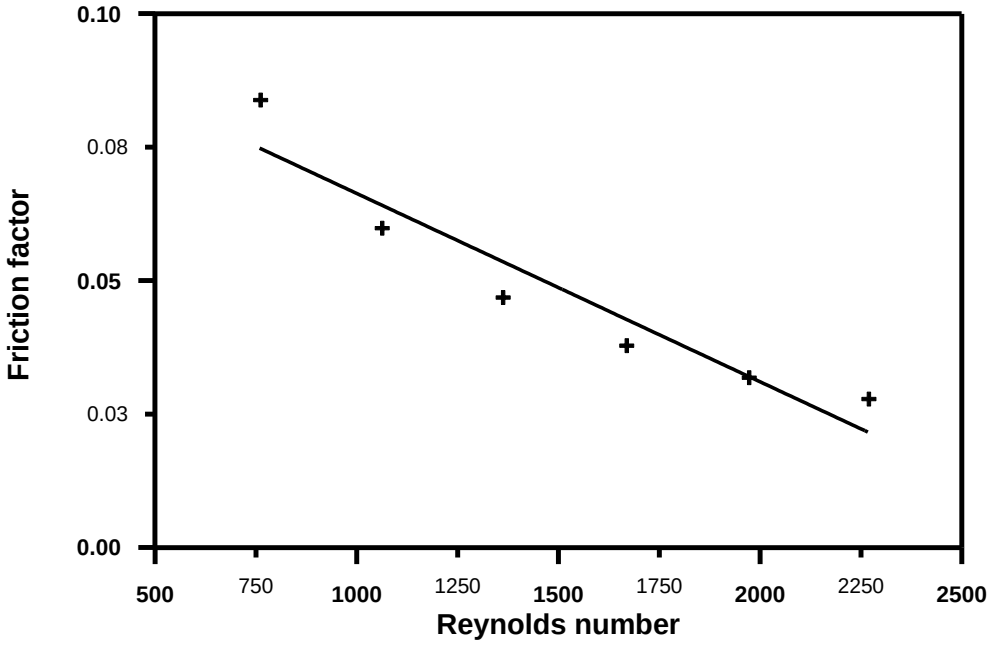

Figure (5-52) the relation between friction factor and Reynolds number for laminar water flow.

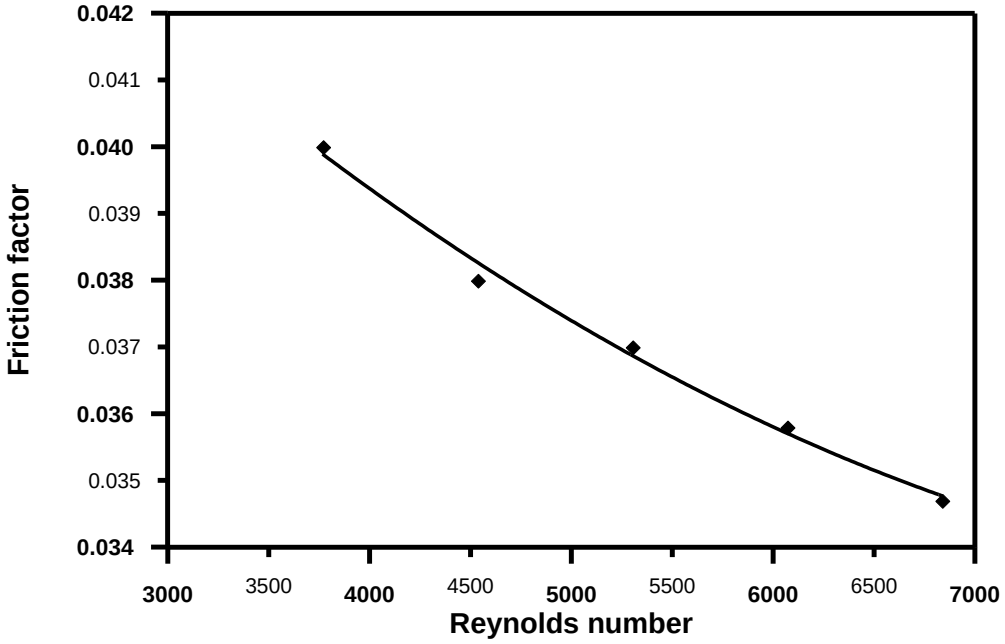

Figure (5-53) the relation between friction factor and Reynolds number for turbulent water flow.

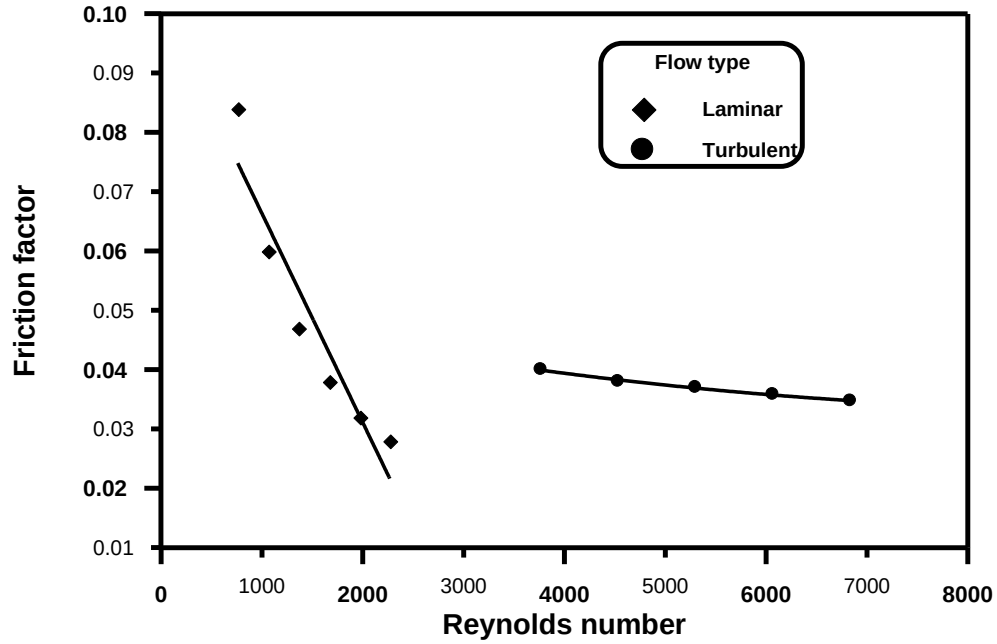

Let

Figure (5-54) the relation between friction factor and Reynolds number for laminar and turbulent water flow.

Conclusions and Suggestions for Future Work

6.1. Conclusions

From the results of the theoretical analysis and the experimental work of flow through circular tube, the following conclusions are deduced :

1. It can be seen that the boundary layer developed faster for lower Reynolds number. The maximum velocity is at the centerline of the tube .The velocity profile becomes fully developed at approximately ($\frac{L_e}{d} = 0.05\,\mathrm{Re}$) for laminar flow and ($\frac{Le}{d} \cong 4.4\,Re^{\frac{1}{6}}$) for turbulent flow (from experimental work).

   However, the flow field is similar for all studied cases .

2. From experimental work, the pressure drop at the entrance region increase with increasing distance in the axial direction ,this is due to decrease of local pressure because of increasing of friction factor.

3. From experimental work, the pressure difference at the fully developed region remains approximately constant .

4. The maximum dimensionless temperature for constant wall temperature is at the centerline of the tube but for constant wall heat flux boundary condition is at the walls.

5. The thermal boundary layer developed faster for lower Reynolds and Prandtl numbers. The dimensionless temperature distribution becomes fully developed at approximately ($\frac{L_{et}}{2a} = 0.05\,\mathrm{Re}\,.\,\mathrm{Pr}$).

however., the flow field is similar to the studied cases

6. The effect of the fluid flow features on the heat transfer behavior appears clearly in calculating bulk temperature, where the bulk temperature decreases in the developing region for constant wall temperature boundary condition, and the bulk temperature increases linearly in developing region for constant heat flux boundary condition. The bulk temperature decreases for constant wall temperature and increases for constant heat flux until its slope becomes zero. The zero slope of bulk temperature means that there is no heat transfer ($\Delta T \approx 0$), because the fluid temperature was reached to a value close to the wall temperature.

7. The Nusselt number has the maximum value at the start of entrance region and then decreases gradually until it will be close to thermal fully developed region. This is due to the higher velocity at the inlet of the tube as comparing with that when moving far away in the axial direction from the inlet of the tube.

8. The Nusselt number at constant heat flux boundary condition is greater than Nusselt number at constant wall temperature boundary condition. However, the flow field is similar for all studied cases.

9. The gradient of friction factor for laminar flow is more than that for turbulent flow. This is due to the lower limit of Reynolds number for laminar flow than that for turbulent flow.

6.2. Suggestions for Future Work

1. Performing a laminar fluid flow and heat transfer at the entrance region of annular ducts by using the implicit finite difference method.
2. Developing a new method for measuring the pressure drop like differential pressure transducer.
3. Performing an entrance region of turbulent fluid flow and heat transfer to power-law fluids through circular pipe.
4. Performing a fully developed laminar flow of non-Newtonian fluid in a rectangular duct by the finite element method.
5. Performing a laminar fluid flow and heat transfer through circular tube with porous walls by using finite difference method.
6. Developing a new method for measuring the velocity profiles across the cross-section of straight circular tubes using laser Doppler velocimetry.

Contents

Page No.

Chapter Four :Experimental Work

Chapter Five : Results and Discussion

PART-I

Nomenclature

Latin Symbols		
Symbol	**Definition**	**Unit**
a	The radius of circular tube	m
d	Diameter of circular tube	m
D	Dimensionless diameter of circular tube	m
h	Heat transfer coefficient	$W/m^2.K$
k	Thermal conductivity	$W/m.K$
L	Length of tube	m
Le	Hydrodynamic entry length	m
Let	Thermal entry length	m
m	Number of mesh points in the z-axis direction	——
n	Number of mesh points in the r-axis direction	——
p	Pressure	N/m^2
P	Dimensionless pressure	——
q	Heat transfer rate	W
q"	Heat flux	W/m^2
T	Temperature	^oC
T_b	Bulk temperature	^oC
θ	Dimensionless temperature	——
θ_b	Dimensionless bulk temperature	——
u	Velocity in axial direction	m/s
U	Dimensionless velocity in axial direction	——
v	Velocity in vertical direction	m/s
V	Dimensionless velocity in vertical direction	——
z	Axial direction of the tube	m
Z	Dimensionless axial direction of the tube	——
Δz	The distance between two nodal points in the axial direction	m
ΔZ	The dimensionless distance between two nodal points in the axial direction	——
r	Vertical direction of the tube	m
R	Dimensionless vertical direction of the tube	——
Δr	The distance between two nodal points in the vertical direction	m
ΔR	The dimensionless distance between two nodal points in the vertical direction	——
Q	Water flow rate	L/min
A	Cross section area of pipe	m^2
H_l	Head loss	m
ΔP	Pressure drop	pa

τ_w	Wall shear stress	N/m^2
f	Darcy friction factor	———
C_f	Fanning friction factor	———

Greek Symbols

Symbol	Definition	Unit
α	Thermal diffusivity	m^2/s
ν	Kinematic viscosity	m^2/s
μ	Dynamic viscosity	kg/m.s
ρ	Density of fluid	kg/m^3
C_p	Specific heat at constant pressure	kJ/kg.°C
δ	Hydrodynamic boundary layer thickness	m
δ t	Thermal boundary layer thickness	m
$\beta_0, \Omega_0, \Phi_0,$ $\alpha_j, \beta_j, \Omega_j, \Phi_j$	Elements of matrix (3.72)	———
$\beta'_0, \Omega'_0, \Phi'_0,$ $\alpha'_j, \beta'_j, \Omega'_j, \Phi'_j$	Elements of matrices (3.83) and (3.86)	———

Dimensionless Numbers

Symbol	Definition	Equation
Re	Reynolds number	$\mathrm{Re} = \rho.u_o.d/\mu$
Pr	Prandtl number	$\mathrm{Pr} = c_p.\mu/k = \nu/\alpha$
Nu	Nusselt number	$Nu = h.d/k$

Subscripts

Symbol	Definition	Unit
i, j	The indexes increment along the axial and vertical direction	———
o	Inlet	———
w	Refers to wall	———

Abbreviation

C.H.F	Constant Heat Flux
C.W.T	Constant Wall Temperature

References

[1] Frank Kreith and Mark S.Bohn "*Principle of Heat Transfer* " McGraw-Hill Book Company, New York, second edition , *1977.*

[2] Incropera, F.P. and Dewitt, D.P., *"Fundamentals of Heat and Mass Transfer",* John Wiley & Sons, New York, 1996.

[3] Holman, J.P., *"Heat Transfer*", McGraw-Hill Book Company, New York, sixth edition, 2000.

[4] Kays ,W.M and Crawford, M.E *"Convective Heat and Mass Transfer"* McGraw-Hill Book Company, New York, second edition ,1966.

[5] **Lien, K., Chong, M.S.,** and **Ooi, A.,** "*The Entrance Length for Fully Developed Turbulent Channel Flow*", J .of Australasian Fluid Mechanics Conference, University of Sydney, Australia, 13-17 December, 2004.

[6] Moller ,M.Y *"Forced Convection Heat Transfer in Straight Tubes "***,** M.Sc. thesis, Mechanical Engineering Department, University of Cranfield, 1968**.**

[7] Schmidt, F.W. and Zeldin, B., *"Laminar Heat Transfer in the Entrance Region of Ducts",* Int. J. Heat Mass Transfer, Vol. 23, No. 1, 1970.

[8] Cony,J.E and El- shaarawi,M.A *"Laminar Heat Transfer in the Entrance Region of Concentric Annuli with Rotating Inner Walls* "ASME Journal of heat transfer ,Vol. 105,pp.560-561,1974 .

[9] Emery, A.F and Gessner, F.B., *"The Numerical Prediction of Turbulent Flow and Heat transfer in The Entrance Region of a Parallel Plate Duct",* ASME Journal of Heat Transfer, Vol. 98, No. 4, pp.594-600, 1976.

[10] Render ,D.J, *"Momentum and Heat Transfer for Pulsating Laminar Flow"* Thesis /Dissertation, Ph.D thesis ,New York University ,Jan.1977.

[11] Kuehn ,T.H .and Goldstein ,R.J *"A parametric Study of Prandtl Number and Diameter Ratio Effects on Natural Convection Heat Transfer in Horizontal Cylinders",* ASME Journal of Heat Transfer ,Vol.102,pp.768-770,1980**.**

[12] Ching, J.C., and Jenq, S.C., "*Laminar and Turbulent Heat Transfer in the Pipe Entrance Region for Liquid Metals",* Int. J. Heat Mass Transfer, Vol. 24, pp.1179-1189, 1981.

[13] Al-Ali ,H.H. "*Simultaneously Developing Laminar Flow and Heat Transfer in the Entrance Region of Flat and Circular Conduits* " Ph.D thesis, Colorado School of Mines, Golden, CO (USA), Jan. ,1988.

[14] Uysal,U , and Sozbir , *"Numerical Analysis of Unsteady Laminar Forced Convection in a Rectangular Ducts* ",department of Mechanical Engineering ,1989.

[15] Alan L. Brigg *"Transient Conjugate Heat Transfer in a Circular Ducts for Power-Law Fluid with Viscous Dissipation "* Ph.D thesis ,University of Pittsburgh ,1989.

[16] Bigyani Das*" Entrance Region Flow of the Hershel – Bulkley Fluid in a Circular Tube "* Department of Mathematics And Statistics ,University of New Mexico ,Albuquerque ,NM 87131 ,USA, Fluid Dynamics Research ,Vol.10 ,PP.39-53 ,Jun.1992.

[17] Zhao ,T.S and Cheng,P *"A numerical Study of Laminar Reciprocating Flow in a Pipe of Finite Length"* Department of Mechanical Engineering ,The Hong Kong University of Science & Technology. Applied Scientific Research ,Vol.59,pp.11-25,1998.

[18] Cuccruiio,G and Beradi ,P.G *"Developing of Velocity and Temperature in the Entrance Pipe Flow for Power Law Fluids* " Proceeding of the 11th International heat transfer conference ,Vol.3,pp.15-20,1998.

[19] Benhamous,B.,Galanis,N. and Laneville,A *"A transient Effects of Orthogonal Pipe Oscillations on Laminar Developing in Compressible Flow* "Int. J. Heat and Mass transfer ,Vol .34,Issue 7 ,pp.561-584,2000.

[20] Shariff, M.M. and Greywall, M.S., *"Stream wise computation of parabolized axisymmetric laminar flows with heat transfer",* ASME Fluids Engineering Division Summer Meeting, Boston, Massachusetts, June 11-15, 2000.

[21] Barber, R.W. and Emerson, D.R., *"A numerical study of low Reynolds number slip flow in the hydrodynamic development region of circular and parallel plate ducts",* Center for Microfluidics, Department of Computational Science and Engineering ,CLRC Daresbury Laboratory, Warrington, 2001

[22] Patnaik Patnaik, B.S., Gowda, Y.T., Ravisankar, M.S., Narayana, P.A., and Seetharamu, K.N., *"Finite element simulation of internal flows with heat transfer using a velocity correction approach",* 2001, E-mail: {bsv_patnaik,knseetharamu}@hotmail.com.

[23] Viana, M.J.G, Nascimento, U.C.S., Quaresma, J.N.N and. Macedo, E.N , *" Integral Transform Method For Laminar Heat Transfer Convection of Hersdhel-Bulkley Fluids Within Concentric Annular Ducts"* Braz. J. Chem. Eng. vol.18, no.4 Sao Paulo Dec. 2001

[24] Tien-Chien Jen , Sunil Eapen, and Guang-Jyh Hwang, *Fully Developed Laminar Fluid Flow in a Rotating Isothermal Isosceles Triangular Channel "*, International Journal of Rotating Machinery, 8(1):1-12,2002.

[25] Maia ,M.C.A and Gasparetto,C.A ," *A numerical Solution for the Entrance Region of non-Newtonian Flow in Annuli"* University of Federal Rio de Janeiro, ,Braz.J.Chem.Eng.Vol.20,No2,June.2003.

[26] Iyad Talal Al-Zaharah ,*"Entropy Analysis in Pipe Flow Subjected to External Heating "*Mechanical Engineering Department ,Saudi Arabia, Int. J. Entropy ,Vol.5,pp .391-403, Dec.2003.

[27] Erbay, L.B., Ercan, M.S., Sulus, B., and Yalcin, M.M.,"*Entropy generation during fluid flow between two parallel plates with moving bottom plate*", Int. J. Entropy, Vol. 5, pp. 506-518, 2003.

[28] Ahmet Sahin, A.Z. and Rached Ben-Mansour, R., *"Entropy generation in laminar fluid flow through a circular pipe"*, Int. J. Entropy, Vol. 5, pp. 404-416, 2003.

[29] Muzychka, Y.S. and Yovanovich, M.M., *"Laminar Forced Convection Heat Transfer in the Combined Entry Region of Non-Circular Ducts",* ASME Journal of Heat Transfer, Vol. 126, pp. 54-61, 2004.

[30] Oyumi, S.M., *"Laminar fluid flow and heat transfer in channels"*, University of California, Department of Nuclear Engineering, Berkeley,CA 94720, 2004.

[31] Ibrahim, A.N., "*Developing Turbulent Flow and Heat Transfer through Rectangular and Circular Duct Cross Section",* M.Sc. thesis, Mechanical Engineering Department, University of Babylon, 2005.

[32] Shaker , A.A.,*" Heat Transfer Calculations of Developing Steady Laminar Flow Between Parallel Plates Channel ",* M.Sc. thesis, Mechanical Engineering Department, University of Babylon, 2006.

[33] Shirly ,C,C, Nascimenton and Joao, N.N Quaresma" *Generalized Integral Transform Solution For Hydrodynamically Developing Non-Newtonian Flow in Circular Tubes"* J. of the Braz. Soc. Of Mech.Sci and Eng.,2006.

[34] Babus'haq, R.F., *"Heat transfer by forced convection in the entrance region of pipes",* M.Sc. thesis, Mechanical Engineering Department ,University of Technology, 1978.

[35] Goswami, D.Y *"Velocity Profiles of Liquid Flow Through Circular Tubes and How They Affects Flow Measurment",* Journal Article ,Journal of Solar Energy Engineering, Vol/Issue :113:3 ;DOE Project. Aug.1991.

[36] Nikuradse, J ., "*Laws of Flow in Rough Pipes"* NACA Tech. Mem 1937.

[37] Fall,H.G., "*Frictional Losses in Piping Systems*", **EML4141L ,Experiment I, 2003.**

[38] Hornbeck, R.W*., "Numerical Marching Techniques for Fluid Flows with Heat Transfer",* National Aeronautics and Space Administration, Washington, 1973.

[39] Adams, J.A. and Rogers D.F., *"Computer-Aided Heat Transfer Analysis",* McGraw-Hill Book Company, New York, 1973.

[40] Schlichting, H., *"Boundary-Layer Theory*", McGraw-Hill Book Company, New York, Sixth edition ,1968.

[41] Anderson, D.A., Tannehill, J.C., and Pletcher, R.H., *"Computational Fluid Mechanics and Heat Transfer",* McGraw-Hill Book Company, New York, 1984.

[**42**] **Virk**, **P.S.,** "*Drag Reduction Fundamentals*", Journal of AIChE, Vol. 21, No.4, PP. 625-656, 1975.

[43]Karlkar ,B.v .and Desmond, R.M., *"Heat Transfer"* **,**West Publishing company , Second edition, 1982.

[44] Abid,E.M., *"Flow Increase in Liquid Pipe line Using Drag Reducing Additives"* , M.Sc theses. from University of Babylon.2007.